ALLOSTERIC REGULATION OF THE CANCER ASSOCIATED MITOCHONDRIAL GLUTAMINASE GAC

A dissertation

Presented to the Faculty of the Graduate School

Of Cornell University

In partial Fulfillment of the Requirement of the Degree of

Doctor of Philosophy

by

Yunxing (Stella) Li

May 2018

ALLOSTERIC REGULATION OF THE CANCER ASSOCIATED MITOCHONDRIAL GLUTAMINASE GAC

Yunxing Li, Ph.D.

Cornell University 2018

Glutamine-derived carbon becomes available for anabolic biosynthesis in cancer cells via the hydrolysis of glutamine to glutamate, as catalyzed by GAC, a splice variant of kidney-type glutaminase (GLS). Thus, there is significant interest in understanding the regulation of GAC activity, with the suggestion being that higher order oligomerization is required for its activation.

The first objective of my thesis study is to use x-ray crystallography, together with site directed mutagenesis, to determine the minimal enzymatic unit capable of robust catalytic activity. Mutagenesis of the helical interface between the two pairs of dimers comprising a GAC tetramer yielded a non-active, GAC dimer whose x-ray structure displays a stationary loop ('activation loop') essential for coupling the binding of allosteric activators like inorganic phosphate to catalytic activity.

A subsequent study using a tryptophan fluorescence probe to understand the regulation of GAC activity, and the mechanistic details of small molecule, allosteric inhibitors, is guided in part by the development of spectroscopic approaches that can directly measure glutaminase activity and the interaction of activators and inhibitors of GAC in real time.

BIOGRAPHICAL SKETCH

The author was born April 16th, 1984 in Beijing, China and raised by her parents, Haiying Li and Zhenyu Yang. As a young child, she had always been amazed watching her father using paint and brush to create beautiful oil paintings at home, and she had this dream of being an artist when she grew up. However, the author's dad, as a person who attended art school but then gave up his dream of being an artist, told her that she could always keep art as a hobby, just don't make it your profession, because it is very hard to make a living by drawing and painting. When she asked her dad what stopped him from pursuing art, he said "Because you were born" (But today she feels really thankful that her dad persuaded her to pursue science over art).

The author then joined the "army" of hundreds of thousands of high school students for the "battle" of taking entrance exams to qualify for attendance at academic colleges. She was accepted by Peking University (it was actually her second try to this school) in 2003 and chose to pursue physics as her major because she thought people in physics are usually very smart and being around them might make her smart too. But she soon grew to feel that physics, as the oldest scientific field besides math, left few general questions left to be answered and the ones that remained are for the "super genius" who would be willing to marry science for life. As she had always been interested in biology, which is a much younger field with so many interesting but unanswered questions, she wanted to change her emphasis to use her training in physics as a means to address biological questions. The author did her

undergraduate research in the Chinese Academy of Sciences focusing on a project involving molecular dynamic simulations. She then followed her undergraduate advisor's suggestion and applied to Oklahoma University in the US and there worked in computational biology studying the mechanism of proton transfer in proteins using a density functional theory based approach.

During her time training as a computational biophysicist, the author realized that she did not enjoy sitting in front of computer and getting virtual data, instead, she sought to use her own hands to perform experiments and generate real results. It was with this in mind, when she arrived at Cornell University as a PhD candidate in biophysics, she chose Dr. Richard Cerione's research group mainly because of the diversity of experiments that were carried out in his lab and of course also because of the warmth and humor evident among the laboratory members. During the time she spent in Dr. Cerione's lab, the author focused on using biophysical methods to investigate the activation mechanism of a therapeutic target that plays an important role in glutamine metabolism in cancer; glutataminase C. The author now looks forward to publishing her thesis work and continuing her scientific journey.

For the Art of Science!

The figure above presents the important role of glutaminase C (GAC) in the mitochondria (engine) of cancer cells as a delicate machine (the car), and we as mechanics use a protein engineering approach to reveal the secret of its activation mechanism. (The work related to this figure is described in Chapter II, and the digital painting was made in fall 2016 by Yunxing Li)

ACKNOWLEDGMENT

First and foremost, I would like to thank my advisor Rick Cerione, who not only has always been a supportive mentor (sometimes plays the role of my parent), but for the passion and enthusiasm that he brings to science that inspires every member in lab every single day. I feel really lucky to have been part of the “Cerione Family” for the past few years as the love and support that I have received from the group will always be remembered. I really appreciate that, as an advisor, Rick does not only care about making us improve our scientific skills, but more importantly, wants us to live our lives simply, as happy people.

To my committee members: Barbara Baird and Holger Sondermann. I really enjoyed working with and talking to Holger whenever I had questions about my project, especially hopping over to their station in CHESS to chat about crystallography (and horror movies!) and watch these experts collect their diffraction data in a masterful way. I would also like to acknowledge Barbara, who is an exemplary advisor and scientist. It was my pleasure to have her on my committee.

I have been very fortunate to have two great mentors in my time here: Jon Erickson and Sekar Ramachandran. To Ram, thank you for accepting me as a rotation student and training me with zero experience in biochemistry and always being there with great advice whenever I needed an expert to talk to. I will miss all the brain storming and sleepless nights we fought through during beam time. To Jon, thank you

for being a great coach who always gave me useful guidance and feedback as I prepared my talks. It was a great pleasure for me to work with two excellent scientists.

I would like to give special thanks to the staff scientists at CHESS for helping me during the multiple beam times during my PhD studies. Especially Dr. Richard Gillilan, and Dr. Irina Kriksunov. Both of them are terrific scientists specializing in SAXS and crystallography and it has been exciting to learn new things from these experts during each beam time. Also thanks to David Schuller who was instrumental in helping me solve my first crystal structure.

And for the rest of my family members in the Cerione Lab: I really enjoyed the unique warm family atmosphere in our lab and I feel very lucky to have shared the last few years at Cornell with you. In no particular order, I would like to thank: Yeyun Zhou, Jingwen Zhang, Jared Johnson, Bo Li, Lindsey Boroughs, Joe Druso, Joy Lin, Laura Deroschers, Kelly Sullivan, Bridget Kreger, Yang Gao, Kristin Wilson, Marc Antonyak, Kathy Rojas, Kai Su Greene, Mike Lukey, Bill Katt, Chengliang Zhang, Arash Latifkir, Julio Sanchez, Yun Ha Hur, Shawn Milano and past Cerione lab members.

For people outside my research life, first I definitely would acknowledge my parents, who brought me to this world and have been understanding and supportive at each step/decision I have made in my life. I would also like to give special acknowledgement to Frank He. Even though we only met each other towards the end of our PhD journeys, you have been there for me and helped me negotiate some uncertain and tough times; both as a partner and as my best friend.

A very special thanks to my unique group of friends outside of lab who made my PhD experience filled with adventure and happy memories. Joshua Tokuda whose creativity and cheerful personality has always inspired people around him, and often led us to some very cool group projects that we would have never thought of doing. David Ackerman as one of my oldest buddies in Cornell, his chillness and unique sense of humor have made him one of the most fun person to hang out with. Avtar Singh, who is always willing to give help and support to his friends, has been a great person to talk to. Jeahoo Kwon's unique personality has definitely brought us a lot of special happy moments during the time we have spent in Cornell. And I will always appreciate the "biophysics T-shirts' that he brought all the way from Korea to us. Rupa Shah as a friend outside the "nerd circle" always helps us to "stay normal" and she is a talented interview coach. Julie Sutten has been my ice skating buddy ever since my first year in Cornell. I will always remember those flip jumps we have practiced together and hopefully we will have chance to skate together in the future as well. Thank you all!

TABLE OF CONTENTS

LIST OF FIGURES

CHAPTER ONE

INTRODUCTION

Cancer cells undergo metabolic remodeling

Genetic and epigenetic modifications to the cellular genome underlie a host of changes that allow tumor cells to proliferate and outcompete their normal counterparts (1,2). Alterations in metabolic processes that accompany transformation are often critically important in supporting tumor growth and this involves invoking a number of strategies to scavenge and utilize nutrients in novel ways (3). In addition to altered glucose metabolism, many cancers are known to catabolize glutamine for energy and as a source of biosynthetic building blocks for other pathways. For this reason, glutamine metabolism has emerged as an effective therapeutic target for cancer researchers and, consequently, a number of drugs are being developed to exploit this metabolic vulnerability.

The accumulation of somatic mutations is often central to tumor progression and can be the driving force for phenotypic differences between normal and transformed cells (4). Mutations in signaling pathways or cell cycle checkpoints can have dramatic consequences for cell proliferation and provide tumor cells with a survival advantage (5). Genetic changes underlying cancer are often classified into two categories: tumor suppressors and oncogenes (6). Tumor suppressors are genes whose inactivation often yields a transformed phenotype as

their protein products regulate a wide range of cellular activities, including cell cycle checkpoints, DNA damage detection and repair, protein degradation and ubiquitination, mitogenic signaling, cell migration, specification, differentiation and angiogenesis (7). Perhaps the best known example of a tumor suppressor is p53, which plays a role in detecting DNA damage and participates in multiple cell cycle checkpoints, and is the single most frequently mutated gene in human cancers (>50%, 8). In contrast, oncogenes are activated versions of their native forms (proto-oncogenes). Proteins encoded by proto-oncogenes typically control cell proliferation, apoptosis or both. These gene products fall into six broad functional categories: chromatin remodelers, transcription factors, growth factors, growth factor receptors, signal transducers and apoptosis regulators (11,12). These mutations bestow tumors with characteristic properties that include enhanced proliferation compared to normal tissue, insensitivity to anti-growth signals, evasion of apoptotic pathways and immunity checkpoints, and often, the capability for angiogenesis and metastatic potential (11). These distinct behaviors also give rise to heightened metabolic demands, which tumors are able to satisfy by modifying their capacity for nutrient uptake and processing (14,15).

Glucose metabolism in cancer and the Warburg effect

The classic example of altered metabolic activity in cancer cells is described as the Warburg effect, whereby tumor cells increase their glycolytic activity and

shift from normal aerobic respiration through the TCA cycle to glycolysis. A key enzyme in glycolysis, pyruvate kinase (PK), was identified to play an important role in the Warburg effect (14). As the enzyme for the final step of catalysis in glycolysis, pyruvate kinase transfers a phosphate group from phosphoenolpyruvate (PEP) to ADP, thus yielding pyruvate; with the last rate limiting step being the entry of the pyruvate derived from glucose into the mitochondria. Here, pyruvate dehydrogenase (PDH) converts pyruvate to acetyl-CoA which is incorporated into the TCA cycle (17,18). It has been shown that pyruvate kinase isoform 2 (PKM2) is predominantly expressed in cancer cells, while in normal cells the expression was switched to the constitutively active isoform PKM1 (17). Although PKM2 only differs from PKM1 by 22 residues, the regulation of these two isoforms is very different. Interestingly, it has been shown that a glycolysis intermediate, fructose 1,6-bisphosphate (FBP), is an allosteric activator of pyruvate kinase M2 but not M1. The binding site on PKM2 is at the dimer-dimer interface, where PKM2 differs from PMK1, and the binding of FBP can induce tetramer formation (20,21). Therefore, PKM2 activation is FBP-dependent while PMK1 is constitutively active (20). Taken together, the increased PKM2 expression in cancer cells leads to decreased pyruvate kinase activity (14). In light of this, the tetramer promoted activation of PKM2 provides a potential therapeutic target to overcome the loss of enzymatic activity of pyruvate kinase in cancer cells. In fact, there have been small molecule activators developed to stimulate the PKM2 activity by inducing tetramer formation, and these molecules are being examined in relevant mouse models

(23,24,25). In addition, a second novel allosteric activator that can specifically regulate PKM2 but not PKM1, known as SAICAR (N-Succinyl-5-aminoimidazole-4-carboxamide Ribose 5'-Phosphate), has been identified. SAICAR is an intermediate of the *de novo* nucleotide synthesis pathway, with its cellular levels being dependent upon the pentose phosphate pathway (24).

The Warburg effect is dependent upon the upregulation of lactate dehydrogenase (LDH-A), which catalyzes the conversion of pyruvate to lactate, helping tumors survive under hypoxic conditions, resulting in the secretion of glucose carbons as lactate (11,12,13). This metabolic adaptation allows tumor cells to produce ATP at a rate that is 200-fold higher than that of normal cells (14,15). To carry out this altered metabolic program, cancer cells increase their rate of glucose uptake, often in response to hypoxic conditions in solid tumors. Hypoxia-inducible factor-1-α (HIF-1α) is a transcription factor upregulated under these conditions that plays a major role in glucose metabolism by increasing the expression of glucose transporters and glycolytic enzymes (16,17,18).

In addition to changes in the glycolytic pathway, modifications to TCA cycle regulation are a common feature of cancer cell metabolic reprogramming. The TCA cycle is an essential pathway that cells use to convert sugars, lipids and amino acids to the universal energy molecule, ATP (33). Enzymes carrying out reactions in the TCA cycle have recently been shown to be associated with rare cancers. Three TCA cycle enzymes have been shown to be mutated in certain cancers: succinate dehydrogenase, fumarate dehydrogenase and isocitrate dehydrogenase 2,

resulting in the accumulation of succinate, fumarate and (R)-2-hydroxyglutarate, respectively (20,21,22,23,24).

Glutamine metabolism in cancer

As a consequence of their altered glucose metabolism, cancer cells are required to use alternative sources of carbon for energy and biosynthesis. Glutamine is an abundant nonessential amino acid that can serve this need and has been shown to be essential for cancer cell viability. It is a major nitrogen donor for the enzymatic steps responsible for purine and pyrimidine synthesis. Glutamine is hydrolyzed to glutamic acid, with the production of ammonia, in the mitochondria through the catalytic actions of the glutaminase enzymes. Glutamic acid is then converted to α-ketoglutarate, by glutamate dehydrogenase, thus generating a precursor to the synthesis of amino acids such as serine, alanine, aspartate and ornithine (18,19). Tumors have a particularly high demand for nucleotides and other building blocks due to their elevated rates of proliferation, and so glutamine metabolism is critical for cancer cell growth and survival. In some cancer cell lines, glutamine consumption is 10-fold higher than that of any other amino acid (41).

Figure 1.1 Glucose and glutamine metabolism in normal cells and cancer cells. Schematic highlights key differences in many cancer cells compared to normal tissue. Normal cells use glycolysis prior to respiration in the mitochondria (yellow) and the complete breakdown of glucose by the tricarboxylic acid (TCA) cycle (green). In cancer cells, glycolysis becomes the primary mode of glucose metabolism resulting in lactate and its secretion. Glutaminolysis provides the cancer cell with an alternate source of biosynthetic precursors, fueling the TCA cycle with glutamine derived α-ketoglutarate. The anti-tumor compounds 968 and BPTES inhibit glutamine metabolism by inhibiting the enzyme glutaminase (GLS).

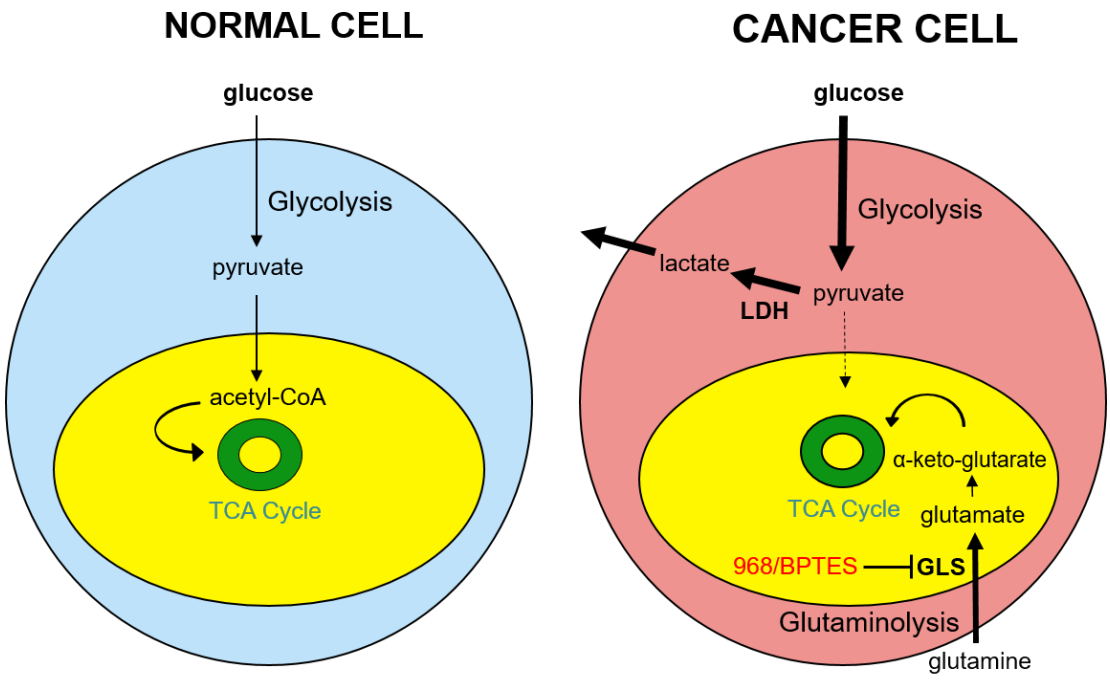
NORMAL CELL
glucose
Glycolysis
pyruvate
acetyl-CoA
TCA Cycle
CANCER CELL
glucose
Glycolysis
lactate
LDH
pyruvate
α-keto-glutarate
TCA Cycle
glutamate
968/BPTES
GLS
Glutaminolysis
glutamine

There is increasing interest in the proteins that are responsible for the altered metabolism exhibited by cancer cells that result in them being “addicted” to certain nutrients that are not used by non-transformed cells. This metabolic reprogramming results in a vulnerability of some cancer cells and may offer a worthwhile opportunity for developing new therapeutic strategies. In this regard, inhibitors directly targeting glutamine metabolism have been shown to significantly affect the growth of glutamine-addicted cell lines while minimally affecting normal cells (42).

Recent studies have shown that both the tissue of origin and the specific oncogenes present in a cancer can affect whether a tumor consumes or produces glutamine. For example, liver tumors induced by the expression of the oncogene Myc catabolize glutamine, while hepatic tumors induced by MET produce it. In humans, the lungs are one of the major sources of glutamine release into the blood plasma (22,23). Stress-induced glutamine biosynthesis is largely regulated by the expression of glutamine synthetase, which is significantly elevated in transformed cells compared to normal cells in lung tissue (45). Liver and kidney also have the capacity to synthesize or catabolize glutamine but do not appear to be major contributors to the plasma glutamine pool (25,26). Evidence from transgenic mouse model systems has shown that during tumorigenesis, both organs change modes from primarily releasing glutamine to consuming it (30,31,32,28).

Not all cancer cell lines need an external supply of glutamine. For instance, a panel of lung cancer cell lines showed different levels of glutamine addiction, with some even exhibiting complete glutamine independence (51). Meanwhile, breast cancer cell lines have exhibiting systematic glutamine dependence, with luminal cells tending to be glutamine-addicted while basal cells are glutamine-independent (52). Methods to quantify glutamine accumulation in solid tumors, similar to positron emission tomography for fluorodeoxyglucose (FDG-PET), would be a very useful tool for diagnosing glutamine-addicted cancers (53).

Identification of GLS as a metabolic target for cancer therapy.

Rho-family GTPases activate different signaling pathways that impact a variety of cellular activities including cell polarity, migration, cell growth, membrane trafficking, and malignant transformation (45,46), all of which play important roles in oncogenesis. In fact, overexpression of Rho GTPases has been demonstrated in a number of different cancer cell lines (including advanced stage breast cancers) (47,48,49). In particular, two Rho-family GTPases, RhoA and RhoC, have been implicated in the progression of malignancy, metastasis, and local invasiveness (50,51,52). As a consequence, Rho GTPases may provide novel targets for anticancer therapies. Along these lines, while screening for small molecule inhibitors that can block cellular transformation by the Rho family GEF, oncogenic

Dbl, a small molecule inhibitor of the benzo[α]phenanthridinone family (968) was identified by our laboratory (62). The most essential features of 968 that gave maximal inhibition of cell transformation are the para-dimethyl amino group and the meta-positioned bromine on the phenyl ring. The fact that 968 can inhibit the transformation of a number of different types of constitutively active Rho GTPases suggested that its target was not an individual Rho protein or its GEF binding partner. Further experiments aimed at identifying the small molecule's target were carried out; in particular, a biotin-labeled 968 molecule was used to affinity precipitate a candidate protein target from transformed cell lysates. Microsequence analysis indicated that the putative 968 target was the mouse isoform of human glutaminase C (GAC) (62). GAC has a molecular weight of 66 kDa, and is one of two splice variant isoforms of kidney-type glutaminase, GLS (63). The same study showed that the addition of α-ketoglutarate, which is the product of the next step in glutamine metabolism catalyzed by glutamate dehydrogenase, can restore the ability of both GLS knockdown and 968 treated Dbl expressing MEFs, as well as the breast cancer cell lines MDA-MB231 and SKBR3, to grow in low serum. Subsequently, it was shown that 968 was neither a competitive inhibitor of inorganic phosphate (an activator of the enzyme) nor glutamine (64), which suggested that 968 acts in an allosteric manner.

Because of their central role in initiating glutaminolysis, the glutaminase enzymes have emerged as possible metabolic targets for cancer therapy (40,41,66).

Two different genes encode the glutaminase enzymes: kidney-type glutaminase (KGA), which is encoded by the GLS gene, and liver-type glutaminase (LGA) is encoded by the GLS2 gene. The two alternatively spliced forms of GLS are referred to as KGA (which is the longer form) and a carboxyl-terminal splice variant, GAC (67,68). GAC has been of particular interest in cancer as it is highly expressed in a number of types of cancer cell lines, including those of breast, lung, cervix, brain, prostate, and B cells. These cancer cells also exhibit glutamine addiction and are susceptible to inhibition by the 968 and BPTES compounds (27,33,34,35).

Glutaminase activity is upregulated in cancer cells, either by increasing its expression level or by alterations in its specific activity (72,73). The expression level of GAC was first found to be significantly increased in human B cell lymphoma as well as prostate cancer (71). GAC expression was then shown to be elevated in an aggressive breast cancer cell line (MDA-MB231) compared to non-transformed mammary epithelial cells (62). However, in the latter studies, the expression level of GAC alone could not fully account for the elevated glutaminase activity, suggesting that the specific activity of the enzyme was also increased. Indeed, this appears to be the case in a number of cancer cell lines. For example, in both Dbl-transformed NIH-3T3 cells and SKBR3 breast cancer cells, the expression level of GLS is similar to that of normal fibroblasts. However, the specific activity of the enzyme is significantly increased in the transformed cells (70).

Regulation of glutaminase

While the patterns of glutamine metabolism in solid tumors are often determined by tissue microenvironment and the tissue of origin (72), at the cellular level there two primary mechanisms for mediating the upregulation of enzyme activity. The first is by increasing the expression level of the enzyme, i.e. as the total concentration of enzyme increases, activity is elevated by the increase in the amount of active, oligomeric enzyme by mass action. A second mode of regulation that is less well characterized is through the post-translational modification of the enzyme, so as to increase its specific ability. In the latter case, it was reported that oncogenic Dbl can signal through NF-κB to increase the expression of a protein kinase that promotes the phosphorylation of GLS in NIH-3T3 cells, with a corresponding increase in its enzymatic activity (62). With regard to the regulation of GLS expression, one mechanism involves c-Myc, which upregulates GLS expression through the binding and sequestration of micro-RNAs miR-23a/b that normally suppress GLS translation (71). However, the relationship between c-Myc and glutamine metabolism is complicated, tissue specific, and tumor specific (75,76). The recently published studies from our own laboratory suggest that, in oncogenic-Dbl transformed cells, Rho GTPases signal the activation of the c-Jun N-terminal kinase (JNK), which then directly phosphorylates and activates the transcription factor c-Jun. This results in the increased expression of GLS by directly binding to its promoter at a consensus motif. Since c-Jun regulates GLS directly at

the transcriptional level, the high expression of c-Jun that occurs in some breast cancer cells appears sufficient to upregulate the expression of GLS (74).

Apart from upstream oncogenic regulators, some tumor suppressors can also regulate glutamine metabolism (75). For example, the retinoblastoma (Rb) gene is dysregulated in a wide range of human cancers, where it normally acts as a tumor suppressor. It has been reported that genomic deletion of all three Rb family members ((Rb-1, Rb11, and Rb12) causes a significant increase in the levels of GLS and the glutamine transporter ASCT2, which in turn leads to a strong dependence on glutamine for cell survival and proliferation (76).

Glutaminase structure and inhibitors

Glutaminases belong to a larger protein family with homologs in bacteria as well as eukaryotes (39,40). They are soluble proteins with a relatively low affinity for their substrate glutamine (K_m ~1.5 – 9.5 mM) (79). A comparison of the active sites from different glutaminases indicates the conservation of a β-lactamase fold structure together with several conserved key residues in the active site of the enzyme (42,43).

Glutaminase inhibition has been a therapeutic goal for some time. One of the earliest inhibitors, 6-diazo-5-oxy-L-norleucine (DON; **Figure 1.2**), competes with glutamine by binding and crosslinking to the active site of GLS. The irreversible nature of its binding makes DON a potent inhibitor; however, the fact that it binds

to multiple targets reflects its overall lack of selectivity which remains a significant drawback to its development as a therapeutic agent (82).

Some progress in developing clinically useful glutaminase inhibitors has been made in the last decade, as allosteric, reversible inhibitors of KGA and GAC have been reported. One of these, named 968, was developed by our laboratory and validated in a number of cancer cell types (38,43). However, because of its relatively low (micromolar) binding affinity and poor solubility, it has been challenging to obtain a co-crystal structure of 968 bound to GAC, making it difficult to definitively determine its mechanism of inhibition (84). Kinetic analysis suggests that 968 does not function as a competitive inhibitor (64). Furthermore, *in silica* docking experiments performed in our laboratory suggest that the binding pocket for 968 is located at the hydrophobic interface between the two monomers that constitute the dimer (see **Fig.1.3**). The development of a direct spectroscopic binding assay for 968 showed that the inhibitor preferentially binds to the monomeric state of GAC (85). Thus, the best evidence to date would suggest that 968 initially binds to a hydrophobic patch on GAC monomers, and upon GAC dimer formation, it then fits into a cove between the two enzyme monomers and traps the enzyme in an inactive conformational state.

Figure 1.2 Chemical structures of inhibitors of GLS. Examples of inhibitors of glutaminase reported in the literature, including 6-diazo-5-oxy-L-norleucine (DON), 968 (70), bis-2-(5-phenylacetamido-1,2,4-thiadiazol-2-yl)ethyl sulfide (BPTES), and their analogs.

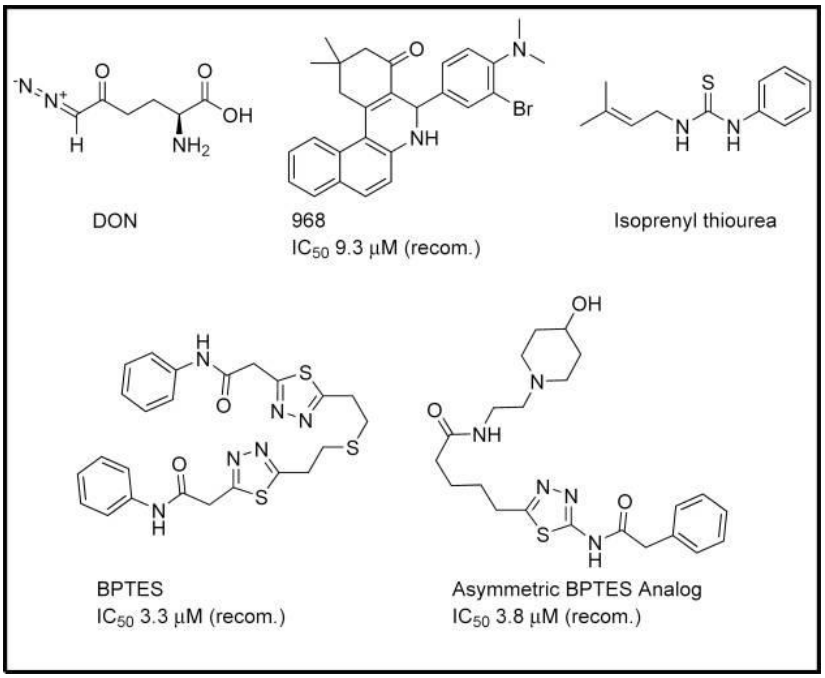
DON
968
IC50 9.3 μM (recom.)
Isoprenyl thiourea
BPTES
IC50 3.3 μM (recom.)
Asymmetric BPTES Analog
IC50 3.8 μM (recom.)

Another recently identified inhibitor is BPTES (bis-2-phenylacetoamido-1,3,4-thiadiazol-2-ylethyl sulfide), which exhibits selective inhibition towards GLS over GLS2 (86). The higher binding affinity of BPTES and related analogs for GAC, compared to 968, has led to its development as a therapeutic agent. In fact, a more recently described BPTES analog, CB-839, is currently in clinical trials for triple-negative breast cancer and multiple myeloma. The ability of BPTES to bind to GAC with relatively high affinity (sub-micromolar) has led to a co-crystal structure for the enzyme-inhibitor complex (46,44). As shown in **Figure 1.2**, BPTES has a symmetric structure, though some BPTES analogs with improved solubility do not possess this symmetry (83). The crystal structure shown in **Figure 1.3 C**, revealed the binding site of BPTES and provided insight into its mechanism of inhibition, showing that the drug folds onto itself and binds two opposing loops at the GAC dimer-dimer interface to form an inactive GAC tetramer. The loop that represents the BPTES binding site is able to undergo a conformational change during both tetramerization and phosphate (activator) binding and, as described in **Chapter II**, plays a fundamental role in regulating glutaminase activity.

Although the physiologically relevant activator of GAC in cancer cells remains in question, several inorganic activators have been reported, such as inorganic phosphate and sulfate (47,48). Inorganic phosphate is a well-studied activator, although in the absence of structures of inorganic, multivalent anions bound to GAC, the mechanism of action of these allosteric activators remains

speculative. The sole co-crystal structure with inorganic sulfate was determined with a highly truncated and inactive form of GAC. In this structure, both inhibitor (BPTES) and activator (inorganic sulfate) are seen to undergo direct interactions with the “activation loop” (89), providing support for the view that this region of the enzyme is important for catalysis. Inorganic phosphate has also been shown to promote the polymerization of full-length GAC, which may result in a heterogeneous population of GAC oligomers and help explain why it has been challenging to obtain a co-crystal structure for the native protein (90).

Figure 1.3 Comparison of GAC allosteric inhibitors, BPTES and 968. A, Chemical structure of BPTES. **B,** Chemical structure of 968. **C,** X-ray crystal structure of GAC in complex with BPTES. The two dimers in the tetramer structure of GAC make contact at a helical interface. Two BPTES molecules bridge the two dimers, binding at the dimer-dimer interface of the GAC tetramer through their interaction with the "activation loop". **D**, The molecular docking model of 968 in complex with GAC. One molecule of 968 is proposed to bind to each dimer, inserting into the hydrophobic pocket at the monomer-monomer interface.

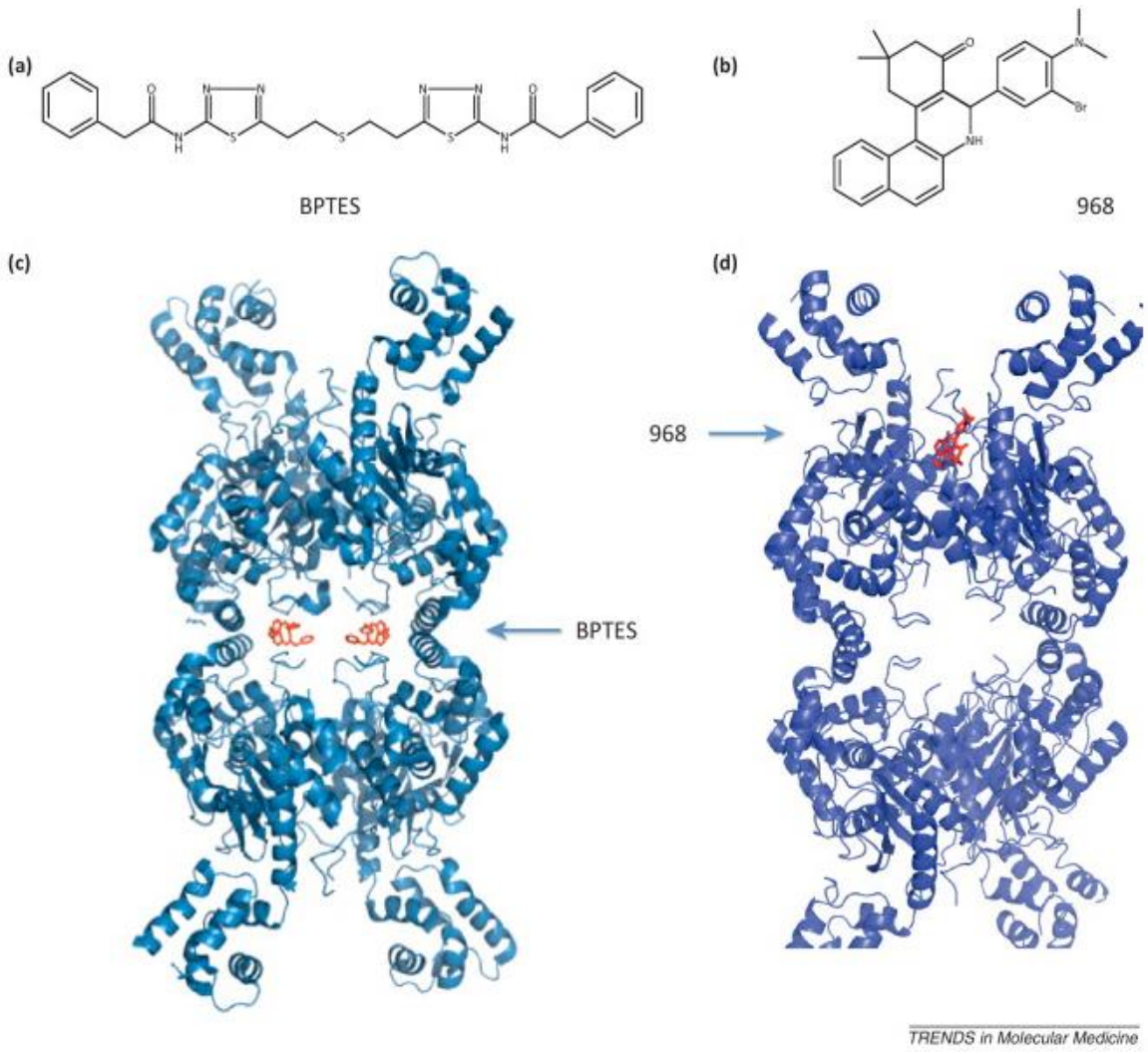
(a)
BPTES
(b)
968
(c)
BPTES
(d)
968
TRENDS in Molecular Medicine

The importance of the dimer to tetramer transition in the activation of GAC

Previous studies of GAC have suggested that the essential step for enzyme activation is the transition of a GAC dimer to a tetrameric species (80, 83, 55). In order to monitor GAC oligomerization, FRET assays were developed in our laboratory as a real-time read out to monitor the dimer to tetramer transition at the low concentrations of GAC typically used when assaying enzyme activity. Two populations of purified recombinant GAC were labeled with fluorescent donor and acceptor probes, respectively. The mixing of the two labeled GAC species resulted in a dose-dependent quenching of the donor emission, which was reversible with the addition of unlabeled GAC. This result revealed that the GAC dimer to tetramer transition is a dynamic process. The titration profile of the donor fluorescence (dimer to tetramer titration) was directly correlated to the basal activity of GAC, as a function of increasing enzyme concentration, which supported the view that the GAC tetramer was necessary for enzymatic activity (85).

Effects of small molecule inhibitors of GAC activity on the dimer to tetramer transition

Using the real-time FRET assay, the effects of 968, versus BPTES on the GAC dimer to tetramer transition were also investigated. For BPTES, it was found that

the addition of the inhibitor to the mixture of donor and accepter labeled GAC caused an immediate quenching of the 488-GAC (donor) fluorescence, as a result of the formation of donor-acceptor tetramers induced by the binding of BPTES. In these experiments, the GAC:BPTES complex was observed to be very stable, as evidenced by the difficulty in reversing dimer-dimer binding by the addition of unlabeled GAC. This result was consistent with the previous published studies that as an inhibitor, BPTES stabilized an inactive tetrameric form of GAC.

In contrast to BPTES, 968 showed a significantly different effect on the GAC dimer to tetramer transition. Adding 968 caused a significant amount of quenching in the fluorescence emission of 488-GAC, where the addition of excess unlabeled GAC resulted in a partial fluorescence recovery. The partial recovery of 488 fluorescence reflected a situation where 968 did not interfere with GAC tetramer formation since the GAC:968 tetramer could still dissociate and form mixed tetramers between donor or acceptor labeled GAC and unlabeled GAC. However, the inability to fully recover the fluorescence emission was due to the fact that 968 interacts at a site close to the location of the donor fluorescent probe, thereby causing a change in its fluorescence (85). This then made it possible to directly monitor the binding of 968 to GAC labeled with a fluorescent reporter group, i.e. by monitoring changes in the reporter group fluorescence. Further studies were carried out by our laboratory to investigate in more detail the interaction between 968 and GAC and the nature of its inhibition of enzyme activity. To this end, a real-

time fluorescence based enzyme activity assay which monitors NADH production of glutamate was refined in our laboratory. Thus, it became possible to monitor simultaneously the direct binding of 968 to GAC and the effects of the inhibitor on enzymatic activity. The results revealed an overlapping dose-dependence for 968 inhibition of GAC and its direct binding to the enzyme. These binding experiments also showed that 968 preferentially binds to the monomeric form of GAC before fitting into a cove that forms when two GAC monomers come together to form a dimer, consistent with our docking prediction (**Fig.1.3**, (86)).

OVERVIEW

The central aim of the thesis work presented below is to gain structural and functional insights into the mechanism of GAC activation and the details of inhibition of GAC activity by small molecules. The work was undertaken in order to use biophysical structures of GAC bound to its regulators in order to better understand their mode of action and obtain direct evidence showing how these small molecules interact with the enzyme at the atomic level to modulate protein activity.

In Chapter II, I describe the X-ray crystal structure of a 'constitutive dimer', where the helical interface that mediates the dimer to tetramer transition is disrupted by site-directed mutagenesis. Using this structure, I go on to perform structural and kinetic experiments to further probe the mechanism of GAC activation. The X-ray crystal structure of this dimeric form of GAC enabled us to

identify the “activation loop” of the enzyme that is subsequently shown to play a critical role in both activation and inhibition of the enzyme. In Chapter III, I then go on to develop a direct fluorescence readout for substrate (glutamine) binding by placing a tryptophan close, first to the activation loop (GACF327W), and then at the glutamine (substrate) binding site (GAC(Y471W), which allows for direct real-time assays of glutamine binding to the enzyme and the effects of activators and inhibitors at these sites. These spectroscopic probes of GAC have made it possible to study the influence that small molecule regulators have on substrate-enzyme interactions and provide insight regarding GAC mechanism of action. Finally, Chapter IV is a summary presenting our current working model of GAC structure and function that forms the basis for future studies of glutaminase catalysis and inhibition.

REFERENCES:

1. You, J., and Jones, P. (2012) Cancer Genetics and Epigenetics : Two Sides of the Same Coin ? *Cancer Cell*. **22**, 9–20

2. Choi, J. D., and Lee, J.-S. (2013) Interplay between Epigenetics and Genetics in Cancer. *Genomics Inform.* **11**, 164

3. Phan, L. M., Yeung, S.-C. J., and Lee, M.-H. (2014) Cancer metabolic reprogramming: importance, main features, and potentials for precise targeted anti-cancer therapies. *Cancer Biol. Med.* **11**, 1–19

4. Loeb, L. A., Loeb, K. R., and Anderson, J. P. (2003) Multiple mutations and cancer. *Proc. Natl. Acad. Sci. U. S. A.* **100**, 776–81

5. Rhind, N., and Russell, P. (2012) Signaling Pathways that Regulate Cell Division. *Cold Spring Harb. Perspect. Biol.* **4**, a005942–a005942

6. Lee, E. Y. H. P., and Muller, W. J. (2010) Oncogenes and tumor suppressor genes. *Cold Spring Harb. Perspect. Biol.* **2**, 1–18

7. Sherr, C. J. (2004) Principles of Tumor Suppression Review. *Cell*. **116**, 235–246

8. Sherr, C. J., and McCormick, F. (2002) The RB and p53 pathways in cancer. *Cancer Cell*. **2**, 103–112

9. Stehelin, D. (1995) Oncogenes and cancer. *Science (80-.).* **267**, 1408–1409

10. Pardal, R., Molofsky, a V, and He, S. (2005) Stem Cell Self-Renewal and Cancer Cell Proliferation Are Regulated by Common Networks That Balance the Activation of Proto-oncogenes and Tumor Suppressors Stem Cell Self-Renewal and Cancer Cell Proliferation Are Regulated by Common Networks That Balance t. 10.1101/sqb.2005.70.057

11. Walker, M., Kublin, J. G., and Zunt, J. R. (2009) On the Origin of Cancer Metastasis. **42**, 115–125

12. Kasner, E., Hunter, C. A., Ph, D., Kariko, K., and Ph, D. (2013) Evading apoptosis in cancer. **70**, 646–656

13. Kasner, E., Hunter, C. A., Ph, D., Kariko, K., and Ph, D. (2013) Mutation of Tumor Suppressor Gene Men1 Acutely Enhances Proliferation of Pancreatic Islet Cells. **70**, 646–656

14. Christofk, H. R., Vander Heiden, M. G., Harris, M. H., Ramanathan, A., Gerszten, R. E., Wei, R., Fleming, M. D., Schreiber, S. L., and Cantley, L. C. (2008) The M2 splice isoform of pyruvate kinase is important for cancer metabolism and tumour growth. *Nature*. **452**, 230–233

15. DeBerardinis, R. J., Lum, J. J., Hatzivassiliou, G., and Thompson, C. B. (2008) The Biology of Cancer: Metabolic Reprogramming Fuels Cell Growth and Proliferation. *Cell Metab.* **7**, 11–20

16. Scrutton, M., and Utter, M. (1968) The regulation of glycolysis and gluconeogenesis in animal tissues. *Annu. Rev. Biochem.* 10.1146/annurev.bi.37.070168.001341

17. Ibsen, K. H. (1977) Interrelationships and Functions of the Pyruvate Kinase Isozymes and Their Variant Forms : A Review Interrelationships and Functions of the Pyruvate Kinase Isozymes and Their Variant Forms : A Review1. *Cancer Res.*

18. Jurica, M. S., Mesecar, A., Heath, P. J., Shi, W., Nowak, T., and Stoddard, B. L. (1998) The allosteric regulation of pyruvate kinase by fructose-1,6-bisphosphate. *Structure*. **6**, 195–210

19. Dombrauckas, J. D., Santarsiero, B. D., and Mesecar, A. D. (2005) Structural basis for tumor pyruvate kinase M2 allosteric regulation and catalysis. *Biochemistry*. **44**, 9417–9429

20. Mazurek, S. (2011) Pyruvate kinase type M2: A key regulator of the metabolic budget system in tumor cells. *Int. J. Biochem. Cell Biol.* **43**, 969–980

21. Anastasiou, D., Yu, Y., Israelsen, W. J., Jiang, J.-K., Boxer, M. B., Hong, B. S., Tempel, W., Dimov, S., Shen, M., Jha, A., Yang, H., Mattaini, K. R., Metallo, C. M., Fiske, B. P., Courtney, K. D., Malstrom, S., Khan, T. M., Kung, C., Skoumbourdis, A. P., Veith, H., Southall, N., Walsh, M. J., Brimacombe, K. R., Leister, W., Lunt, S. Y., Johnson, Z. R., Yen, K. E., Kunii, K., Davidson, S. M., Christofk, H. R., Austin, C. P., Inglese, J., Harris, M. H., Asara, J. M., Stephanopoulos, G., Salituro, F. G., Jin, S., Dang, L., Auld, D. S., Park, H.-W., Cantley, L. C., Thomas, C. J., and Vander Heiden, M. G. (2012) Pyruvate kinase M2 activators promote tetramer formation and suppress tumorigenesis. *Nat. Chem. Biol.* **8**, 839–847

22. Parnell, K. M., Foulks, J. M., Nix, R. N., Clifford, A., Bullough, J., Luo, B., Senina, A., Vollmer, D., Liu, J., McCarthy, V., Xu, Y., Saunders, M., Liu, X.-H., Pearce, S., Wright, K., O'Reilly, M., McCullar, M. V., Ho, K.-K., and Kanner, S. B. (2013) Pharmacologic Activation of PKM2 Slows Lung Tumor Xenograft Growth. *Mol. Cancer Ther.* **12**, 1453–1460

23. Kim, D. J., Park, Y. S., Kim, N. D., Min, S. H., You, Y.-M., Jung, Y., Koo, H., Noh, H., Kim, J.-A., Park, K. C., and Yeom, Y. Il (2015) A novel pyruvate kinase M2 activator compound that suppresses lung cancer cell viability under hypoxia. *Mol. Cells*. **38**, 373–379

24. Malik, A. B., Toth, M., Fridman, R., and Sambasivarao, S. V (2013) SAICAR

stimulates pyruvate kinase isoform M2 and promotes cancer cell survival in glucose-limited conditions. **18**, 1199–1216

25. Gatenby, R. A., and Gillies, R. J. (2004) Why do cancers have high aerobic glycolysis? *Nat. Rev. Cancer*. **4**, 891–899

26. Kim, J. W., and Dang, C. V. (2006) Cancer's molecular sweet tooth and the Warburg effect. *Cancer Res.* **66**, 8927–8930

27. Fantin, V. R., St-Pierre, J., and Leder, P. (2006) Attenuation of LDH-A expression uncovers a link between glycolysis, mitochondrial physiology, and tumor maintenance. *Cancer Cell*. **9**, 425–434

28. Alfarouk, K. O., Verduzco, D., Rauch, C., Muddathir, A. K., Adil, H. H. B., Elhassan, G. O., Ibrahim, M. E., David Polo Orozco, J., Cardone, R. A., Reshkin, S. J., and Harguindey, S. (2014) Glycolysis, tumor metabolism, cancer growth and dissemination. A new pH-based etiopathogenic perspective and therapeutic approach to an old cancer question. *Oncoscience*. **1**, 777–802

29. Alfarouk, K. O. (2016) Tumor metabolism, cancer cell transporters, and microenvironmental resistance. *J. Enzyme Inhib. Med. Chem.* **6366**, 1–8

30. Eales, K. L., Hollinshead, K. E. R., and Tennant, D. A. (2016) Hypoxia and metabolic adaptation of cancer cells. *Oncogenesis*. **5**, e190

31. Denko, N. C. (2008) Hypoxia, HIF1 and glucose metabolism in the solid tumour. *Nat. Rev. Cancer*. **8**, 705–713

32. Courtnay, R., Ngo, D. C., Malik, N., Ververis, K., Tortorella, S. M., and Karagiannis, T. C. (2015) Cancer metabolism and the Warburg effect: the role of HIF-1 and PI3K. *Mol. Biol. Rep.* **42**, 841–851

33. I. E. Scheffler (2008) *Mitochondria, John Wiley & Sons, 2nd edition*

34. Cardaci, S., and Ciriolo, M. R. (2012) TCA cycle defects and cancer: When metabolism tunes redox state. *Int. J. Cell Biol.* 10.1155/2012/161837

35. Yang, M., Soga, T., and Pollard, P. J. (2013) Oncometabolites: Linking altered metabolism with cancer. *J. Clin. Invest.* **123**, 3652–3658

36. Emerging, T. H. E., Of, H., and Metabolism, C. (2017) the Emerging Hallmarks of Cancer Metabolism. **23**, 27–47

37. Reitman, Z. J., and Yan, H. (2010) Isocitrate dehydrogenase 1 and 2 mutations in cancer: Alterations at a crossroads of cellular metabolism. *J. Natl. Cancer Inst.* **102**, 932–941

38. Gaude, E., and Frezza, C. (2014) Defects in mitochondrial metabolism and cancer. *Cancer Metab.* **2**, 10

39. Ahluwalia, G. S., Grem, J. L., Hao, Z., and Cooney, D. A. (1990) Metabolism and action of amino acid analog anti-cancer agents. *Pharmacol. Ther.* **46**, 243–271

40. Wilmore, D., and Rombeau, J. (2001) Glutamine metabolism: Nutritional and clinical significance. *J. Nutr.* 0022-3166/01

41. Cultu, T. (1955) of Mammali. **122**, 501–504

42. Wise, D. R., and Thompson, C. B. (2011) Glutamine Addiction: A New Therapeutic Target in Cancer. *Trends Biochem. Sci.* **35**, 427–433

43. Plumley, D. A., Souba, W. W., Hautamaki, R. D., Martin, T. D., Flynn, T. C., Rout, W. R., and Copeland, E. M. (1990) Accelerated lung amino acid release in hyperdynamic septic surgical patients. *Arch. Surg.* **125**, 57–61

44. Hulsewé, K. W. E., Van Der Hulst, R. R. W. J., Ramsay, G., Van Berlo, C. L. H., Deutz, N. E. P., and Soeters, P. B. (2003) Pulmonary glutamine production: Effects of sepsis and pulmonary infiltrates. *Intensive Care Med.* **29**, 1833–1836

45. Pan, M., Wasa, M., Ryan, U., and Souba, W. (1995) Inhibition of pulmonary microvascular endothelial glutamine transport by glucocorticoids and endotoxin. *J. Parenter. Enter. Nutr.* **19**, 477–481

46. Dudrick, P. S., Inoue, Y., Espat, N. J., and Souba, W. W. (1993) Na(+)-dependent glutamine transport in the liver of tumour-bearing rats. *Surg. Oncol.* **2**, 205–215

47. Felig, P., Wahren, J., and Raf, L. (1973) Evidence of Inter-organ Amino-Acid Transport by Blood Cells in Humans. *Proc. Natl. Acad. Sci.* **70**, 1775–1779

48. Dang, C. V (2013) MYC, metabolism, cell growth, and tumorigenesis. *Cold Spring Harb. Perspect. Med.* **3**, 1–15

49. Souba, W. W., Strebel, F. R., Bull, J. M., Copeland, E. M., Teagtmeyer, H., and Cleary, K. (1988) Interorgan glutamine metabolism in the tumor-bearing rat. *J. Surg. Res.* **44**, 720–726

50. Chen, M. K., Espat, N. J., Bland, K. I., Copeland, E. M., and Souba, W. W. (1993) Influence of progressive tumor growth on glutamine metabolism in skeletal muscle and kidney. *Ann. Surg.* **217**, 655-66–7

51. van den Heuvel, A. P. J., Jing, J., Wooster, R. F., and Bachman, K. E. (2012) Analysis of glutamine dependency in non-small cell lung cancer. *Cancer Biol. Ther.* **13**, 1185–1194

52. Kung, H. N., Marks, J. R., and Chi, J. T. (2011) Glutamine synthetase is a genetic determinant of cell type-specific glutamine independence in breast epithelia. *PLoS Genet.* 10.1371/journal.pgen.1002229

53. Rajagopalan, K. N., and DeBerardinis, R. J. (2011) Role of Glutamine in Cancer: Therapeutic and Imaging Implications. *J. Nucl. Med.* **52**, 1005–1008

54. Manneville, S. E.-, and Hall, A. (2002) Rho GTPases in cell biology. *Nature*. **420**, 629–635

55. Vega, F. M., and Ridley, A. J. (2008) Rho GTPases in cancer cell biology. *FEBS Lett.* **582**, 2093–2101

56. Fritz, G., Brachetti, C., Bahlmann, F., Schmidt, M., and Kaina, B. (2002) Rho GTPases in human breast tumours: expression and mutation analyses and correlation with clinical parameters. *Br. J. Cancer*. **87**, 635–644

57. Mira, J.-P., Benard, V., Groffen, J., Sanders, L. C., and Knaus, U. G. (2000) Endogenous, hyperactive Rac3 controls proliferation of breast cancer cells by a p21-activated kinase-dependent pathway. *Proc. Natl. Acad. Sci.* **97**, 185–189

58. Suwa, H., Ohshio, G., Imamura, T., Watanabe, G., Arii, S., Imamura, M., Narumiya, S., Hiai, H., and Fukumoto, M. (1998) Overexpression of the rhoC gene correlates with progression of ductal adenocarcinoma of the pancreas. *Br. J. Cancer*. **77**, 147–52

59. Kleer, C. G., van Golen, K. L., Zhang, Y., Wu, Z.-F., Rubin, M. A., and Merajver, S. D. (2002) Characterization of RhoC expression in benign and malignant breast disease: a potential new marker for small breast carcinomas with metastatic ability. *Am. J. Pathol.* **160**, 579–84

60. Burbelo, P., Wellstein, A., and Pestell, R. G. (2004) Altered Rho GTPase signaling pathways in breast cancer cells. *Breast Cancer Res. Treat.* **84**, 43–48

61. Clark, E. a, Golub, T. R., Lander, E. S., and Hynes, R. O. (2000) Genomic Analysis of metastasis reveals an essential role for RhoC. *Nature*. **406**, 532–535

62. Wang, J., Erickson, J. W., Fuji, R., Ramachandran, S., Gao, P., Dinavahi, R., Wilson, K. F., Ambrosio, A. L. B., Dias, S. M. G., Chi, V., and Cerione, R. A. (2011) Targeting mitochondrial glutaminase activity inhibits oncogenic transformation. **18**, 207–219

63. Curthoys, N. P., Collins, F., and Watford, M. Regulation of glutaminase activity and glutamine metabolism

64. Kenny, J., Bao, Y., Hamm, B., Taylor, L., Toth, A., Wagers, B., and Curthoys, N. P. (2003) Bacterial expression, purification, and characterization of rat kidney-type mitochondrial glutaminase. *Protein Expr. Purif.* **31**, 140–148

65. Xiang, Y., Stine, Z. E., Xia, J., Lu, Y., O'Connor, R. S., Altman, B. J., Hsieh, A. L., Gouw, A. M., Thomas, A. G., Gao, P., Sun, L., Song, L., Yan, B., Slusher, B. S., Zhuo, J., Ooi, L. L., Lee, C. G. L., Mancuso, A., McCallion, A. S., Le, A., Milone, M.

C., Rayport, S., Felsher, D. W., and Dang, C. V. (2015) Targeted inhibition of tumor-specific glutaminase diminishes cell-autonomous tumorigenesis. *J. Clin. Invest.* **125**, 2293–2306

66. Szeliga, M., and Obara-Michlewska, M. (2009) Glutamine in neoplastic cells: Focus on the expression and roles of glutaminases. *Neurochem. Int.* **55**, 71–75

67. Huang, W., Choi, W., Chen, Y., Zhang, Q., Deng, H., He, W., and Shi, Y. (2013) A proposed role for glutamine in cancer cell growth through acid resistance. *Cell Res.* **23**, 724–727

68. Le, A., Lane, A. N., Hamaker, M., Bose, S., Gouw, A., Barbi, J., Tsukamoto, T., Rojas, C. J., Slusher, B. S., Zhang, H., Lisa, J., Liebler, D. C., Slebos, R. J. C., Lorkiewicz, P. K., Richard, M., Fan, T. W. M., and Dang, C. V (2013) Glucose-independent glutamine metabolism via TCA cycling for proliferation and survival in B cells. **15**, 110–121

69. Seltzer, M. J., Bennett, B. D., Joshi, A. D., Gao, P., Thomas, A. G., Ferraris, D. V, Tsukamoto, T., Rojas, C. J., Slusher, B. S., Rabinowitz, D., Dang, C. V, and Riggins, G. J. (2011) Inhibition of glutaminase preferentially slows growth of glioma cells with mutant IDH1. **70**, 8981–8987

70. Erickson, J. W., and Cerione, R. a (2010) Glutaminase: a hot spot for regulation of cancer cell metabolism? *Oncotarget*. **1**, 734–740

71. Gao, Ping, E. Al (2009) c-Myc suppression of miR-23a/b enhances mitochondrial glutaminase expression and glutamine metabolism. *Nature*. **458**, 762–765

72. Ahmad A. Cluntun, , Michael J. Lukey, , Richard A. Cerione, J. W. L. (2017) Glutamine Metabolism in Cancer: Understanding the Heterogeneity. *Cell Press*

73. Certo, M. T., Gwiazda, K. S., Kuhar, R., Sather, B., Mandt, T., Brault, M., Lambert, A. R., Baxter, S. K., Ryu, B. Y., Kiem, H., Gouble, A., and Paques, F. (2013) The metabolic profile of tumors depends on both the responsible genetic lesion and tissue type. **9**, 973–975

74. Lukey, M. J., Greene, K. S., Erickson, J. W., Wilson, K. F., and Cerione, R. A. (2016) The oncogenic transcription factor c-Jun regulates glutaminase expression and sensitizes cells to glutaminase-targeted therapy. *Nat. Commun.* **7**, 11321

75. Nicolay, B. N., Gameiro, P. A., Tschöp, K., Korenjak, M., Heilmann, A. M., Asara, J. M., Stephanopoulos, G., Iliopoulos, O., and Dyson, N. J. (2013) Loss of RBF1 changes glutamine catabolism. *Genes Dev.* **27**, 182–196

76. Reynolds, M. R., Lane, A. N., Robertson, B., Kemp, S., Hill, B. G., Dean, D. C., and Clem, B. F. (2014) Control of Glutamine Metabolism By the Tumor

Suppressor Rb. **33**, 556–566

77. Nandakumar, R., Wakayama, M., Nagano, Y., Kawamura, T., Sakai, K., and Moriguchi, M. (1999) Overexpression of salt-tolerant glutaminase from Micrococcus luteus K-3 in Escherichia coli and its purification. *Protein Expr. Purif.* **15**, 155–161

78. Nandakumar, R., Yoshimune, K., Wakayama, M., and Moriguchi, M. (2003) Microbial glutaminase: Biochemistry, molecular approaches and applications in the food industry. *J. Mol. Catal. B Enzym.* **23**, 87–100

79. Yoshimune, K., Shirakihara, Y., Shiratori, A., Wakayama, M., Chantawannakul, P., and Moriguchi, M. (2006) Crystal structure of a major fragment of the salt-tolerant glutaminase from Micrococcus luteus K-3. *Biochem. Biophys. Res. Commun.* **346**, 1118–1124

80. Paetzel, M., Danel, F., de Castro, L., Mosimann, S. C., Page, M. G., and Strynadka, N. C. (2000) Crystal structure of the class D beta-lactamase OXA-10. *Nat. Struct. Biol.* **7**, 918–925

81. Strynadka, N. C. J., Adachi, H., Jensen, S. E., Johns, K., Sielecki, A., Betzel, C., Sutoh, K., and James, M. N. G. (1992) Molecular structure of the acyl-enzyme intermediate in β-lactam hydrolysis at 1.7 Å resolution. *Nature*. **359**, 700–705

82. MPinkus, L. (2018) Allosteric regulation of the cancer association. *Methods in Enzymology* **357**, 700-705

83. Warner, W. A., Sanchez, R., Dawoodian, A., Li, E., and Momand, J. (2013) Dibenzophenanthridines as inhibitors of glutaminase C and cancer cell proliferation. **80**, 631–637

84. Katt, W.P., Cerione,R. A. (2015) Glutaminase regulation in cancer cells: a druggable chain of events. *Drug Discov. Today* **19**, 450–457

85. Stalnecker, C. A., Ulrich, S. M., Li, Y., Ramachandran, S., McBrayer, M. K., DeBerardinis, R. J., Cerione, R. A., and Erickson, J. W. (2015) Mechanism by which a recently discovered allosteric inhibitor blocks glutamine metabolism in transformed cells. *Proc. Natl. Acad. Sci.* **112**, 394–399

86. Windmueller, G., and Chem, J. B. (1977) Phosphate-Dependent Glutaminase of Small Intestine : Localization and Role in Intestinal Glutamine Metabolism ’ take and metabolism by the small intestine in rats and in a in rats , intestine is the only tissue which exhibits appreciable annual meeting

87. Robinson, M. M., McBryant, S. J., Tsukamoto, T., Rojas, C., Ferraris, D. V, Hamilton, S. K., Hansen, J. C., and Curthoys, N. P. (2007) Novel mechanism of inhibition of rat kidney-type glutaminase by bis-2-(5-phenylacetamido-1,2,4-thiadiazol-2-yl)ethyl sulfide (BPTES). *Biochem. J.* **406**, 407–14

88. Campos-Sandoval, J. A., López de la Oliva, A. R., Lobo, C., Segura, J. A., Matés, J. M., Alonso, F. J., and Márquez, J. (2007) Expression of functional human glutaminase in baculovirus system: affinity purification, kinetic and molecular characterization. *Int. J. Biochem. Cell Biol.* **39**, 765–773

89. Delabarre, B., Gross, S., Fang, C., Gao, Y., Jha, A., Jiang, F., Song J., J., Wei, W., and Hurov, J. B. (2011) Full-length human glutaminase in complex with an allosteric inhibitor. *Biochemistry*. **50**, 10764–10770

90. Suzuki, S., Tanaka, T., Poyurovsky, M. V., Nagano, H., Mayama, T., Ohkubo, S., Lokshin, M., Hosokawa, H., Nakayama, T., Suzuki, Y., Sugano, S., Sato, E., Nagao, T., Yokote, K., Tatsuno, I., and Prives, C. (2010) Phosphate-activated glutaminase (GLS2), a p53-inducible regulator of glutamine metabolism and reactive oxygen species. *Proc. Natl. Acad. Sci.* **107**, 7461–7466

91. Godfrey, S., Kuhlenschmidt, T., and Curthoys, P. (1977) Correlation between activation and dimer formation of rat renal phosphate-dependent glutaminase. *J. Biol. Chem.* **252**, 1927–1931

CHAPTER 2

MECHANISTIC BASIS OF GLUTAMINASE ACTIVATION: A KEY ENZYME THAT PROMOTES GLUTAMINE METABOLISM IN CANCER CELLS[1]

ABSTRACT

Glutamine-derived carbon becomes available for anabolic biosynthesis in cancer cells via the hydrolysis of glutamine to glutamate, as catalyzed by GAC, a splice variant of kidney-type glutaminase (GLS). Thus, there is significant interest in understanding the regulation of GAC activity, with the suggestion being that higher order oligomerization is required for its activation. We used x-ray crystallography, together with site directed mutagenesis, to determine the minimal enzymatic unit capable of robust catalytic activity. Mutagenesis of the helical interface between the two pairs of dimers comprising a GAC tetramer yielded a non-active, GAC dimer whose x-ray structure displays a stationary loop ('activation loop') essential for coupling the binding of allosteric activators like inorganic phosphate to catalytic activity. Further mutagenesis that removed constraints on the activation loop yielded a constitutively active dimer, providing clues regarding how the activation loop communicates with the active site, as well as with a peptide segment that serves as a 'lid' to close off the

[1] This chapter was previously published as: Mechanistic basis of glutaminase activation: Li Y, Erickson JW, Stalnecker CA, Katt WP, Huang Q, Cerione RA, Ramachandran S. A key enzyme that promotes glutamine metabolism in cancer cells J. Biol. Chem. (2016) 291 (40), 20900-20910.

active site following substrate binding. Our studies show that the formation of large GAC oligomers is not a pre-requisite for full enzymatic activity. They also offer a mechanism by which the binding of activators like inorganic phosphate enables the activation loop to communicate with the active site to ensure maximal rates of catalysis, and promotes the opening of the lid to achieve optimal product release. Moreover, these findings provide new insights into how other regulatory events might induce GAC activation within cancer cells.

INTRODUCTION

In order to accommodate the cellular changes underlying tumor establishment and maintenance, metabolic remodeling occurs, resulting in dramatic increases in aerobic glycolysis (1-5; i. e., the "Warburg effect"). This is often accompanied by an acquired reliance on glutamine as a carbon source for anabolic processes such as fatty acid and nucleotide synthesis, as well as serving as a fuel for the tricarboxylic acid cycle. The marked increases in glutamine metabolism in tumor cells represent a critical difference in the physiology of normal and transformed tissues that may offer novel therapeutic targets for the treatment of cancer. Transcriptional and post-translational responses to transformation that determine the glutamine dependence of certain tumors are therefore of great interest as they identify microscopic changes that give rise to "glutamine addicted" neoplasms (6).

One such change is the increased expression and catalytic activity of mitochondrial kidney-type glutaminase (GLS) (7,8). Glutamine is the most abundant

amino acid in blood serum, thus providing a ready precursor for macromolecular synthesis after conversion to glutamate, as catalyzed by GLS. Thus, GLS provides a molecular gateway to glutamine-derived biosynthesis within cells undergoing Warburg glycolysis, and in doing so offers a potentially attractive target for inhibiting cancer cell growth (9,10). The two alternatively spliced isoforms of GLS, most often designated as KGA and GAC, account for the majority of glutamine to glutamate conversion in cells, with the over-expression of GAC being observed in a number of cancer cell types (11). The elevated activity of GLS has been linked to oncogenes such as Myc (12,13) and Ras (14), as well as to the hyper-activation of Rho GTPases (9,15).

It has been reported that oligomerization is both necessary and sufficient for activating GAC, with the formation of GAC tetramers and higher order oligomers being suggested to be essential for full enzymatic activity (16-18). In order to further examine the mechanistic basis for the activation of this key metabolic enzyme, we have made use of structural analysis, determining the x-ray crystal structures for both wild-type GAC and a stable GAC dimer, together with multi-angle light scattering size determinations, mutagenesis and biochemical assays of enzyme activity. By combining these approaches, we were able to design a GAC dimer that was constitutively active, thus demonstrating that higher order oligomerization is not an absolute requirement for maximal catalysis. Closer examination of this constitutively active GAC dimer allowed us to introduce specific mutations that revealed the intramolecular coupling of 1) an activation loop that mediates phosphate-stimulated activity and represents the binding site for a small molecule allosteric inhibitor (19-21), and 2) a peptide 'lid'

that governs product release from the GAC catalytic site. Together these coupled sites provide for a tiered regulation of this important metabolic enzyme, which offers new possibilities for targeted drug therapy of glutamine-addicted cancer cells.

EXPERIMENTAL PROCEDURES

Recombinant GAC preparations

Human GAC (residues 73 to 598) was cloned into the pQE80 vector (Qiagen) containing an N-terminal histidine (His)-tag. The recombinant plasmid was transformed into the E. coli strain BL21(DE3) and then purified using Ni^{2+}-affinity and gel filtration chromatography. The purified protein was snap frozen and stored in gel filtration buffer (5 mM Tris-HCl (pH 7.5) and 0.15 M NaCl) at -80°C.

A mouse kidney type isoform 2 (GAC, NP_001106854.1) plasmid (residues 73-603 for GAC) was cloned into a pET28a vector containing an N-terminal histidine (His)-tag and thrombin cleavage site. The protein was expressed in E. coli and then purified using Co2+ affinity beads (Clontech), followed by His-tag cleavage with human thrombin (Haemetologic Technologies) overnight at 4°C, and further purified by anion exchange (GE Healthcare) and gel filtration chromatography. Purified GAC was snap frozen and stored in a high salt-containing buffer (20 mM Tris-HCl, pH 8.5, 500 mM NaCl, 1 mM NaN3) at -80°C. The human wild-type GAC and the mouse GAC(D391K) mutant were used for crystallization and structural analyses. The mouse GAC was used for all in vitro assays, whereas the human GAC was used for cell transfections and immunocytochemistry. The mouse numbering is used throughout to minimize confusion.

Crystallization, x-ray data collection, and structure determinations

Crystals of human GAC (20 mg/ml) were grown using the hanging drop method at 18°C by mixing 2 µl of the protein solution with 2 µl of the reservoir solution (12% PEG6000 (w/v), 1.0 M LiCl, 1% DMSO (v/v) and 0.1 M Tris-HCl buffer, pH 8.5). Crystals appeared after 24 hours and reached a size of 100x100x200 µm3 after 7 days. Crystals were cry-frozen under high pressure before data collection (33).

For the GAC(D391K) mutant (5 mg/ml), the primary screening was performed on the Phoenix liquid handling system using the Qiagen ComPAS screening kit. Crystallization was performed in 50 mM Tris-HCl, pH 9.0, 9% PEG 10,000, and 100 mM NaCl. The sitting drop vapor diffusion technique was used (4 µl of 5 mg/ml protein plus 4 µl precipitant). Rod shaped crystals appeared in about 3-4 days, and grew for approximately 10 days.

All Datasets were collected at the Cornell High Energy Synchrotron Source (CHESS, Ithaca, NY) on beam lines A1 and F1. The coordinates of the glutaminase domain of human GAC (PDB id: 3CZD) were used as a search model for molecular replacement for human GAC, and those of chain A from mouse glutaminase (3SS5) were used for GAC(D391K). Data reduction was performed prior to phasing and refinement, which were carried out with the software packages HKL2000, CCP4, and COOT.

Glutaminase activity assays

Assays used to evaluate the activity of GAC mutants followed a two-step protocol as described previously (17). Typically, GAC was added at indicated concentrations to 100 µl of a solution containing 20 mM glutamine, 65 mM Tris-acetate, pH 8.6, and 0.2 mM EDTA, in either the presence or absence of the anionic activator K_2HPO_4, and incubated at room temperature for 10 minutes. The reaction was quenched by the addition of ice-cold hydrochloric acid to a final concentration of 0.3 M. An aliquot of this was added to a buffer (glutamate dehydrogenase assay

buffer: 160 mM Tris-HCl (pH 9.4)) containing 0.35 mM adenosine diphosphate, 1.7 mM nicotinamide adenine dinucleotide (NAD) and 6.3 U/mL glutamate dehydrogenase) in a UV-transparent Costar 96well plate (Corning), and incubated at room temperature for 50 minutes. The absorbance at 340 nm was measured and converted to glutamate concentrations using the extinction coefficient for the conversion of NAD to NADH of 6220 M-1cm-1.

Cell culture and immunocytochemistry

NIH-3T3 cells were transformed by oncogenic Dbl as previously described (24). The cells were transfected with full length wild-type human GAC (reference sequence NM_001256310.1) or with the constitutively active GAC triple mutant (GAC(K316Q/K325A/D391K)) using Lipofectamine (Life Technologies). SKBR3 human breast cancer cells were obtained from ATTC and cultured according to supplier specifications. The breast cancer cells were transfected with full length human GAC, Cterminally tagged with the V5 epitope, using Lipofectamine. Immunocytochemistry was performed 48 hours post transfection by fixation (10 minutes) in 3.7% CH2O in PBS, followed by 5 minutes of permeabilization in PBS supplemented with 0.05% TX-100. Cells were rinsed 3X in PBS and incubated with mouse anti-V5 (ThermoFisher) 1:100 in PBS and rabbit anti-DLST (Cell Signaling; D2281) 1:50 for 3 hours at room temperature, followed by PBS washing (3X). Secondary fluorescently conjugated antibodies (Invitrogen) were used to visualize protein localization with a Zeiss Axioplot fluorescence microscope.

Size exclusion chromatography with coupled multi-angle light scattering (SEC-MALS)

Purified GAC and GAC mutants were examined using multi-angle light scattering (MALS) as previously described by Moller et al. (17). Briefly, 50 µL samples of 5 or 10 mg/mL GAC were injected onto a WTC-030S5 size exclusion column (Wyatt Technology) coupled to a static 18-angle light scattering detector (DAWN HELEOS-II)

and a refractive index detector (OptiLab T-rEX, Wyatt Technology) kept at 23°C. The size exclusion column was equilibrated with 20 mM Tris-HCl, pH 8.5, and 200 mM NaCl, with or without 50 mM K_2HPO_4. The flow rate was normally kept at 1 mL/min for all MALS analyses. RMS radius and mass distribution (polydispersity) were analyzed using the ASTRA software and monomeric BSA (Sigma) was used to normalize the light scattering signal.

RESULTS

Disruption of the GAC helical interface results in an inactive dimer

Previous studies have suggested that mammalian glutaminases exist as dimers in their inactive state and need to oligomerize into tetramers and higher order oligomers to be capable of catalytic activity (1618). Several x-ray crystal structures of wild-type glutaminase, as well as our own analysis of human GAC, reveal the presence of four molecules in the asymmetric unit (**Fig.2.1 A**). This quaternary assembly is formed by the association of two inactive GAC dimers and involves two sets of interfaces. One interface is made up of the contacts between monomers i and ii, and those between monomers iii and iv (**Fig.2.1 A**), which buries considerably more surface area than the second interface between monomers i and iii, and monomers ii and iv. The latter pairing of dimers to form a tetramer has been suggested to be a critical step in the stimulation of glutaminase activity by the allosteric activator, inorganic phosphate (21). The GAC dimer-dimer interface results from the interaction between two pairs of anti-parallel α-helices contributed by two monomers that are twisted 180^o relative to one another. Closer inspection of the interactions between the two helices, referred to as the interface helices, reveals the presence of a salt bridge between aspartic acid 391 and lysine 401 (**Fig.2.1 A, inset**). The anti-parallel configuration of the helices therefore consists of four of these interactions for each

GAC tetramer. This observation led us to hypothesize that the disruption of this salt bridge by mutagenesis might destabilize the tetrameric assembly and yield a GAC species trapped as a dimer.

In order to test this idea, we mutated aspartic acid 391 to a lysine residue (GAC(D391K)), thereby introducing an electrostatic repulsion between the newly introduced lysine 391 residue and the wild-type lysine 401 residue. The GAC(D391K) mutant was expressed in E. coli to levels comparable to that of wild-type GAC and its oligomeric status was examined using SEC-MALS. Initial SEC-MALS analysis of wild-type GAC indicated the presence of a heterogeneous species with a calculated molecular mass that was intermediate between that of a dimer (~115 kDa) and a tetramer (~230 kDa; **Fig.2.1 B**). The apparent molecular mass for wild-type GAC, as determined by SEC-MALS, increased with increasing protein concentration suggesting the rapid inter-conversion between the dimeric and tetrameric GAC species with respect to the timescale of the gel filtration experiment. In contrast, the GAC(D391K) mutant behaved as a homogeneous species with a molecular weight of ~115 kDa, corresponding to that of a GAC dimer (**Fig.2.1 B**), which persisted at high concentrations of GAC(D391K) (>100 μM).

Wild-type GAC, at a concentration of 50 nM, exhibits low enzymatic activity in the absence of any activators such as inorganic phosphate, although, its activity increases with the addition of inorganic phosphate in a dose-dependent manner (**Fig.2.1 C, red**). However, the GAC(D391K) mutant fails to exhibit detectable activity, even when assayed at inorganic phosphate concentrations as high as 100 mM (**Fig.2.1 C, black**).

Figure 2.1 A single mutation in the helical interface of glutaminase results in an inactive, dimeric form of the enzyme. A, X-ray crystal structure of wild-type human GAC (PDB: 5D3O) showing the antiparallel salt bridge at the helical interface of two dimers (inset). **B**, SEC-MALS analysis of wild-type GAC and GAC(D391K). The signal from the 90° scattering detector is shown as red (wild-type GAC) and green (GAC(D391K)) lines [Left, Y axis]. Arrows indicate the average molecular weight as calculated (each second) across the protein elution peak [Right, Y axis]. Predicted molecular weights based on the primary sequences for the GAC dimer and the tetramer are indicated as horizontal dashed lines. Protein samples (100 μM) were injected into the SEC-MALS system for analysis. **C**, Comparison of specific activities of 50 nM wild-type GAC or GAC(D391K) with increasing phosphate concentration. The GAC catalyzed conversion of glutamine to glutamate was assayed as described in 'Experimental Procedures'. Results are representative of three independent titrations.

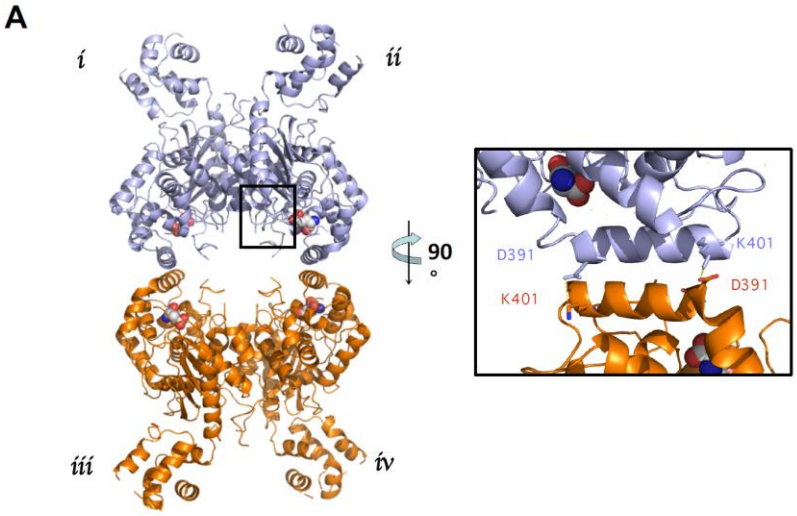
A
i
ii
iii
iv
90
°
D391
K401
K401
D391

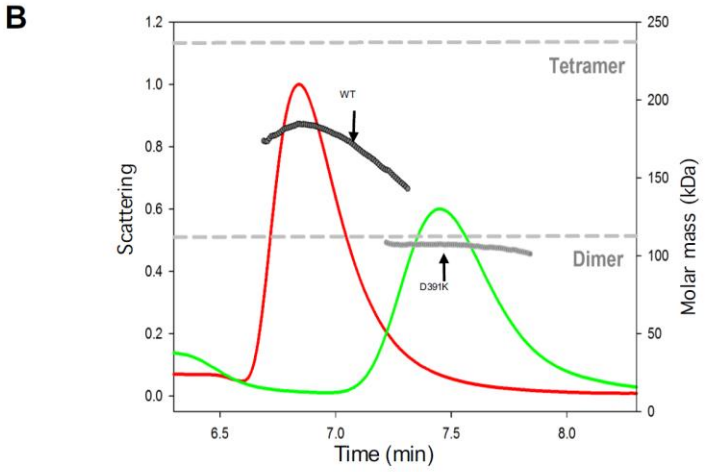
B
Tetramer
Dimer
WT
D391K
Scattering
Molar mass (kDa)
Time (min)

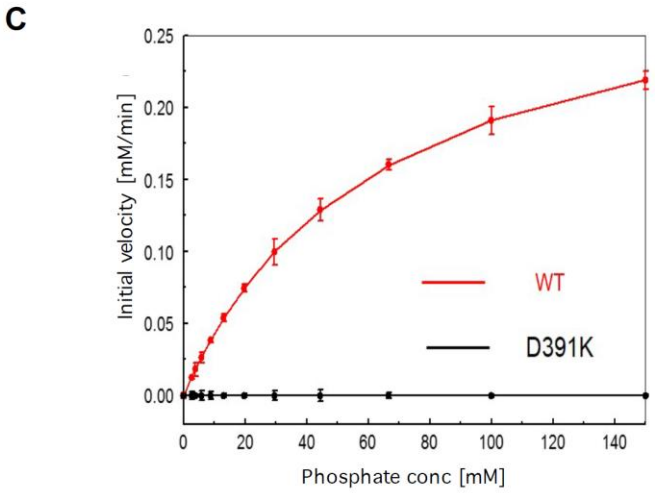
C
Initial velocity [mM/min]
WT
D391K
Phosphate conc [mM]

The x-ray crystal structure of the GAC(D391K) mutant reveals a stationary activation loop in contrast to wild-type GAC structures

Crystals of GAC(D391K) were grown under conditions that were markedly different from those for the crystallization of wild-type GAC, and were observed to diffract to a resolution of 2.3 Å (see Table). The structure for GAC(D391K) was solved by molecular replacement, using the x-ray structure for wildtype GAC as a search model (**Fig.2.2 A**). Unlike the structure for wild-type GAC, only two molecules of GAC(D391K) were present in the asymmetric unit, consistent with the homogeneous dimeric species observed in the SEC-MALS experiments (**Fig.2.1 B**). The overall three dimensional structures of the individual monomers in GAC(D391K) are highly similar to those for wild-type GAC, with the calculated RMSD value being 0.55 Å. Of particular interest was the essentially identical positioning of the active site residues in wild-type GAC and the dimeric, inactive GAC(D391K) mutant (**Fig.2.2 B**), suggesting that wild-type GAC, while a tetramer in the x-ray crystal structure, apparently is in a catalytically inactive state.

In the x-ray crystal structure of the GAC(D391K) mutant, a peptide loop was observed that extends from glycine 315 to methionine 338, with the central portion (leucine 321 to leucine 326) being unresolved in the structure of wild-type GAC. Interestingly, an allosteric inhibitor of GAC, BPTES, was recently co-crystallized with GAC (20,22) and shown to interact with this loop, forming a bridge between two dimers that stabilizes an inactive tetramer (18,23). When comparing the backbone

structures of wild-type GAC and the GAC(D391K) mutant, the calculated RMSD plot revealed that the largest difference between these structures exists for residues glycine 320 and phenylalanine 327, which are present at either end of the unresolved stretch of residues (designated with the dashed line in **Fig.2.2 C**). Thus, the structure of the GAC(D391K) mutant revealed that this loop, henceforth referred to as the activation loop, is less flexible in the dimeric structure, much like the case for the BPTES inhibited structure, whereas, this region of GAC is not resolvable in the wildtype enzyme crystal structures.

Mutation of lysine 325 in the GAC(D391K) background results in a constitutively active enzyme

The fact that the binding of BPTES to the activation loop of GAC results in an inactive enzyme suggests that conformational changes in this loop are important for enzymatic activity. In an effort to identify the individual loop residues important for activity, alanine-scanning mutagenesis was carried out on residues leucine 321 to phenylalanine 327 (**Fig.2.3 A**). Each loop mutation was made in the GAC(D391K) background, and then assayed for enzyme activity in the presence and absence of 50 mM inorganic phosphate. Alanine substitution of arginine 322, phenylalanine 323, asparagine 324 and leucine 326 within the GAC(D391K) background yielded GAC double mutants that were catalytically inactive (data not shown). Mutation of either leucine 321 or phenylalanine 327 to alanine resulted in an enzyme with enhanced

Figure 2.2 Structure determination of GAC(D391K) and comparison with wild-type GAC coordinates. A, Ribbon depiction of GAC(D391K) showing the location of the active site based on the structure for the product of the GAC-catalyzed reaction, glutamate (yellow), bound to wild-type GAC (PDB: 3SS5), and the resolved activation loop (colored in green indicated with black arrows) near the helical interface. **B**, Details of the glutamine/glutamate binding site (bound glutamate is shown) where wild-type GAC tetramer (orange) and GAC(D391K)-dimer (blue) contact residues are superimposed. **C**, RMSD plot of carbon atom coordinates in the two crystalline forms of GAC illustrating the apparent flexibility of the activation loop in wild-type but not GAC(D391K) dimeric GAC. The dashed line indicates the region lacking resolvable electron density in the tetrameric structure. Differences in the backbone structures also occur at the helical interface and the substrate 'lid' (see text).

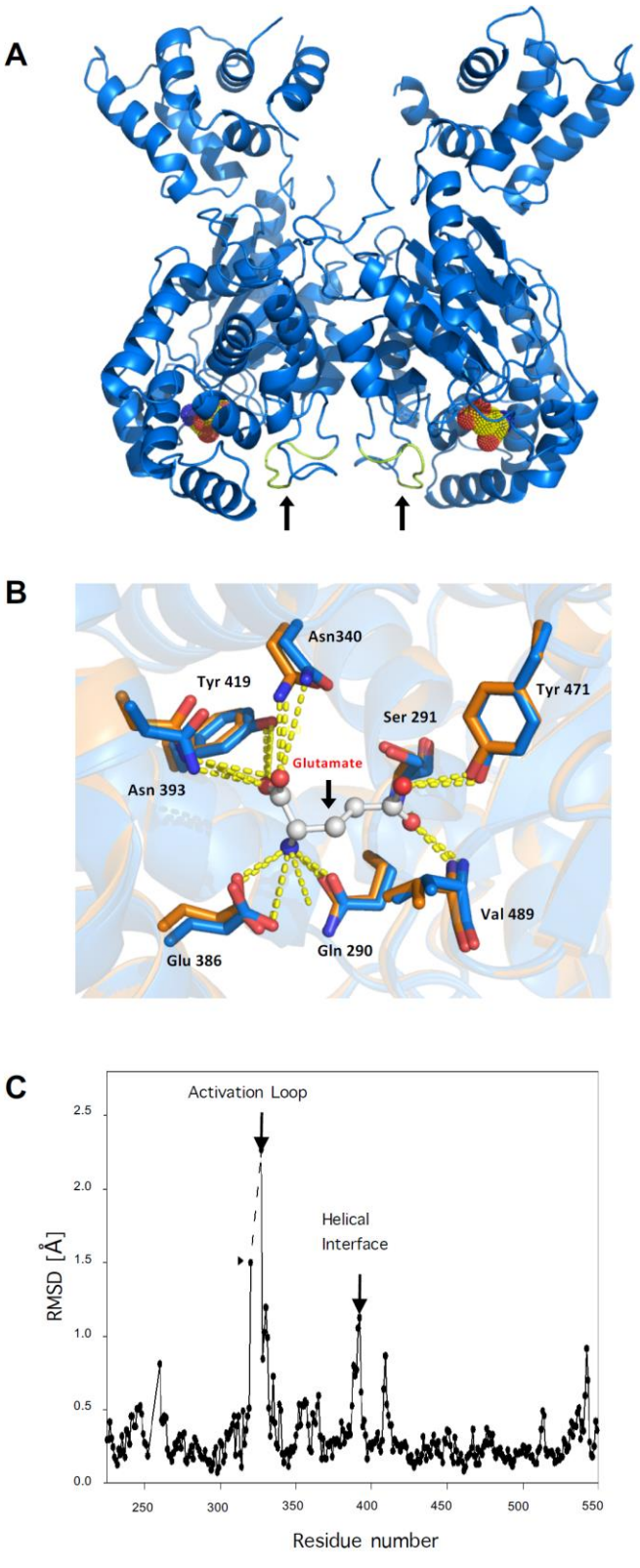
A
B
Asn340
Tyr 419
Tyr 471
Ser 291
Glutamate
Asn 393
Val 489
Gln 290
Glu 386
C
Activation Loop
Helical
Interface
RMSD [Å]
2.5
2.0
1.5
1.0
0.5
0.0
250
300
350
400
450
500
550
Residue number

basal activity (i.e., measured in the absence of inorganic phosphate), compared to GAC(D391K), that was ~50% and 90% of the basal activity measured for wild-type GAC (**Fig.2.3 B**). However, the mutation of lysine 325 to alanine within the GAC(D391K) background yielded an enzyme, GAC(K325A/D391K), with basal activity comparable to that for wild-type GAC measured in the presence of 50 mM inorganic phosphate, with no additional stimulation occurring upon phosphate addition (**Fig.2.3 B**).

Ferreira et al. had previously reported that mutating lysine 325 to alanine in a wild-type GAC background resulted in an enzyme that was active in the absence of inorganic phosphate, but formed a large higher order oligomer via the interactions of the N-terminal domains of GAC tetramers (18). The formation of this higher order GAC oligomer was suggested to be a prerequisite for full enzyme activity. Analysis of the GAC(K325A/D391K) double mutant at a concentration of ~100 µM by SEC-MALS revealed a poly-disperse species with a molecular mass intermediate between the predicted size of a dimer and a tetramer (**Fig.2.3 C**). Upon ectopically expressing the GAC(K325A/D391K) double mutant in the SKBR3 human breast cancer cell line, immunofluorescence microscopy showed the presence of rod-like bodies (**Fig.2.3 D**, **top panel**) that did not show an exact co-localization with the mitochondrial marker DLST (**Fig.2.3 D, bottom panel**). These micron size structures may incorporate endogenous GAC as well, since we observed less total GAC in the mitochondria of cells ectopically expressing the GAC(K325A/D391K) double mutant (data not shown). Attempts at isolating cell clones that stably expressed the constitutively active forms of GAC were unsuccessful, suggesting that the higher oligomeric form of GAC is toxic or at least inhibitory for cell growth.

Data collection and refinement statistics

	GAC D391K
Data collection	
Space group	P21212
Cell dimensions	1
a, b, c (Å)	85.2, 101.4, 145.2
α, β, γ (°)	90.0, 90.0, 90.0
Resolution (Å)	2.3
I/σI	7.2/3.9
Completeness (%)	92.87
Redundancy	7.3
Refinement	
Resolution (Å)	50.0-2.30
No. reflections	51086
Rwork/Rfree	0.19641/0.22761
No. atoms	
protein	6669
water	172
Average B factor (Å^2)	30.712
r.m.s. deviations	
Bond lengths (Å)	0.001
Bond angles (°)	1.4

Figure 2.3 Alanine scanning of the activation loop reveals lysine 325 as a critical residue for GAC enzyme activity. A, Numbered residues constituting the activation loop and their proximity to the active site. **B**, Alanine substitution in the inactive dimeric GAC(D391K) background and the resulting effects on glutaminase activity in the presence or absence of 50 mM phosphate. The specific activity of all recombinant proteins (50 nM) with or without 50 mM phosphate was tested and the relative activity normalized with respect to wild-type GAC. Results are the average of three independent determinations with error bars representing standard error. **C**, SEC-MALS determination of GAC(K325A/D391K) oligomer size distribution demonstrates that the activation loop mutant induces the formation of a heterogeneous population of tetramers. The signals from the 90° scattering detector are shown as red (GAC(K325A/D391K)) and green (GAC(D391K)) lines [Left, Y axis]. Arrows indicate the average molecular weight as calculated (each second) across the protein elution peak [Right, Y axis]. Theoretical molecular weights based on the primary sequence for the dimer and the tetramer are indicated as horizontal dashed lines. **D**, Subcellular localization of V5-tagged GAC(K325A/D391K) (green; upper panel) compared to the mitochondrial marker, DLST (red; lower panel) in SKBR3 cells. Arrows highlight macroscopic oligomeric forms of GAC(K325A/D391K) or the distribution of the mitochondrial marker DLST.

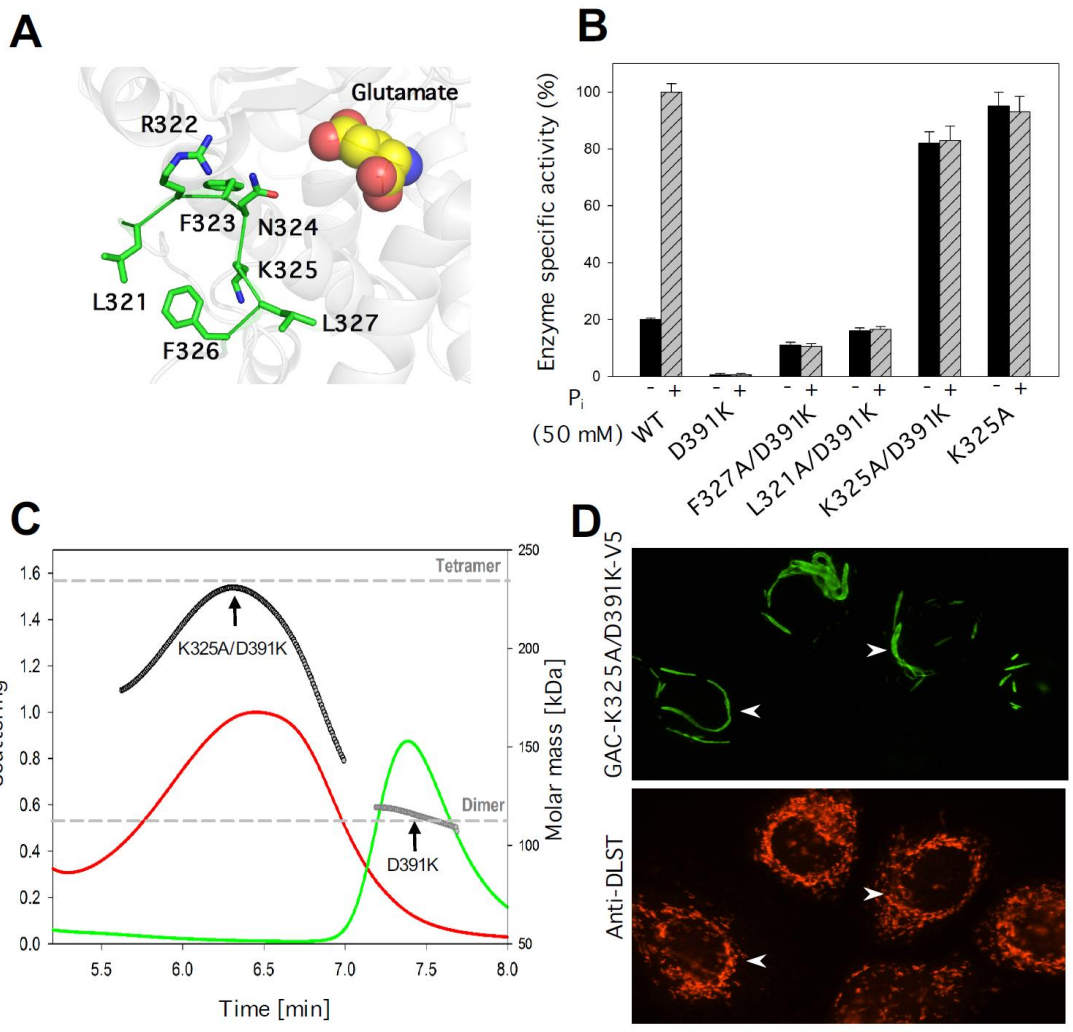
A
Glutamate
R322
F323
N324
K325
L321
L327
F326
B
Enzyme specific activity (%)
100
80
60
40
20
0
- + - + - + - + - + - +
Pi
(50 mM)
WT
D391K
F327A/D391K
L321A/D391K
K325A/D391K
K325A
C
Tetramer
Dimer
K325A/D391K
D391K
Scattering
Molar mass [kDa]
Time [min]
1.6
1.4
1.2
1.0
0.8
0.6
0.4
0.2
0.0
250
200
150
100
50
5.5
6.0
6.5
7.0
7.5
8.0
D
GAC-K325A/D391K-V5
Anti-DLST

Generation of a constitutively active GAC dimer

The mutation of lysine 316 to glutamine in GAC(K325A) was suggested to prevent the formation of large oligomers of GAC (18). Therefore, we introduced the K316Q substitution into the GAC(K325A/D391K) background and found that it exhibited a level of activity comparable to that of either the GAC(K325A/D391K) double mutant or wild-type GAC in the presence of 50 mM inorganic phosphate (**Fig.2.4A**). Analysis of the GAC(K316Q/K325A/D391K) triple mutant by SEC-MALS showed the presence of a single mono-disperse species with a molecular mass corresponding to a dimer (**Fig.2.4 B; "triple"**). Moreover, the triple mutant is able to localize properly to the mitochondria in SKBR3 cells, similar to what we observe for wild-type GAC (compare top to bottom micrographs in **Fig.2.4 C, left panel**). Thus, we have been able to engineer a dimeric form of GAC, which exhibits constitutive enzyme activity that is completely uncoupled from the formation of higher oligomeric species.

We compared the ability of the constitutively active GAC(K316Q/K325A/D391K) triple mutant, versus wild-type GAC, to enhance the transforming activity induced by the hyper activation of Rho GTPases due to the expression of the oncogenic Rho-GEF, Dbl (for Diffuse B cell lymphoma) (24). Previously, we showed that the co-expression of wild-type GAC with the activated Cdc42(F28L) mutant displayed a marked synergy in promoting NIH-3T3 cells to form foci (9). Similar results are obtained upon co-expressing wild-type GAC with oncogenic Dbl (**Fig.2.4 C, right panel**). However, surprisingly, given the increased glutamine dependence induced by Dbl expression (15), the constitutively active GAC triple mutant did not significantly enhance the transformation potential of the oncogenic form of Dbl relative to wild-type GAC (**Fig.2.4 C, right panel**).

Communication between the activation loop and the enzyme catalytic site

Serine 291 and lysine 294 are part of a conserved SXXK motif, part of the catalytic triad present in the active sites of all glutaminases that are essential for enzymatic activity (9). Therefore, we examined whether the communication between these active site residues and the activation loop could be altered by mutating residues within an intervening connecting peptide segment (i.e., serine 291 to lysine 325; **Fig.2.4 D** shows this segment for mouse GAC aligned with sequences from additional solved x-ray crystal structures of glutaminase enzymes). Within this connecting segment is a highly conserved glycine (residue 320 indicated by the red arrow in **Fig.2.4 D** and **E**), which we changed to a proline to restrict the rotational freedom of the connecting segment, to see whether flexibility at this site is necessary for enzyme activation. When this substitution was made within a wild-type GAC background, there was a complete loss of both basal and phosphate stimulated enzymatic activity (**Fig.2.4 F**). Similarly, the G320P substitution within the constitutively active GAC(K325A) mutant markedly reduced enzymatic activity, both in the presence and absence of the allosteric activator, inorganic phosphate (**Fig.2.4 F**). Similar results were obtained with a more conservative substitution (G320A), confirming a critical role for this peptide segment in linking the activation loop to the site of catalysis.

Figure 2.4 Uncoupling the necessity of GAC oligomerization for enzyme activation and the connection between the activation loop and the glutaminase active site.

A, Engineering a constitutively active dimeric form of GAC. The specific activity of each recombinant GAC (50 nM) was assayed with or without 50 mM phosphate. **B**, SEC-MALS analysis of GAC(D391K), GAC(K325A/D391K), and the triple mutant GAC(K316Q/K325A/D391K). The signals from the 90° scattering detector are shown as red (GAC(K325A/D391K)), green (GAC(D391K)), and blue (GAC(K316Q/K325A/D391K)) lines [Left, Y axis]. Arrows are pointing to the average molecular weight, which is calculated (each second) across the protein elution peak [Right, Y axis]. Theoretical molecular weight based on primary sequence for the dimer and tetramer are indicated as horizontal dashed lines. **C**, Subcellular localization of V5-tagged wild-type GAC or the triple mutant GAC(K316Q/K325A/D391K) (green; left panels) compared to the mitochondrial marker, DLST (red; right panels) in SKBR3 cells. The K316Q substitution restores wildtype mitochondrial localization to GAC. Right panel: Dbl-induced focus formation is enhanced by co-expression of either GAC(WT) or GAC(K316Q/K325A/D391K). NIH-3T3 cells were co-transfected with the indicated amounts of Dbl plasmid and 1 μg of either GAC(WT) or mutant plasmid. Cells were grown for 12 days, fixed with 3.7% formaldehyde in PBS and stained with 1% crystal violet in methanol to visualize foci. **D**, Primary sequence alignment of several bacterial glutaminases whose structures are known illustrating the conservation of the transducing peptide containing the active site serine 286 (black arrow), glycine 320

(red arrow), and lysine 325 in mammalian glutaminase (green arrow). **E**, Relative positions of the catalytic site serine 291 to the activation loop residue lysine 325, and glycine 320 within the connecting peptide between serine 291 and lysine 325. Colored arrowheads point to residues and correspond to those indicated in the sequence alignment shown in **D.** **F**, Glycine 320 is critical for activation loop communication to serine 291 in the GAC active site. The specific activity of all the proteins at 50 nM was assayed with and without added phosphate (50 mM) and standard errors are based on three independent experiments.

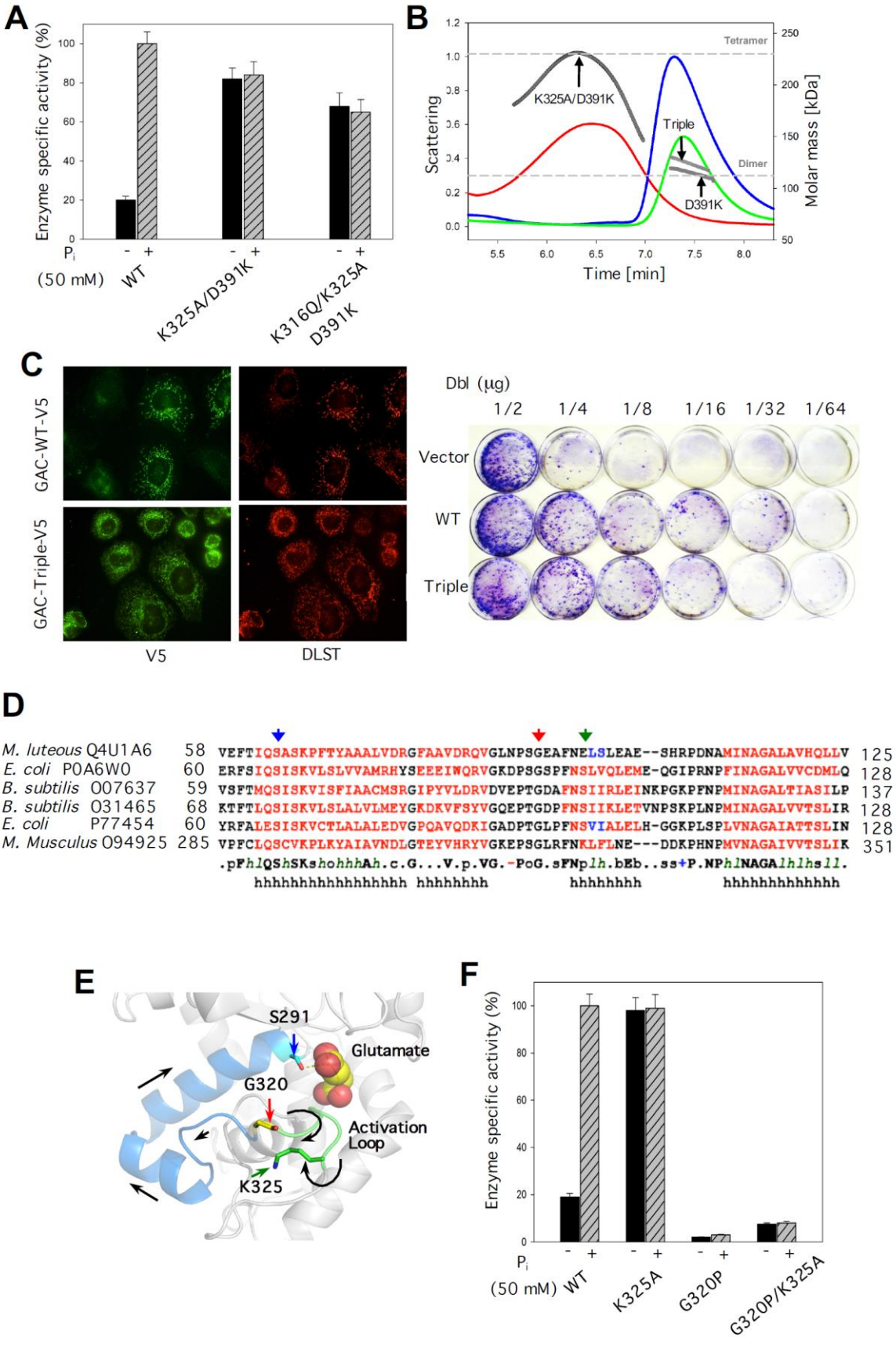
A
Enzyme specific activity (%)
100
80
60
40
20
0
Pi
- +
- +
- +
(50 mM)
WT
K325A/D391K
K316Q/K325A
D391K
B
Scattering
Molar mass [kDa]
Tetramer
Dimer
K325A/D391K
Triple
D391K
Time [min]
C
GAC-WT-V5
GAC-Triple-V5
V5
DLST
Dbl (µg)
1/2
1/4
1/8
1/16
1/32
1/64
Vector
WT
Triple
D
M. luteous Q4U1A6 58 VEFTIQSASKPFTYAAALVDRGFAAVDRQVGLNPSGEAFNELSLEAE--SHRPDNAMINAGALAVHQLLV 125
E. coli P0A6W0 60 ERFSIQSISKVLSLVVAMRHYSEEEIWQRVGKDPSGSPFNSLVQLEME-QGIPRNPFINAGALVVCDMLQ 128
B. subtilis O07637 59 VSFTMQSISKVISFIAACMSRGIPYVLDRVDVEPTGDAFNSIIRLEINKPGKPFNPMINAGALTIASILP 137
B. subtilis O31465 68 KTFTLQSISKVLSLALVLMEYGKDKVFSYVGQEPTGDPFNSIIKLETVNPSKPLNPMINAGALVVTSLIR 128
E. coli P77454 60 YRFALESISKVCTLALALEDVGPQAVQDKIGADPTGLPFNSVIALELH-GGKPLSPLVNAGAIATTSLIN 128
M. Musculus O94925 285 VPFCLQSCVKPLKYAIAVNDLGTEYVHRYVGKEPSGLRFNKLFLNE---DDKPHNPMVNAGAIVVTSLIK 351
.pFhlQShSKshohhhAh.c.G...V.p.VG.-PoG.sFNplh.bEb..ss+P.NPhlNAGAlhlhsll.
hhhhhhhhhhhhhhhhh hhhhhhhh hhhhhhhh hhhhhhhhhhhhh
E
S291
Glutamate
G320
Activation Loop
K325
F
Enzyme specific activity (%)
100
80
60
40
20
0
Pi
- +
- +
- +
- +
(50 mM)
WT
K325A
G320P
G320P/K325A

Cooperation between the activation loop and a conserved motif that encloses the catalytic site upon substrate binding

Analysis of the available x-ray crystal structures of the complex between wild-type GAC and its catalytic product, glutamate (25), reveals that a highly conserved YIP motif (**Fig.2.5 A, boxed residues**) provides contacts for the bound substrate and product (**Fig.2.5 B**). Moreover, superimposing the x-ray crystal structures of wild-type GAC, in the presence and absence of bound glutamate, revealed movement in this conserved motif, such that it would form a 'lid' over the catalytic site when it is occupied (i.e. by substrate), as illustrated by the comparison of **Fig.2.5 B** and **C**. We therefore examined whether mutations introduced into this active site lid could influence enzymatic activity by affecting accessibility to the catalytic site. Indeed, a Y254F substitution, within a wild-type GAC background, yielded an enzyme with markedly enhanced basal activity (i.e., in the absence of inorganic phosphate) compared to the wild-type protein, while the same substitution, when introduced within the GAC(D391K) dimer background, failed to activate enzyme activity (**Fig.2.5 D**). GAC was also inactive when the Y254F substitution caused a significant shift in the dose-response for inorganic phosphate (**Fig.2.5 E**), indicating that disrupting the active site lid with a conservative Y to F substitution can significantly enhance the binding of phosphate and alter the specific activity of the enzyme (**Fig.2.5 F**; see Discussion). As will be described further below, these results, and those presented in the preceding sections, now offer a fresh picture of how the enzymatic activity of GAC is activated in response to allosteric activators such as inorganic phosphate.

Figure 2.5 Phosphate activation of GAC influences substrate accessibility and product release. A, Sequence alignment guided by the available glutaminase structures as in **Fig.2.4 A** highlighting the conservation of the YIP motif constituting the substrate pocket lid. **B**, Proximal relationship of the activation loop and the substrate accessibility lid when either glutamate or glutamine is bound (PDB: 3SS5). **C**, Ligand free depiction of GAC where the dashed line segments designate unresolved regions in the crystal structure (PDB: 3SS3). **D**, Effect of YIP motif disruption on the activity of recombinant GAC. The specific activity of all purified proteins at 50 nM was assayed with and without added inorganic phosphate (50 mM). **E**, YIP motif lid disruption results in a higher apparent affinity of inorganic phosphate for GAC(Y254F). Dose dependence of phosphate activation of 50 nM GAC**(**Y254F) vs GAC(WT). The titrations and fits are representative of three independent experiments. F, Initial velocity analysis showing the V_{max} difference between GAC**(**Y254F) vs GAC(WT). GAC was assayed at 300 nM with increasing glutamine concentrations. Michaelis–Menten parameters for the best fits shown by the solid curves are: GAC(WT) K_m=5.6 mM, V_{max}=0.09 mM/min, and for GAC(Y254F) K_m=9.5 mM, V_{max}=0.30 mM/min. Results are representative of three independent trials.

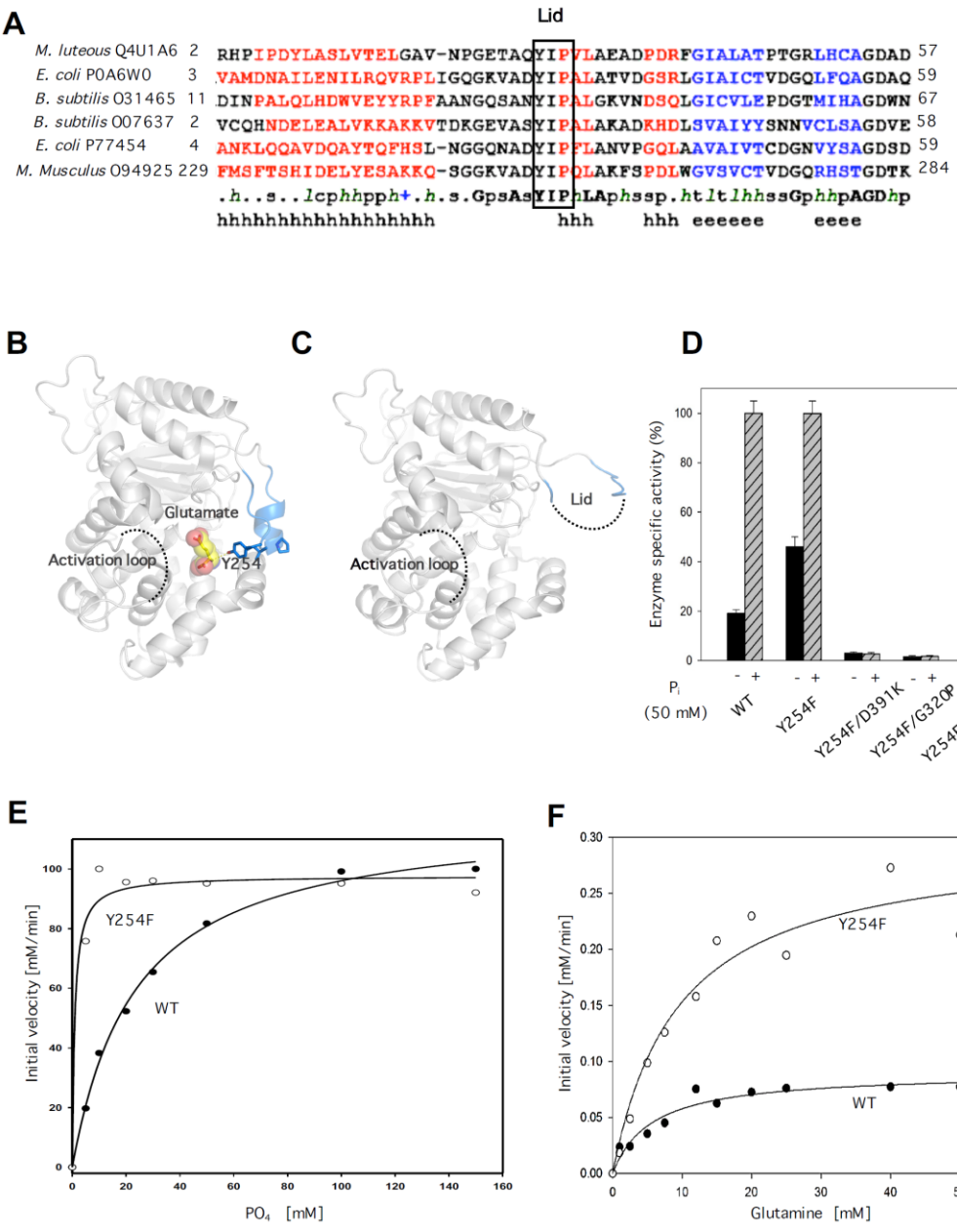
A
Lid
M. luteous Q4U1A6 2 RHPIPDYLASLVTELGAV-NPGETAQYIPVLAEADPDRFGIALATPTGRLHCAGDAD 57
E. coli P0A6W0 3 VAMDNAILENILRQVRPLIGQGKVADYIPALATVDGSRLGIAICTVDGQLFQAGDAQ 59
B. subtilis O31465 11 DINPALQLHDWVEYYRPFAANGQSANYIPALGKVNDSQLGICVLEPDGTMIHAGDWN 67
B. subtilis O07637 2 VCQHNDELEALVKKAKKVTDKGEVASYIPALAKADKHDLSVAIYYSNNVCLSAGDVE 58
E. coli P77454 4 ANKLQQAVDQAYTQFHSL-NGGQNADYIPFLANVPGQLAAVAIVTCDGNVYSAGDSD 59
M. Musculus O94925 229 FMSFTSHIDELYESAKKQ-SGGKVADYIPQLAKFSPDLWGVSVCTVDGQRHSTGDTK 284
.h..s..lcphhpph+.h.s.GpsAsYIPhLAphssp.htltlhhssGphhpAGDhp
hhhhhhhhhhhhhhhhhh hhh hhh eeeeee eeee
B
Glutamate
Activation loop
Y254
C
Lid
Activation loop
D
Enzyme specific activity (%)
Pi
(50 mM)
WT
Y254F
Y254F/D391K
Y254F/G320P
Y254F/G320P K325A
E
Initial velocity [mM/min]
Y254F
WT
PO4 [mM]
F
Initial velocity [mM/min]
Y254F
WT
Glutamine [mM]

DISCUSSION

Members of the glutaminase family of mitochondrial enzymes are responsible for catalyzing the key first step in glutamine metabolism, specifically, the conversion of glutamine to glutamate with the generation of ammonia. This becomes an especially important reaction in a number of cancer cells undergoing Warburg glycolysis. It provides a pathway by which glutamine-derived carbon enters the TCA cycle as α-ketoglutarate, thereby compensating for the majority of pyruvate being converted to lactic acid rather than to citrate, which normally starts the cycle (26). Depending on the degree to which a given cancer cell requires glutamine-dependent anaplerosis (i.e. becomes "glutamine-addicted"), glutamine withdrawal, or small molecule inhibition of glutaminase activity, slows or halts the growth of cancer cells and inhibits tumor growth in mouse models (9,12,15,27,28). Cancer cells often exhibit high levels of GLS expression, which is especially the case for the GAC splice variant, as well as providing signals that ensure its maximal activation (29). Thus, the potential for targeting GAC as a clinical strategy makes it of great importance to understand the molecular and mechanistic aspects of its activation.

Previous studies have suggested that the transition of the enzyme from a dimeric to a tetrameric species was tightly correlated with enzyme activation (21). However, GAC was observed to undergo even higher order oligomerization under conditions where it was catalytically active, leading to the proposal that the formation of super-aggregates of the enzyme is a pre-requisite for full catalytic activity (18). If this were the case, there would be a number of questions that would need to be

considered. For example, how is the generation of super aggregates of GAC achieved in cancer cells and what are the consequences of forming such large structures to mitochondrial and cellular function? Therefore with these issues in mind, we set out to learn more about what is the minimal enzyme unit capable of full activity, and what might this suggest regarding the regulation of GAC activation.

An examination of the existing x-ray crystal structures of members of the glutaminase family, including that for human GAC (**Fig.2.1**), suggested that the allosteric activator, inorganic phosphate, by stabilizing the tetrameric helical interface of GAC, might help to drive enzyme activation by inducing conformational changes within what we refer to as the 'activation loop' (residues 320-327). Indeed, we show that the introduction of a charge-reversal at the helical interface (i.e. GAC(D391K)) effectively traps GAC as an inactive dimeric species. Importantly, the structure of GAC(D391K) shared a key feature with that for GAC bound to an allosteric inhibitor, BPTES, namely, a resolvable activation loop. This then suggested that the flexibility of this loop might represent a critical element for enzyme activation.

We, and others (21,23), have found that mutation of the activation loop residue lysine 325, within a wild-type GAC background, resulted in a constitutively active enzyme. Introducing this same change into the activation loop of the GAC(D391K) mutant yielded constitutive enzymatic activity. This double mutant (GAC(K325A/D391K)), unlike GAC(D391K), is not stabilized in the dimeric state, but is capable of forming tetramers and higher aggregates through N-terminal dimer-dimer interactions.

By taking advantage of an earlier observation that substitutions at lysine 316 prevented GAC from forming super-aggregates (18), we made an important discovery. Specifically, when this same substitution was introduced into the GAC(K325A/D391K) background, it was possible to generate a constitutively active GAC triple mutant (GAC(K316Q/K325A/D391K)) that was trapped in a dimeric state. Perhaps most important, the ectopically expressed GAC(K316Q/K325A/D391K) triple mutant did not give rise to higher order oligomeric structures in cells, unlike other activated forms of GAC, nor was it cytotoxic, but localized normally to the mitochondria.

In order to examine the effects of enhanced GAC activity on cell growth, we compared the ability of wild-type GAC versus constitutively active GAC to augment the transformation of NIH-3T3 cells. In particular, we examined the abilities of wild-type GAC and the constitutively active GAC triple mutant to potentiate the focus forming activity of low concentrations of oncogenic Dbl. No significant difference was observed between these two forms of GAC in their effectiveness to synergize with Dbl in driving cellular transformation. This suggests that overexpressing wild-type GAC is sufficient to provide the enhanced glutaminase activity that magnifies the effects of oncogene-driven focus formation, such that the supportive role that glutamine metabolism appears to play can be accomplished equally well by both wild-type and mutant forms of GAC. While more subtle effects (e.g., subcellular localization, complex formation) may yet be identified for glutaminase point mutations occurring in the cancer genome (curated in the CbioPortal), the simple up-regulation of intrinsic GLS activity does not appear to impact cell growth by itself.

Thus having established that the activation loop of GAC can induce an activated state, independent of the need for the enzyme to form higher order oligomers, or even simply tetramers, we wanted to better understand how this loop was able to communicate with the catalytic active site. An attractive candidate for making this connection was a peptide segment (residues 291-325), and indeed, mutagenesis analysis showed that changing a highly conserved glycine at position 320 to proline uncoupled the communication between the activation loop and the active site. While comparing the structures of GAC in the presence and absence of the product glutamate, we were led to examine a conserved tyrosine-isoleucine-proline (YIP; **Fig.2.5 A**) motif that forms a lid over the substrate-binding pocket upon the binding of substrate (**Fig.2.5 B** and **C**). Changing a highly conserved tyrosine to phenylalanine within this lid increased the basal activity of wild-type GAC (**Fig.2.5 D**). However, a particularly interesting finding was that the Y254F substitution resulted in an apparent increase in the binding affinity of the enzyme for inorganic phosphate, i.e. shifting the activating doses of inorganic phosphate to lower concentrations (**Fig.2.5 E**). The increase in glutaminase activity observed for the Y254F mutant appears to be a result of more rapid substrate (glutamine)/product (glutamate) exchange (i.e. due to the opening of the lid), as suggested by an initial velocity analysis where the V_{max} of the Y254F mutant glutaminase was fivefold higher without a change in K_m (**Fig.2.5 F**).

When taken together, these different observations now lead to a plausible scheme, regarding how allosteric regulators like inorganic phosphate activate GAC (**Fig.2.6**). In this model, the binding of inorganic phosphate is proposed to enhance

interactions between residues within the tetrameric helical interface, thus stabilizing the formation of activated tetramers. Specifically, this would enable the activation loop to assume the proper orientation in order for it to communicate with the connecting peptide segment (containing glycine 320) and thereby optimally position the active site residues for catalysis. Upon the binding of glutamine, additional interactions between the substrate and the lid increase the residence time of glutamine as it awaits the proper orientation of the active site residues for catalysis. The binding of inorganic phosphate, and the resulting changes in the activation loop and connecting peptide segment, would then not only be important for ensuring that the proper orientation of the catalytic residues occurs, but would also weaken the association of the lid with the active center, so as to ensure optimal product release. Note that although inorganic phosphate would weaken the binding of the lid to the active center, in a reciprocal fashion, the interaction of the lid with the active site would weaken the binding of inorganic phosphate to the enzyme. Thus, the Y254F substitution, by weakening the interaction of the lid with the active site, would also give rise to an enhanced interaction between the enzyme and phosphate, resulting in the observed shifting of the dose response curve for phosphate shown in **Fig.2.5 E**.

Our identification of a minimal enzymatic dimeric unit capable of full activity demonstrates that the formation of higher oligomers is not an absolute pre-requisite for full enzyme activation. These findings now also raise some interesting possibilities regarding how specific types of posttranslational modifications within GAC might trigger enzyme activation. Such changes might include the modification of lysine

residues through the addition of acetyl and succinyl moieties (30-32). Future studies will be directed toward understanding how such modifications of GAC within cancer cells might help to mediate the communication between its activation loop and active center, and/or possibly enhance the release of its active site lid in a manner that significantly accelerates product release, thus providing multiple mechanisms by which the activation of this important metabolic enzyme might be achieved.

Figure 2.6 Proposed mechanism of GAC activation illustrating critical points of up-regulation (green) and inhibition (red). 1) The dimeric GAC species has an activation loop orientation that does not support catalysis. 2) Tetrameric GAC has an activation loop that supports catalysis and an open active site lid that facilitates more rapid substrate binding and product release. 3) Close-up of a monomeric species within the tetramer: BPTES or the G320P substitution stabilizes the activation loop in an orientation that does not support catalysis while the GAC(K325A) mutant or the presence of inorganic phosphate results in the positioning of the activation loop required for catalysis. 4) Close-up of a monomeric species within the tetramer. Upon the binding of glutamine, the active site lid closes over the substrate. The Y254F substitution promotes catalysis by facilitating the opening of the active site lid allowing for accelerated substrate binding and release of product.

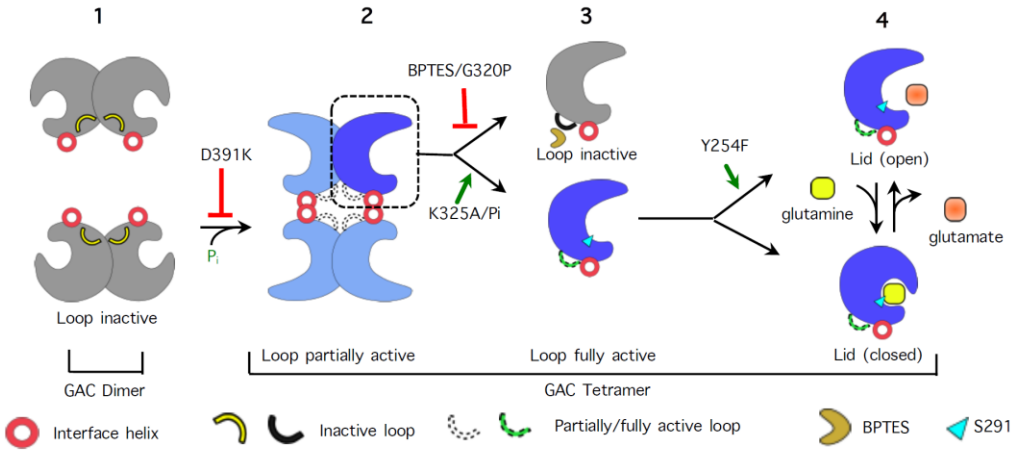
1
2
3
4
BPTES/G320P
D391K
Loop inactive
Y254F
Lid (open)
glutamine
glutamate
K325A/Pi
Pi
Loop inactive
Loop partially active
Loop fully active
Lid (closed)
GAC Dimer
GAC Tetramer
Interface helix
Inactive loop
Partially/fully active loop
BPTES
S291

REFERENCES

1. DeBerardinis, R. J., Lum, J. J., Hatzivassiliou, G., and Thompson, C. B. (2008) The biology of cancer: metabolic reprogramming fuels cell growth and proliferation. Cell Metab. 7, 11-20

2. Cantor, J. R., and Sabatini, D. M. (2012) Cancer cell metabolism: one hallmark, many faces. Cancer Discov. 2, 881-898

3. Hensley, C. T., Wasti, A. T., and DeBerardinis, R. J. (2013) Glutamine and cancer: cell biology, physiology, and clinical opportunities. J. Clin. Invest. 123, 3678-3684

4. Warburg, O. (1956) On the origin of cancer cells. Science 123, 309-314

5. Vander Heiden, M. G., Cantley, L. C., and Thompson, C. B. (2009) Understanding the Warburg effect: the metabolic requirements of cell proliferation. Science 324, 1029-1033

6. Wise, D. R., and Thompson, C. B. (2010) Glutamine addiction: a new therapeutic target in cancer. Trends Biochem. Sci. 35, 427-433

7. Xiang, Y., Stine, Z. E., Xia, J., Lu, Y., O'Connor, R. S., Altman, B. J., Hsieh, A. L., Gouw, A. M., Thomas, A. G., Gao, P., Sun, L., Song, L., Yan, B., Slusher, B. S., Zhuo, J., Ooi, L. L., Lee, C. G., Mancuso, A., McCallion, A. S., Le, A., Milone, M. C., Rayport, S., Felsher, D. W., and Dang, C. V. (2015) Targeted inhibition of tumor-specific glutaminase diminishes cell-autonomous tumorigenesis. Clin. Invest. 125, 2293-2306

8. DeBerardinis, R. J., Mancuso, A., Daikhin, E., Nissim, I., Yudkoff, M., Wehrli, S., and Thompson, C. B. (2007) Beyond aerobic glycolysis: transformed cells can engage in glutamine metabolism that exceeds the requirement for protein and nucleotide synthesis. Proc. Natl. Acad. Sci. U.S.A. 104, 19345-19350

9. Wang, J. B., Erickson, J. W., Fuji, R., Ramachandran, S., Gao, P., Dinavahi, R., Wilson, K. F., Ambrosio, A. L., Dias, S. M., Dang, C. V., and Cerione, R. A. (2010) Targeting mitochondrial glutaminase activity inhibits oncogenic transformation. Cancer Cell 18, 207-219

10. Erickson, J. W., and Cerione, R. A. (2010) Glutaminase: a hot spot for regulation of cancer cell metabolism? Oncotarget 1, 734-740

11. Levine, A. J., and Puzio-Kuter, A. M. (2010) The control of the metabolic switch in cancers by oncogenes and tumor suppressor genes. Science 330, 1340-1344

12. Gao, P., Tchernyshyov, I., Chang, T. C., Lee, Y. S., Kita, K., Ochi, T., Zeller, K. I., De Marzo, A. M., Van Eyk, J. E., Mendell, J. T., and Dang, C. V. (2009) c-Myc suppression of miR-23a/b enhances mitochondrial glutaminase expression and glutamine metabolism. Nature 458, 762-765

13. Wise, D. R., DeBerardinis, R. J., Mancuso, A., Sayed, N., Zhang, X. Y., Pfeiffer, H. K., Nissim, I., Daikhin, E., Yudkoff, M., McMahon, S. B., and Thompson, C. B. (2008) Myc regulates a transcriptional program that stimulates mitochondrial glutaminolysis and leads to glutamine addiction. Proc. Natl. Acad. Sci. U.S.A. 105, 18782-18787

14. Son, J., Lyssiotis, C. A., Ying, H., Wang, X., Hua, S., Ligorio, M., Perera, R. M., Ferrone, C. R., Mullarky, E., Shyh-Chang, N., Kang, Y., Fleming, J. B., Bardeesy, N., Asara, J. M., Haigis, M. C., DePinho, R. A., Cantley, L. C., and Kimmelman A. C. (2013) Glutamine supports pancreatic cancer growth through a KRAS-regulated metabolic pathway. Nature 496, 101-105

15. Lukey, M. J., Greene, K. S., Erickson, J. W., Wilson, K. F., and Cerione, R. A. (2016) The oncogenic transcription factor c-Jun regulates glutaminase expression and sensitizes cells to glutaminase-targeted therapy. Nat. Commun. 7, 11321

16. 16. Godfrey, S., Kuhlenschmidt, T., and Curthoys, N. P. (1977) Correlation between activation and dimer formation of rat renal phosphate-dependent glutaminase. J. Biol. Chem. 252, 1927-1931

17. Moller, M., Nielsen, S. S., Ramachandran, S., Li, Y., Tria, G., Streicher, W., Petoukhov, M. V., Cerione, R. A., Gillilan, R. E., and Vestergaard, B. (2013) Small angle X-ray scattering studies of mitochondrial glutaminase C reveal extended flexible regions, and link oligomeric state with enzyme activity. PLoS One 8, e74783

18. Ferreira, A. P., Cassago, A., de Almeida Goncalves, K., Dias, M. M., Adamoski, D., Ascencao, C. F., Honorato, R. V., de Oliveira, J. F., Ferreira, I. M., Fornezari, C., Bettini, J., Oliveira, P. S., Paes Leme, A. F., Portugal, R. V., Ambrosio, A. L., and Dias, S. M. (2013) Active glutaminase C self-assembles into a supratetrameric oligomer that can be disrupted by an allosteric inhibitor. J. Biol. Chem. 288, 28009-28020

19. Robinson, M. M., McBryant, S. J., Tsukamoto, T., Rojas, C., Ferraris, D. V., Hamilton, S. K., Hansen, J. C., and Curthoys, N. P. (2007) Novel mechanism of inhibition of rat kidney-type glutaminase by bis-2-(5-phenylacetamido-1,2,4-thiadiazol-2-yl)ethyl sulfide (BPTES). Biochem. J. 406, 407-414

20. DeLaBarre, B., Gross, S., Fang, C., Gao, Y., Jha, A., Jiang, F., Song, J. J., Wei, W., and Hurov, J. B. (2011) Full-length human glutaminase in complex with an allosteric inhibitor. Biochemistry 50, 10764-10770

21. Stalnecker, C. A., Ulrich, S. M., Li, Y., Ramachandran, S., McBrayer, M. K., DeBerardinis, R. J., Cerione, R. A., and Erickson, J. W. (2015) Mechanism by which a recently discovered allosteric inhibitor blocks glutamine metabolism in transformed cells. Proc. Natl. Acad. Sci. U.S.A. 112, 394399

22. Thangavelu, K., Pan, C. Q., Karlberg, T., Balaji, G., Uttamchandani, M., Suresh, V., Schüler, H., Low, B. C., and Sivaraman, J. (2012) Structural basis for the allosteric inhibitory mechanism of human kidney-type glutaminase (KGA) and its regulation by Raf-Mek-Erk signaling in cancer cell metabolism. Proc. Natl. Acad. Sci. U.S.A. 109, 7705-7710

23. McDonald, C. J., Acheff, E., Kennedy, R., Taylor, L., and Curthoys, N. P. (2014) Effect of lysine mutations on the phosphate activation and BPTES inhibition of glutaminase. Neurochem. Int. 88, 10-14

24. Hart, M. J., Eva, A., Zangrilli, D., Aaronson, S. A., Evans, T., Cerione, R. A., and Zheng, Y. (1994) Cellular transformation and guanine nucleotide exchange activity are catalyzed by a common domain on the dbl oncogene product. J. Biol. Chem. 269, 62-65

25. Cassago, A., Ferreira, A. P., Ferreira, I. M., Fornezari, C., Gomes, E. R., Greene, K. S., Pereira, H. M., Garratt, R. C., Dias, S. M., and Ambrosio, A. L. (2012) Mitochondrial localization and structurebased phosphate activation mechanism of Glutaminase C with implications for cancer metabolism. Proc. Natl. Acad. Sci. U.S.A. 109, 1092-1097

26. Vander Heiden, M. G., Cantley, L. C., and Thompson, C. B. (2009) Understanding the Warburg effect: the metabolic requirements of cell proliferation. Science 324, 1029-1033

27. Lukey, M. J., Wilson, K. F., and Cerione, R. A. (2013) Therapeutic strategies impacting cancer cell glutamine metabolism. Future Med. Chem. 5, 1685-1700

28. Gross, M. I., Demo, S. D., Dennison, J. B., Chen, L., Chernov-Rogan, T., Goyal, B., Janes, J. R., Laidig, G. J., Lewis, E. R., Li, J., Mackinnon, A. L., Parlati, F., Rodriguez, M. L., Shwonek, P. J., Sjogren, E. B., Stanton, T. F., Wang, T., Yang, J.,

29. Zhao, F., and Bennett, M. K. (2014) Antitumor activity of the glutaminase inhibitor CB-839 in triple-negative breast cancer. Mol. Cancer Ther. 13, 890-901

30. van den Heuvel, A. P., Jing, J., Wooster, R. F., and Bachman, K. E. (2012) Analysis of glutamine dependency in non-small cell lung cancer: GLS1 splice variant GAC is essential for cancer cell growth. Cancer Biol. Ther. 13, 1185-1194

31. Xiong, Y., and Guan, K. L. (2012) Mechanistic insights into the regulation of metabolic enzymes by acetylation. J. Cell Biol. 198, 155-164

32. Hirschey, M. D., and Zhao, Y. (2015) Metabolic regulation by lysine malonylation, succinylation and glutarylation. Mol. Cell. Proteomics 14, 2308-2315

33. McDonald, C. J., Acheff, E., Kennedy, R., Taylor, L., and Curthoys, N. P. (2015) Effect of lysine to alanine mutations on the phosphate activation and BPTES inhibition of glutaminase. Neurochem. Int. 88, 10-14

34. Kim, C. U., Hao, Q., and Gruner, S. M. (2006) Solution of protein crystallographic structures by high-pressure cryocooling and noble-gas phasing. Acta Crystallogr. D Biol. Crystallogr. 62, 687-694

CHAPTER III

ABSTRACT

Aberrant overexpression of the GAC isoform of mitochondrial glutaminase is observed in many "glutamine addicted" cancer cells and therefore represents a potential target for combination therapies. The continued progress in understanding the regulation of GAC activity, and the mechanistic details of small molecule, allosteric inhibitors, is guided in part by the development of spectroscopic approaches that can directly measure glutaminase activity and the interaction of activators and inhibitors of GAC in real time. Previously, we have examined the effects of alanine substitutions in the regulatory region that we designate as the "activation loop" (Chapter 2). In this chapter, we use the identification of the critical role of this region of GAC to engineer a conformational probe of GAC activity by substituting a tryptophan for phenylalanine at position 327. As previously shown by our lab, this GAC mutant was responsive to activator (e.g., phosphate) binding and to the addition of the BPTES-class of inhibitors that binds to the tetramer helical interface, making direct contact with the activation loop and constraining it in an inactive conformation. Here, we extend the usefulness of tryptophan substitution at critical aromatic side chains in GAC by examining the linkage between the activation loop and the substrate glutamine-binding cleft, approximately 12 Å away. Comparison of glutamine binding in the presence and absence of the BPTES analog CB-839 reveals a reciprocal relationship between the constraints imposed on the position of the activation loop and the affinity of GAC for glutamine. Prior binding of inhibitor weakens the affinity for glutamine, resulting in a

lower observed GAC activity. Conversely, pretreatment of GAC with activating anions such as phosphate results in a GAC tetramer with high affinity for glutamine, with a correspondingly higher observed activity. Taken together, these results demonstrate a microscopically reversible linkage between the positioning of the activation loop at the tetramer helical interface and the conformation at the glutamine catalytic site that determines substrate affinity that, in turn, allows for the observed GAC activity.

INTRODUCTION

As discussed in Chapter I, the importance of glutamine metabolism in cancer cell survival has been attracting an increasing amount of attention, which has led to a renewed focus on developing therapeutic approaches that target glutamine metabolism in transformed cells (1, 2). As described earlier, GLS can be viewed as a gateway enzyme for glutamine metabolism as it is responsible for a majority of the glutamine to glutamate conversion in cells (3). This pivotal role for GLS in glutamine metabolism, coupled with the observation that many cancer cell types exhibit an increased requirement for glutamine, underlies the development of a number of inhibitors for GLS to block glutamine metabolism, some of which are undergoing clinical testing (4, 5). As a consequence, the mechanisms by which GLS is activated and inhibited by small molecules is of great interest and is further explored in this chapter.

Tryptophan fluorescence changes in intact, active proteins can be used as a tool to monitor conformational changes induced by protein-small molecule

interactions. Past applications of this approach include monitoring the nucleotide bound state of GTP binding proteins and GTP hydrolysis, as well as revealing the kinetics of protein folding (6, 7, 8, 9). Tryptophan fluorescence has also been used as a probe to monitor the conformational changes in enzymes that are induced by the binding of allosteric inhibitors and activators (10, 11). In some cases, it can also be used as a direct readout for substrate binding and thus serves as a tool to study mechanisms of activation and inhibition, by monitoring the effects that activators and inhibitors have on substrate binding (12, 13).

In this chapter, we extend the utility of earlier work in our laboratory using a direct readout of allosteric activators (phosphate/sulfate) as well as inhibitors (BPTES/CB-839) to monitor the induced conformational changes in the activation loop. X-ray crystal structures of the glutaminase domain of GAC bound to an activator (sulfate) or inhibitor (CB-839) reveal that both small molecules bind near the activation loop as described in Chapter II. This observation provided the rational for developing a “tryptophan sensor” in the activation loop in order to monitor the binding of either activators or inhibitors. Using this approach, our laboratory recently demonstrated that the GAC(F327W) mutant can serve as a reliable fluorescent readout for phosphate and BPTES-type inhibitor binding. Interestingly, phosphate was observed to enhance tryptophan fluorescence in these experiments while BPTES significantly quenched it (14).

Here, using the placement of tryptophan at the GLS binding pocket, we set out to investigate how an inhibitor or activator “communicates” with the active site via the activation loop and by what means the two sites are coupled. As described in Chapter II, the activation loop serves a critical role in GLS activation and inhibition as both allosteric inhibitors and activators bind near the activation loop. Inside the glutamine binding pocket at the active site, approximately 12 Å away from this loop, there are three residues that constitute a catalytic triad that are critical for substrate binding as well as catalysis. Although the individual role for each residue is not completely clear, a comparison of the X-ray structures of active wild type GAC with bound glutamate (product) and an inactive glutaminase domain bound with glutamine (substrate), showed that tyrosine 471 is unique in its interaction with the amide group of the sidechain of glutamine (15). The amide to carboxylic acid conversion that distinguishes the substrate (glutamine) and product (glutamate) of GAC therefore offers GAC(Y471W) as a potential tryptophan sensor for monitoring glutamine binding to the enzyme.

In this chapter, we describe the enzymatic and spectroscopic properties of GAC(Y471W) and demonstrate that it provides a direct readout for monitoring glutamine binding to GAC. This allows for the determination of glutamine binding affinity in the presence and absence of GAC activators and inhibitors. The apparent communication between the activation loop at the tetramer interface with the GAC

active site suggests that the former regulates substrate affinity and by doing so, dictates enzyme activity.

METHODS

Protein production

The recombinant GAC construct (Y471W) was made following the protocol that was described in Chapter II. The mouse kidney-type glutaminase isoform 2 (GAC, NP_001106854.1) encoded plasmid (residues 72-603) was cloned into a pET23a vector with a N-terminal histidine-tag and thrombin cleavage site. The expressed protein was purified using Co^{2+} affinity beads, then followed by anion exchange and gel filtration chromatography. Purified GAC was stored at -80 °C in gel filtration buffer (20 mM Tris-HCl pH 8.5, 500 mM NaCl, 1 mM NaN_3) after the snap freezing in liquid N_2 for long term use.

Fluorescence measurements

Fluorescence measurements were carried out on a Varian Cary Eclipse fluorimeter in counting mode. The sample was held in a 1 mL cuvette with continuous stirring at 20°C in reaction buffer: 50 mM Tris-acetate, pH 8.5, 0.1 mM EDTA. For tryptophan emission scans, the wavelengths for excitation and emission were 285 and 310-390 nm. For kinetic experiments, the wavelengths for excitation and emission were 285 and 340 nm. For glutamine titration experiments, 100 µL of glutamine of appropriate concentration was dissolved in reaction buffer and added to 200 nM GAC (Y471W mutant). Data points for titration curves were taken from the equilibrated portion of

the kinetic curve and fitted with a protein ligand binding equation. Similar to the allosteric activator enhanced substrate binding experiment, 50 mM phosphate (50 µL) was added to 200 nM GAC (Y471W mutant) 90 s prior to the injection of 20 mM glutamine. For inhibitor titrations, CB-839 at indicated concentrations was added to 200 nM GAC (Y471W mutant) with less than 5% (v/v) DMSO. After injection of the drug, incubation was performed for 90s to allow the binding and system to reach equilibration. Points for dose-dependent quenching were taken from the equilibrated kinetic curves. Then 20 mM glutamine dissolved in 100 µL of reaction buffer was added to the solution.

Real-time Glutaminase assays

The real-time activity assays used to evaluate the activity of GAC mutants through the production of NADH were carried out using a Varian Cary Eclipse Fluorimeter. Experiments were prepared in 1-mL cuvet with continuous stirring at 20 °C in reaction buffer (10 units of glutamate dehydrogenase [Sigma] and 2 mM NAD^+ [Sigma] were prepared in 50 mM Tris-Acetate, pH 8.5, 0.1 M EDTA), with an appropriate concentration of K_2HPO_4 added to 200 nM GAC and allowed to equilibrate 60 secs before monitoring the fluorescence for NADH (340 nm excitation, 490 nm emission). The addition of 20 mM glutamine initiated the reaction. The activity of GAC was measured in a coupled assay, by monitoring the NADH produced by glutamate dehydrogenase, which converts glutamate (product of glutaminase-catalysis) to α-ketoglutarate and ammonia by reducing NAD^+ to NADH. Since glutamine also

undergoes non-enzymatic degradation to glutamate, each sample was further analyzed by subtracting the NADH produced in the absence of glutaminase under identical experimental conditions.

RESULTS

Tryptophan substitutions in GAC provide for real time monitoring of GAC activation and inhibition.

The reported crystal structures of BPTES and sulfate-bound GAC demonstrate that both allosteric activators and inhibitors undergo interactions with the activation loop (16). Moreover the comparison between two GAC X-ray crystal structures with and without BPTES/SO_4^{2-} revealed that the activation loop undergoes a significant displacement after binding to BPTES/SO_4^{2-} (**Fig.3.1 A,B,C**). This conformational change at the activation loop suggested a potential way to observe the structural transition in real time by replacing one of the wild-type residues with an aromatic tryptophan as a fluorescence reporter. In previously published work from our own laboratory, tryptophan scanning mutagenesis was performed as described in Chapter 2 with tryptophan substitutions, which yielded a F327W mutant as the best candidate to serve as a reporter for BPTES or phosphate binding (14). The GAC F327W mutant can distinguish between activator and inhibitor binding as phosphate addition enhances tryptophan fluorescence while BPTES-like inhibitors (e.g., CB-839) result in a significant reduction in tryptophan 340 nm emission. This mutant can bind to and form complexes with inhibitors in a manner similar to wild-type GAC and exhibits approximately the same level of phosphate stimulated activity as the wild-type enzyme. Based on the

available crystallographic information, the observed fluorescence changes that the F327W mutant exhibit following BPTES binding are a result of the interactions between the inhibitor and the peptide backbone of the substituted tryptophan, not the direct contact of the inhibitor with the indole side-chain (the WT phenylalanine side chain does not interact with the inhibitor, and the structural analysis performed to date indicates electron density between BPTES and the backbone peptide of residues L326 and F327) (16, 17).

GAC(F327W) can allosterically detect the binding of glutamine at the GAC active site.

We observed that, in addition to serving as a reporter for the binding of phosphate and BPTES analogs to GAC, the F327W can also sense substrate (glutamine) binding. In the presence of 400 nM GAC(F327W), addition of 50 mM phosphate caused an enhancement of the fluorescence signal (15-20%). When glutamine was added at a concentration of 20 mM, the fluorescence signal was decreased over the course of about 2 minutes. On the other hand, when we repeated the experiment with 20 mM of the catalytic product glutamate, there was no observed fluorescence change **Fig.3.2 A**. Additionally, when the order of phosphate and substrate/product addition was reversed, substrate no longer quenched GAC(F327W) fluorescence in the absence of phosphate, while glutamate inhibited any subsequent phosphate induced fluorescence.

Figure 3.1 Rational of making GAC(F327W) mutant A. Overview and zoomed in view of the SO_4^{2-} bound structure of GAC. Each monomer has one SO_4^{2-} bound to the tyrosine 399 at the interface helices (PDB: 3VOY). **B.** Close-up view of aligned SO_4^{2-} bound and ligand free GAC structures (wild type GAC: 3SS3). Tetramer formation creates a hydrophobic pocket (formed by Y399, I396 rom both dimers) which attracts F327 to rotate toward the interface helices. However binding with SO_4^{2-} changes the electrostatic environment of the hydrophobic pocket through Y399, preventing F327 from rotating. **C.** Close-up view of aligned CB-839 bound and dimeric GAC structures (CB-839 bound GAC: 5H11, dimeric GAC (D391K): 5W2J). The arrowhead line indicates the phenylalanine position upon binding of CB-839 which accounts for the F327W fluorescence changes in the presence of inorganic phosphate or BPTES.

A

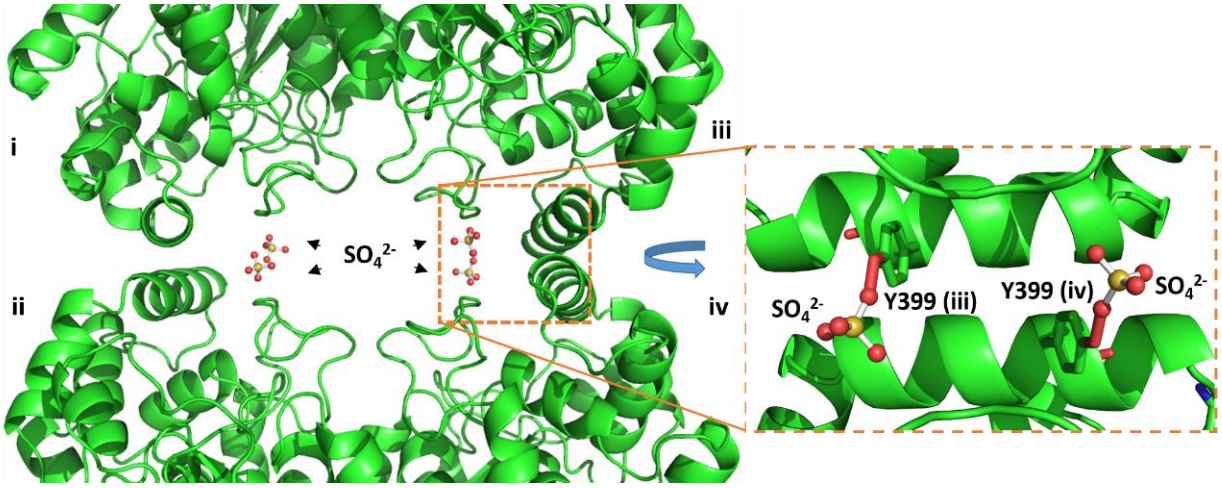
i
ii
iii
iv
SO_4^{2-}
SO_4^{2-}
Y399 (iii)
Y399 (iv)
SO_4^{2-}

B

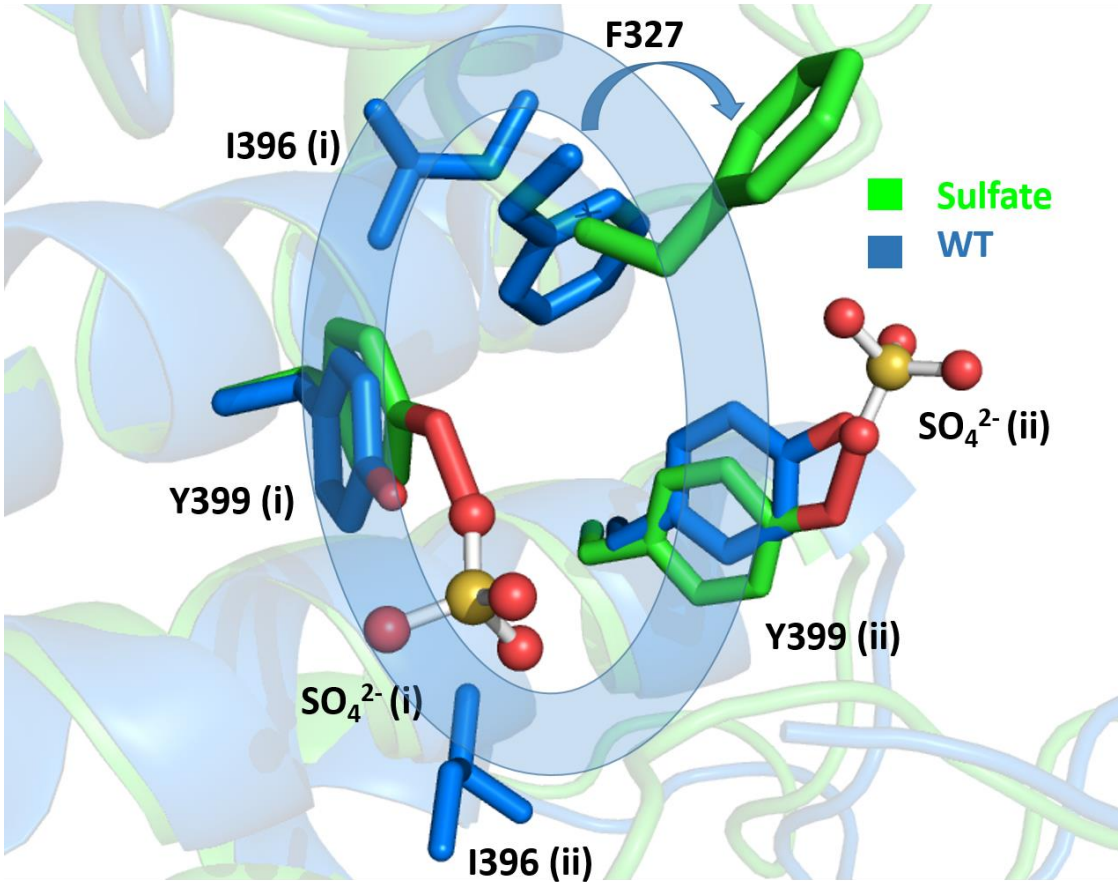
F327
I396 (i)
Sulfate
WT
SO_4^{2-} (ii)
Y399 (i)
Y399 (ii)
SO_4^{2-} (i)
I396 (ii)

C

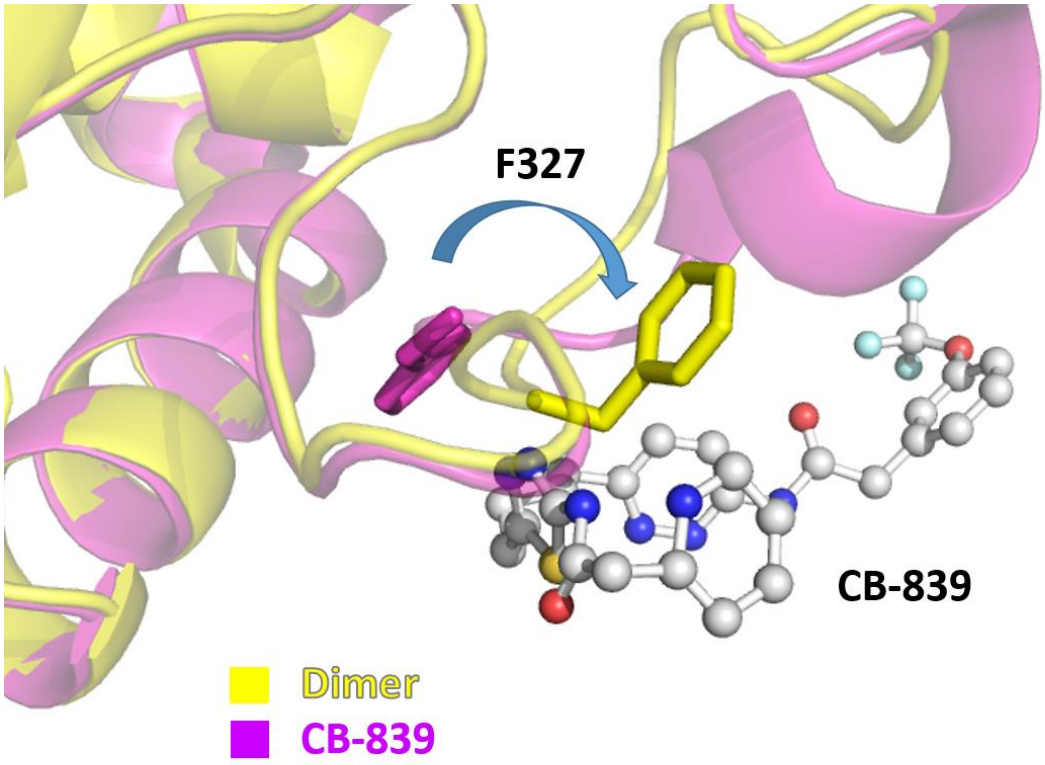

As shown in **Fig.3.2 B**, when the concentration of glutamate added to the solution prior to the addition of 50 mM phosphate was increased incrementally, the amount of fluorescence enhancement by phosphate was similarly reduced in a dose dependent fashion. At a concentration of 20 mM glutamate, the phosphate-stimulated fluorescence was completely blocked, suggesting that glutamate and phosphate behave in an antagonistic manner with regards to the activation loop of GAC.

It is somewhat surprising that a reporter on the activation loop (i.e., tryptophan 327) can sense glutamine binding in the active site, which the available crystallographic data indicate is about 12 Å away. Also, the fact that glutamate can block phosphate binding indicates that the enzyme possesses points of contact that can distinguish the binding of substrate (glutamine) and product (glutamate) and relay information between the tetrameric helical interface and the occupancy of the catalytic site. In order to explore this hypothetical linkage further, we wondered if we could apply the same strategy and identify a residue for sensing glutamine and glutamate at the active site, and position a reporter tryptophan that is sensitive to substrate binding. Since glutamine and glutamate differ only by an amide group on the side chain, we next examined the residues that interact with this amide in the available crystallographic data, in order to identify the best candidates for tryptophan substitution.

Figure 3.2 GAC(F327W) as a reporter for both activator (phosphate) and substrate (glutamine) binding A, Glutamine can quench the F327W fluorescent signal, which is enhanced by phosphate. The GAC(F327W) concentration is 400 nM, and 50 mM phosphate and 20 mM glutamine were added as indicated. **B,** GAC(F32W) fluorescence changes induced by the activator phosphate are inhibited by prior glutamate addition. Concentrations of GAC(F327W) and phosphate are 400 mM and 50 mM, respectively.

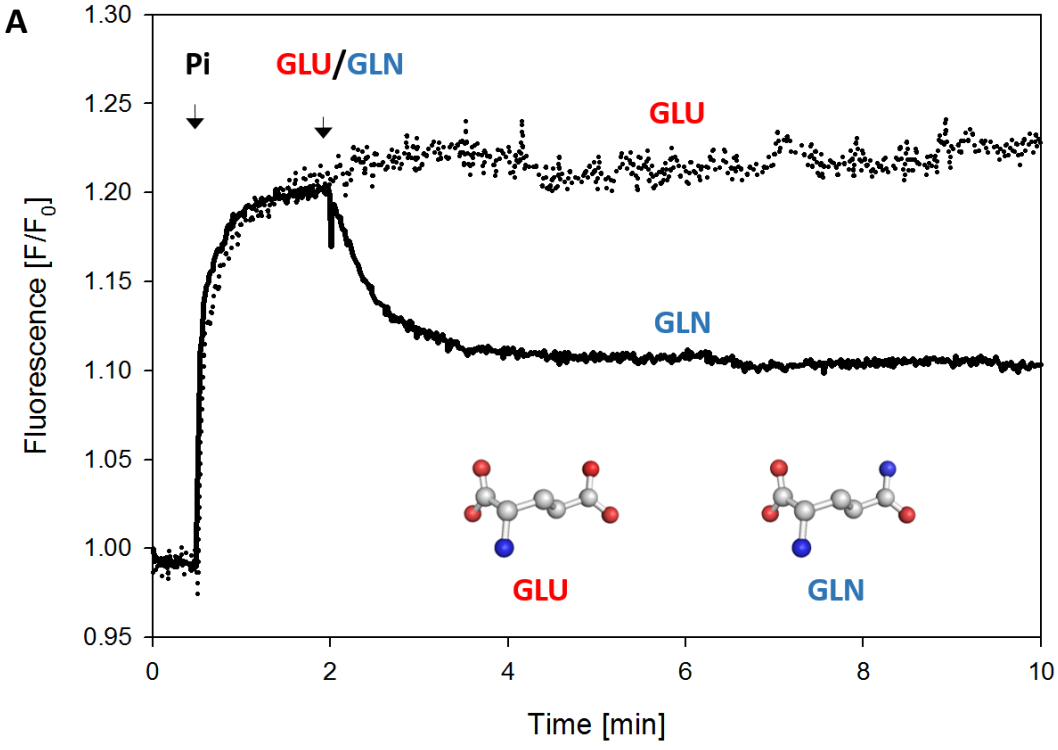
A
Pi
GLU/GLN
GLU
GLN
GLU
GLN
Fluorescence [F/F0]
Time [min]
1.30
1.25
1.20
1.15
1.10
1.05
1.00
0.95
0
2
4
6
8
10

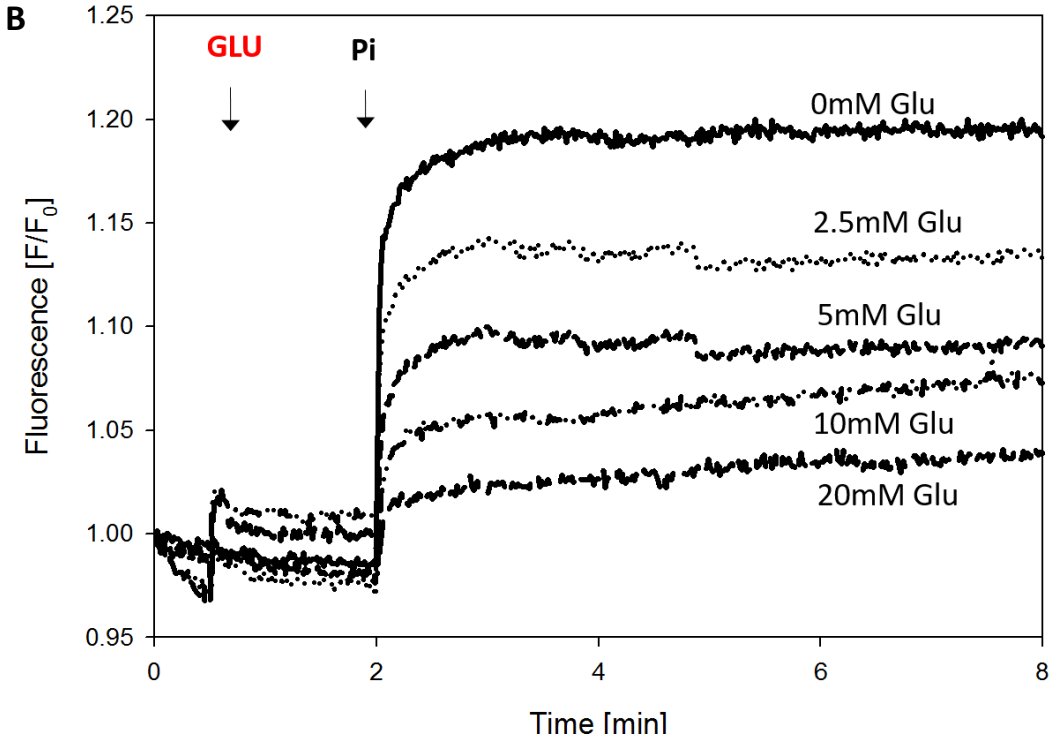
B
GLU
Pi
0mM Glu
2.5mM Glu
5mM Glu
10mM Glu
20mM Glu
Fluorescence [F/F0]
Time [min]
1.25
1.20
1.15
1.10
1.05
1.00
0.95
0
2
4
6
8

Active site tryptophan substitution at GAC tyrosine 471 as a reporter for glutamine binding.

After close examination of the active site of GAC aided by available crystallographic data, residues S291 and Y471 were observed to form hydrogen bonds with glutamine's amide group (shown in **Fig.3.3 A**). These residues have been previously shown to be critical for the catalysis of glutamine (18). Since the tryptophan side chain is relatively bulky and substrate binding is predicted to be sensitive to small alterations in the size of the binding pocket, we chose to mutate Y471 to tryptophan as tyrosine and tryptophan are comparable in size. We initially analyzed the fluorescence emission of the GAC(Y471W) mutant before and after the addition of glutamine. We found that glutamine induced a significant quenching in the tryptophan fluorescence of the GAC(Y471W) mutant, whereas it did not change the fluorescence emission of wild-type GAC(WT) (**Fig.3.3 B**). We then used the GAC(Y471W) mutant for real time binding experiments much like with the GAC(F327W) mutant. We found that 20 mM glutamine quenched tryptophan fluorescence by 50% while the same concentration of glutamate reduced fluorescence by only 5% (**Fig.3.3 C**). There was no change in the extent of quenching when the glutamate concentration was increased to 20 mM. These results demonstrate that GAC(Y471W) can distinguish between glutamine and glutamate binding by virtue of the differences between substrate and product binding. Real-time NADH fluorescence assays used to assess GAC activity revealed that this mutant GAC(Y471W) possesses neither basal nor phosphate stimulated enzymatic activity (**Fig.3.3 D**). This indicates that the fluorescence quench

we observe with the addition of glutamine to GAC(Y471W) represents substrate binding in real time. Thus, it allows us to monitor substrate binding uncoupled from other events associated with catalysis. Upon examining the available crystallographic data, a comparison of the glutamine and glutamate bound glutaminase structures reveals the likely molecular contact responsible for the glutamine-specific tryptophan changes. The ability of the GAC(Y471W) mutation to read-out glutamine but not glutamate binding is likely due to the interactions of the amine group from the glutamine side chain with the aromatic indole side-chain of the substituted tryptophan.

Figure 3.3 GAC(Y471W) can selectively read out glutamine binding. A. X-ray crystal structure of wild-type GAC bound to the substrate glutamine/product glutamate (PDB: 3SS5). As one of the essential amino acids at the active site, Y471 forms a hydrogen bond with the amine group of the substrate glutamine. The tryptophan as a substitution of tyrosine is shown in grey. The activation loop is highlighted with a dashed line. **B&C,** GAC(Y471W) selectively reads out glutamine binding but not that of glutamate. GAC(Y471W) (200 nM) fluorescence as a binding assay for glutamine. Addition of 20 mM glutamine (dashed line) compared to glutamate (solid line). **(D)** Phosphate-stimulated GAC activity (Y471W vs. WT GAC). Real time NADH assays of GAC activity, where the increased NADH fluorescence results from the coupled reaction where GAC catalyzes the hydrolysis of glutamine to glutamate, and GDH converts glutamate to α-ketoglutarate, and reduces NAD^+ to NADH. GAC: 50 nM, glutamine: 20 mM, phosphate: 50mM.

A

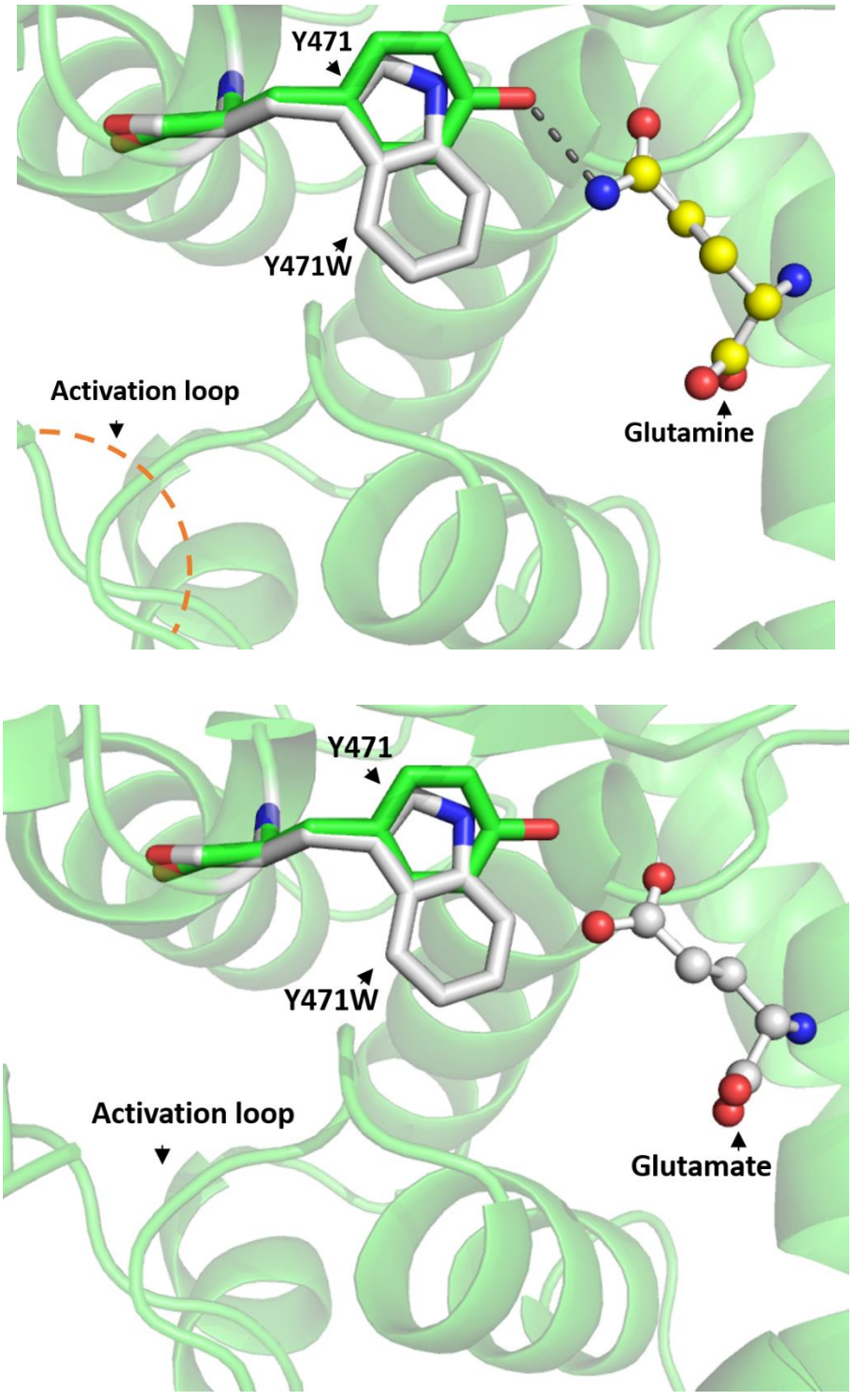
Y471
Y471W
Activation loop
Glutamine
Y471
Y471W
Activation loop
Glutamate

B

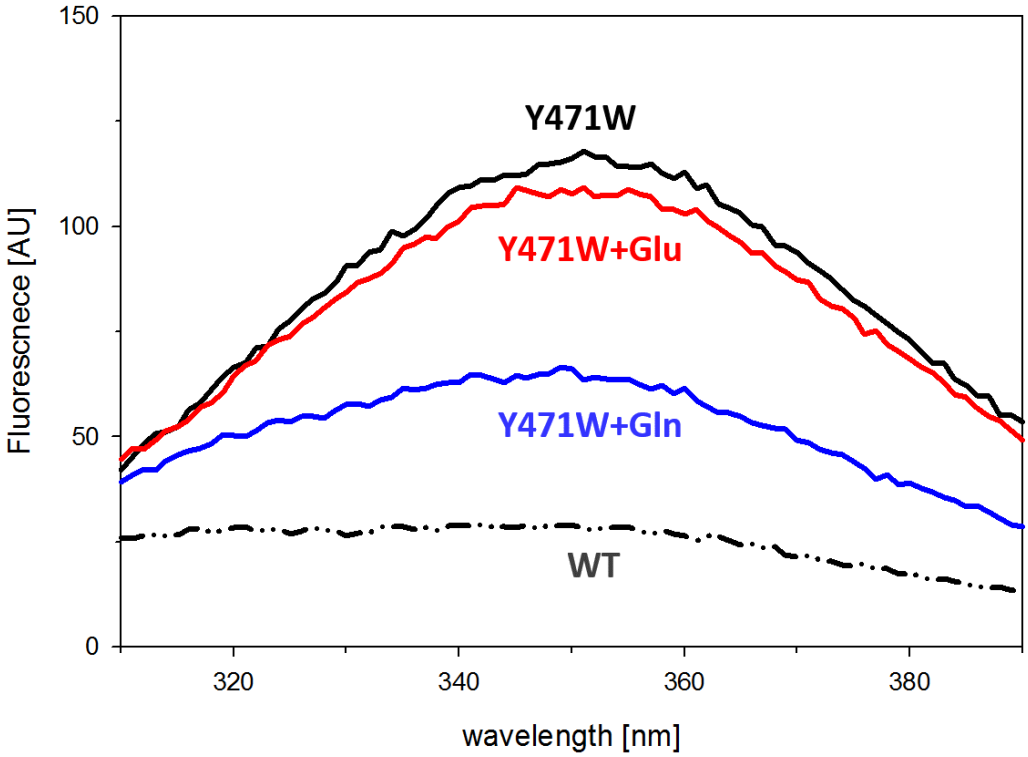
150
100
50
0
Fluorescnece [AU]
Y471W
Y471W+Glu
Y471W+Gln
WT
320
340
360
380
wavelength [nm]

C

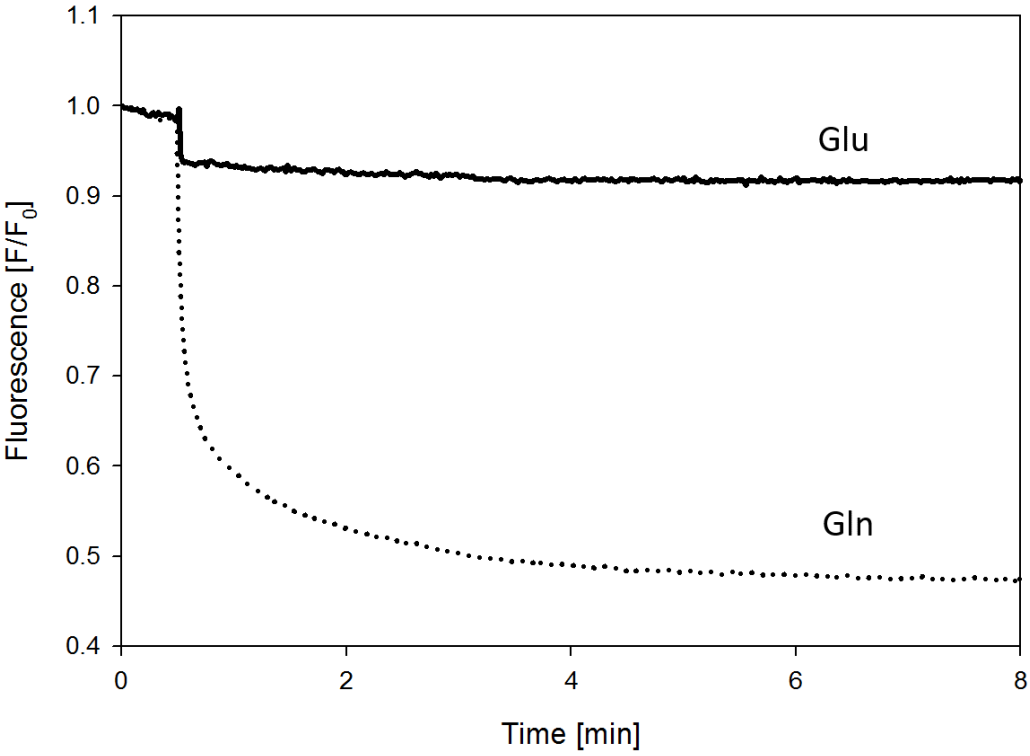
1.1
1.0
0.9
0.8
0.7
0.6
0.5
0.4
Fluorescence [F/F0]
Glu
Gln
0
2
4
6
8
Time [min]

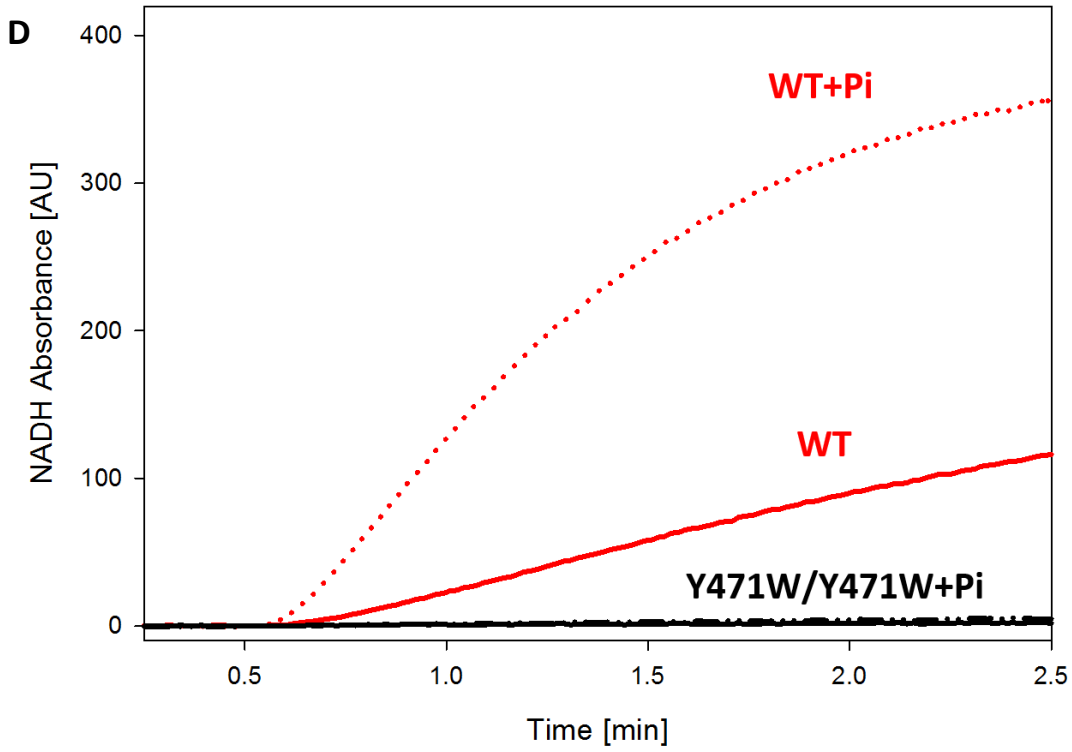
D
400
300
200
100
0
NADH Absorbance [AU]
WT+Pi
WT
Y471W/Y471W+Pi
0.5
1.0
1.5
2.0
2.5
Time [min]

The GAC(Y471W) fluorescence was titrated with increasing concentrations of glutamine where the fluorescence quenching was dose-dependent. As the glutamine concentration was increased from 2.5 to 20 mM, quenching induced by the addition of glutamine increased (**Fig.3.4 A**). Each glutamine concentration reached equilibrium within 8 minutes, with lower concentrations of the substrate displaying slower binding kinetics than higher concentrations (2.5 mM glutamine binding was complete within 8 minutes compared to 20 mM glutamine which required 2 minutes) (**Fig.3.4 B**). By plotting the percentage quenching versus glutamine concentration at equilibrium, we were able to derive a K_d for substrate binding to GAC of 2.5 mM, which is in good agreement with the K_m determined from an initial rate analysis (15). Using the tryptophan fluorescence readout of the GAC(Y471W) mutant, we applied the approach to directly compare the kinetics and binding efficiency of glutamine in the presence of different allosteric inhibitors and activators.

Phosphate allosterically regulates GAC substrate affinity.

As described above, the addition of various inorganic anions can stimulate GAC activity. Among these, the most potent activator is phosphate and, according to the limited crystallographic information, the putative binding site for these anions is near the activation loop (15). However, due to the absence of a fully activated GAC structure, the mechanism of how these bound ions activate the enzyme has remained obscure. In order to investigate whether these activators can affect glutamine binding, the GAC(Y471W) mutant was used as a reporter to monitor the

Figure 3.4 GAC(Y471W) is a spectroscopic reporter of bound substrate (glutamine) for the enzyme A, Concentration dependence of the glutamine induced tryptophan fluorescence change of GAC(Y471W) (300 nM). **B,** Glutamine concentration vs. percentage of quenching induced by adding glutamine.

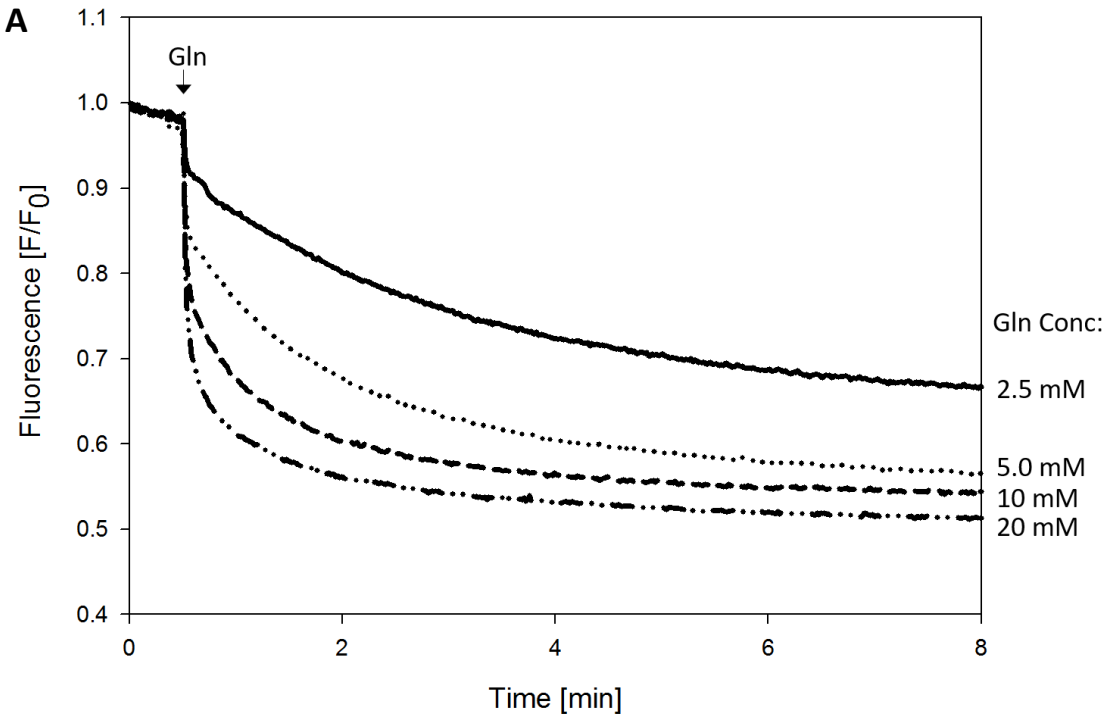
A
Gln
Fluorescence [F/F0]
Time [min]
Gln Conc:
2.5 mM
5.0 mM
10 mM
20 mM

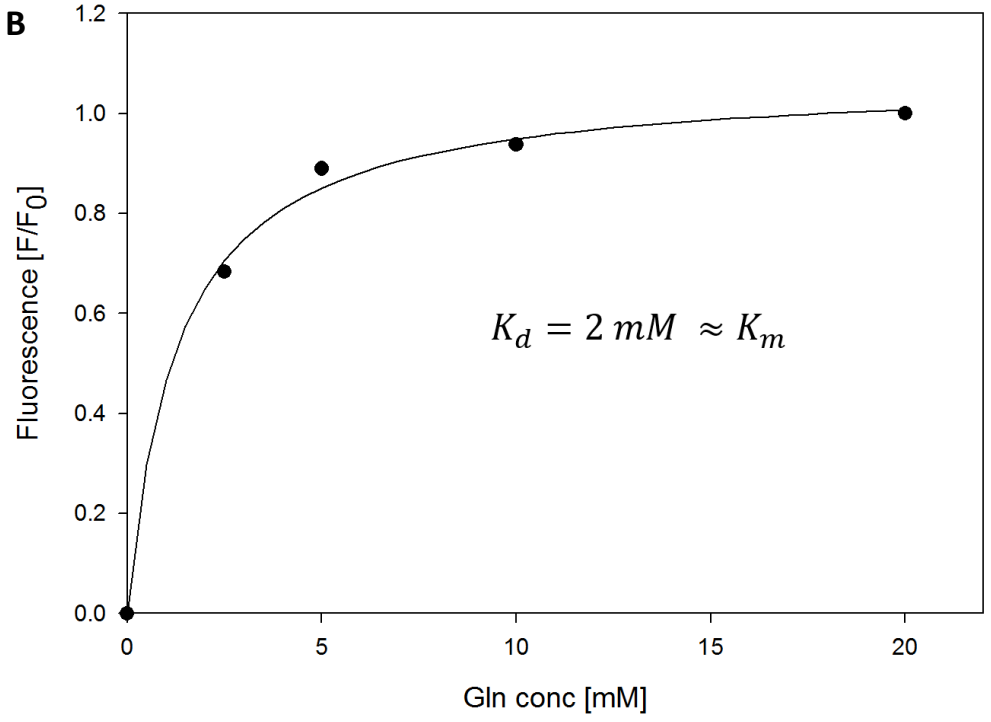
B
Fluorescence [F/F0]
Gln conc [mM]
$K_d = 2\ mM \approx K_m$

changes in glutamine binding that may result from the addition of activators such as phosphate.

Typically, the experiment depicted was carried out at a GAC concentration of 50 nM. In the time course shown, 50 mM phosphate was added to the solution prior to the introduction of glutamine. After 90 sec of incubation of GAC(Y471W) with phosphate, the fluorescent signal stabilized before increasing concentrations of glutamine were added. The effect of phosphate on glutamine binding is illustrated by the kinetic trace in **Fig.3.5 A**, which was performed as above except that at 30 sec there was no phosphate added into the cuvette. At a concentration of glutamine commensurate with the observed K_d (3.8 mM), 50 mM phosphate significantly accelerated substrate binding (**Fig.3.5 B**). Once stabilized, the fluorescence signal under conditions with phosphate added was quenched by about 40%, while the condition without phosphate was quenched by less than 30%. This means that, in addition to accelerating the process of glutamine binding, phosphate appears to increase the glutamine affinity and elevate the amount of substrate bound at equilibrium. Interestingly, these phosphate-induced differences were diminished as the concentration of GAC was increased.

In order to understand the mechanism by which phosphate enhances glutamine binding, we sought to determine possible phosphate binding effects on the enzyme structure. Based on previous SEC-MALS results, it is known that at this concentration (50 nM), GAC is present as a mixture of dimeric and tetrameric forms

(19). The dimeric state is completely inactive while the tetramer has a level of basal activity and can be further stimulated by phosphate. Also, based on the SEC-MALS data presented in Chapter II (**Fig. 2.3**), phosphate binds to and stabilizes the tetrameric form of GAC, which shifts the GAC distribution towards the higher oligomeric state. In order to understand how phosphate might influence glutamine binding, we set out to test how the dimeric and tetrameric versions of GAC compare with regard to their ability to bind substrate. If dimeric GAC has a weaker affinity for glutamine, then the observed higher affinity following phosphate addition may be due to a shift to the higher affinity glutamine-binding tetrameric species. Alternatively, if dimeric GAC binds glutamine with a similar affinity as the tetramer, phosphate binding may be enhancing substrate binding by inducing conformational changes in the dimeric form, presumably in the glutamine binding cleft.

To investigate which model is correct, a constitutively dimeric form of GAC, GAC(D391K) was constructed in the GAC(Y471W) background and tested in the tryptophan fluorescence reporter experiments. **Fig.3.5 C** shows that the constitutively dimeric form of GAC ablated the ability of glutamine to induce a change in the tryptophan fluorescence with or without phosphate at this enzyme concentration (200 nM). Taken together, these data suggest that, in the presence of phosphate, the dimer-tetramer equilibrium is shifted towards the high affinity glutamine binding tetramer. Because phosphate binding is unable to overcome the repulsive charge introduced by the GAC(D391K) mutation, the tetrameric species cannot form. Without the proper

engagement of opposing dimers, the activation loop at this interface is not positioned in a manner that allows high affinity glutamine binding at the active site (see below). However, it remains unclear whether the ability of the tetramer to bind glutamine is further enhanced by the presence of phosphate.

The competition between substrate and product binding detected by using GAC(Y471W).

As presented earlier, GAC(Y471W) does not respond to the addition of glutamate, however the binding of glutamate can still be detected through its inhibition of phosphate binding (**Fig.3.2 B**). Since both the substrate and product occupy the same binding pocket, we wondered whether the binding of glutamate can inhibit the binding of glutamine. We first performed a competitive binding assay between glutamine and glutamate. **Fig.3.6 A** presents the fluorescence signal change after addition of 5 mM glutamine to 300 nM of GAC(Y471W), with increasing concentrations of glutamate added 90 seconds prior. It is observed that the amount of quenching of GAC(Y471W) induced by addition of glutamine decreased as the concentration of glutamate in solution was increased. This result indicated that, binding of glutamine can be blocked by the addition of glutamate. As discussed earlier in Chapter III, phosphate is an activator that can enhance the binding of glutamine, whereas the binding of phosphate can also be blocked by the addition of glutamate.

Figure 3.5 Allosteric activator phosphate enhances glutamine binding to the enzyme through stabilizing the tetrameric form of GAC. **A,** Comparison of the tryptophan fluorescence change with added glutamine at a low concentration of GAC(Y471W) (50 nM) with and without 50 mM phosphate. **B,** Titration of GAC(Y471W) glutamine with a least squares fit of the binding data. **(C)** GAC(D391K, Y471W) does not respond to the addition of glutamine even in the presence of phosphate. Fluorescence assay of GAC(Y471W) vs. GAC(D391K, Y471W) after addition of 50 mM phosphate and 20 mM glutamine. Phosphate was added 90 s prior to addition of glutamine into the solution with 200 nM GAC(Y471W) and GAC(D391K, Y471W).

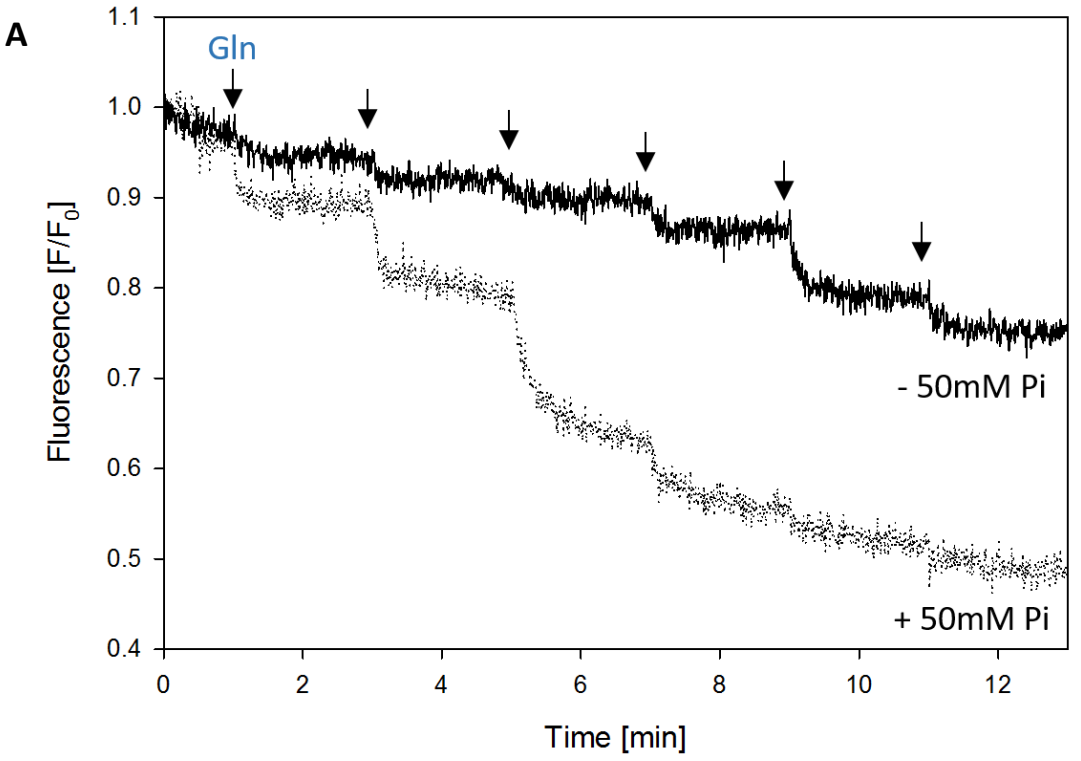
A
Gln
Fluorescence [F/F0]
Time [min]
- 50mM Pi
+ 50mM Pi

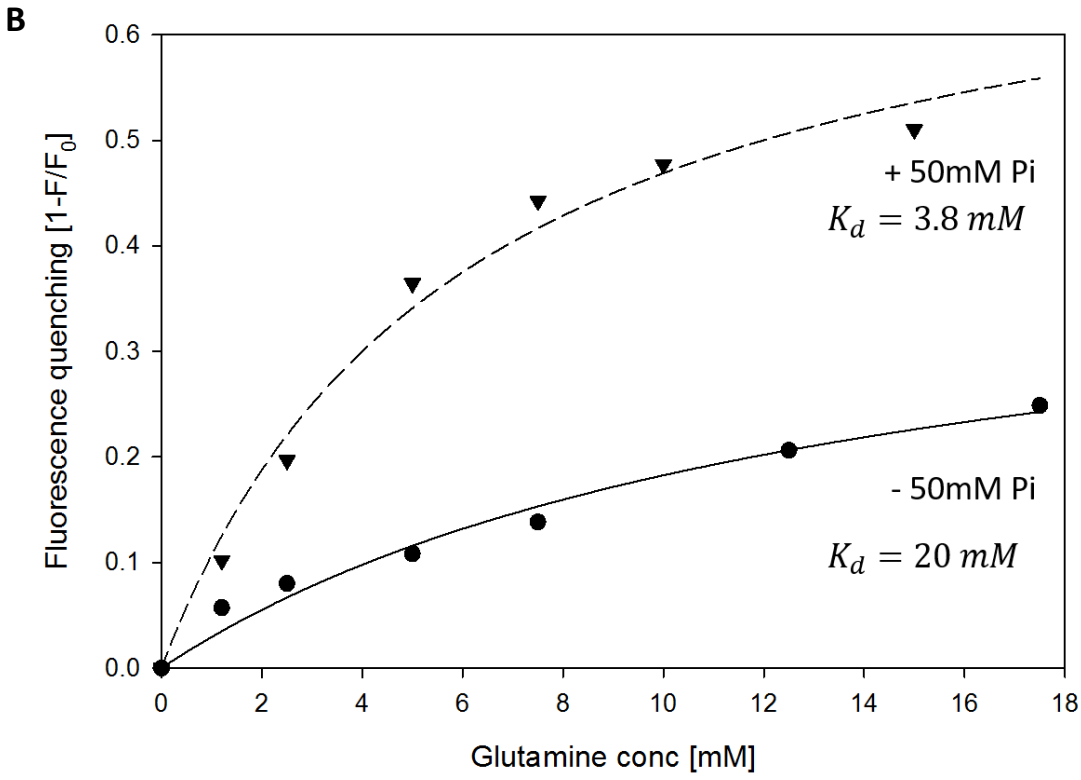
B
Fluorescence quenching [1-F/F0]
Glutamine conc [mM]
+ 50mM Pi
$K_d = 3.8\ mM$
- 50mM Pi
$K_d = 20\ mM$

C

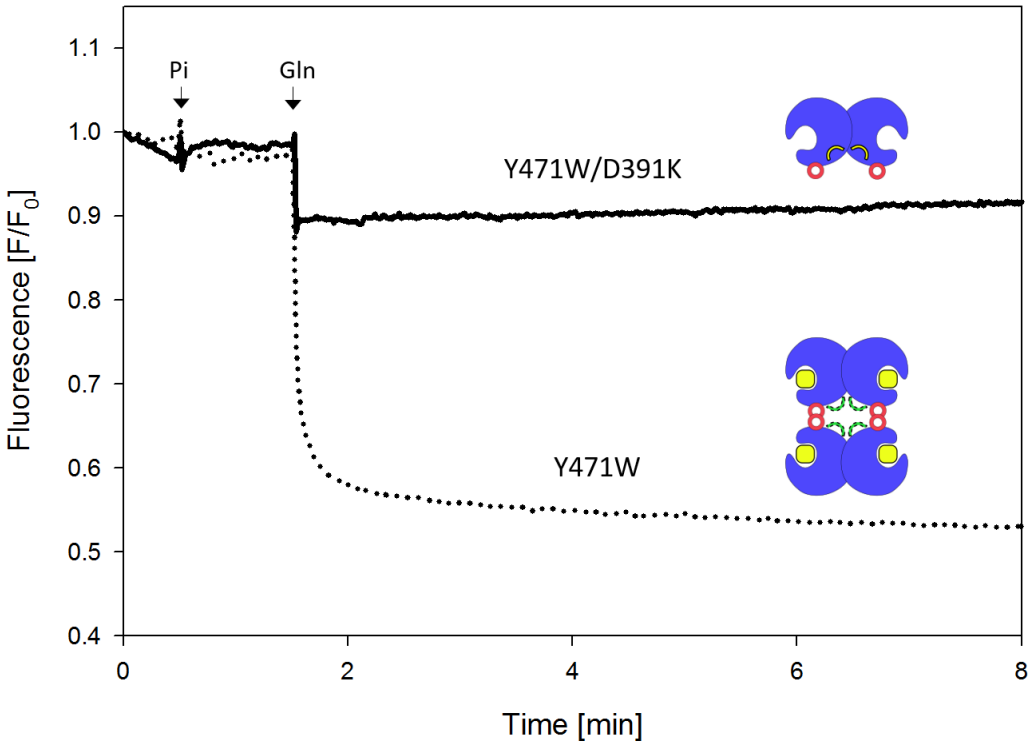
Pi
Gln
Y471W/D391K
Y471W
Fluorescence [F/F0]
Time [min]
1.1
1.0
0.9
0.8
0.7
0.6
0.5
0.4
0
2
4
6
8

Thus, we examined how glutamate and phosphate together might affect the binding of substrate (glutamine) to the enzyme. **Figures 3.6A,B** show the change in fluorescence signal of 300 nM GAC(Y471W) induced by addition of 5 mM glutamine with 50 mM phosphate present or absent and increasing concentrations of glutamate added to block glutamine binding. From the decreasing degree of quenching upon glutamine binding, an approximate K_i for product (glutamate) binding is estimated to be ~125 mM and is insensitive to the presence of phosphate. This is likely due to the degree of preformed tetramers at this concentration of GAC, which, as discussed below, are predicted to bind glutamate with a low affinity. In contrast, when the same experiment is carried out under conditions of low GAC(Y471W) (i.e., 50nM), the proportion of dimeric GAC is much greater even in the presence of 50 mM phosphate, allowing the same concentrations of glutamate to more effectively block glutamine binding (**Figure 3.6C**).

Effect of a small molecule inhibitor on glutamine binding to GAC(Y471W).

A number of allosteric inhibitors of GAC activity have been developed and shown to slow the growth of certain glutamine-addicted cancer cell lines (1, 20, 2). For one of these molecules, BPTES, there are several crystal structures revealing the binding site for this class of inhibitors as the activation loop at the tetramer surface as described in Chapter II. However, as of yet, the precise molecular mechanism of inhibition remains unclear. The GAC(Y471W) mutant provides a way to investigate one aspect of this question by addressing whether these inhibitors function by influencing substrate binding.

Figure 3.6 Glutamate as a product competes with glutamine binding to GAC. A,. Increasing concentrations of glutamate block the tryptophan quenching induced by glutamine (5 mM). The GAC(Y471W) concentration was 300 nM. Glutamate concentrations as indicated were pre-incubated prior to the addition of 5 mM glutamine. **B,** Same conditions as in **A** except for the prior addition of 50 mM phosphate. **C,** Under conditions of low (50 nM) GAC(Y471W), glutamate is more effective at blocking glutamine binding. Glutamate was added as indicated prior to the addition of 50 mM phosphate followed by 5 mM glutamine.

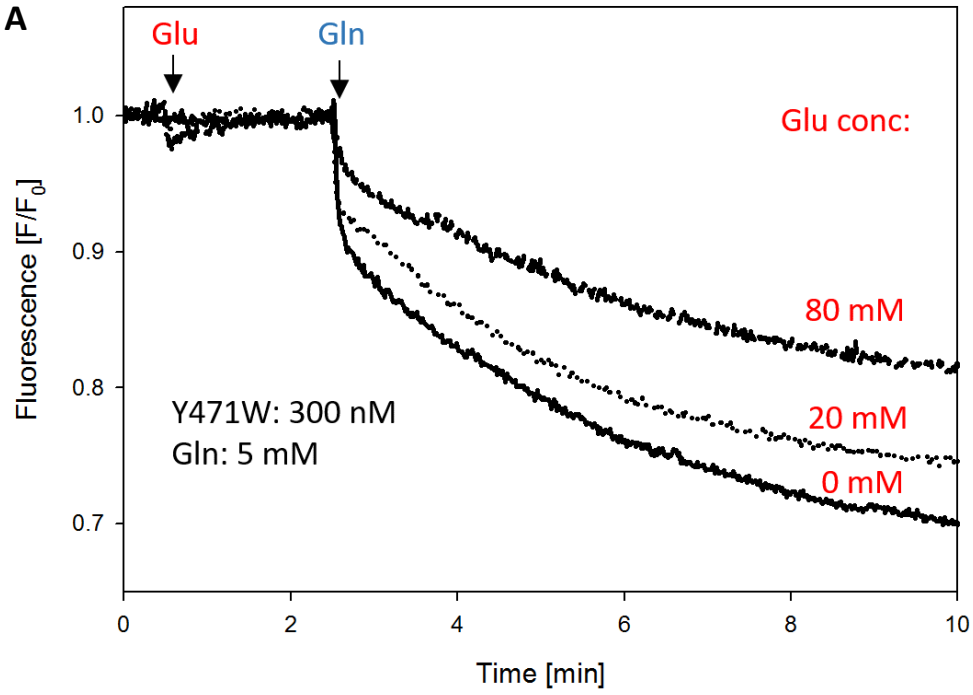
A
Glu
Gln
Glu conc:
80 mM
20 mM
0 mM
Y471W: 300 nM
Gln: 5 mM
Fluorescence [F/F0]
Time [min]
1.0
0.9
0.8
0.7
0
2
4
6
8
10

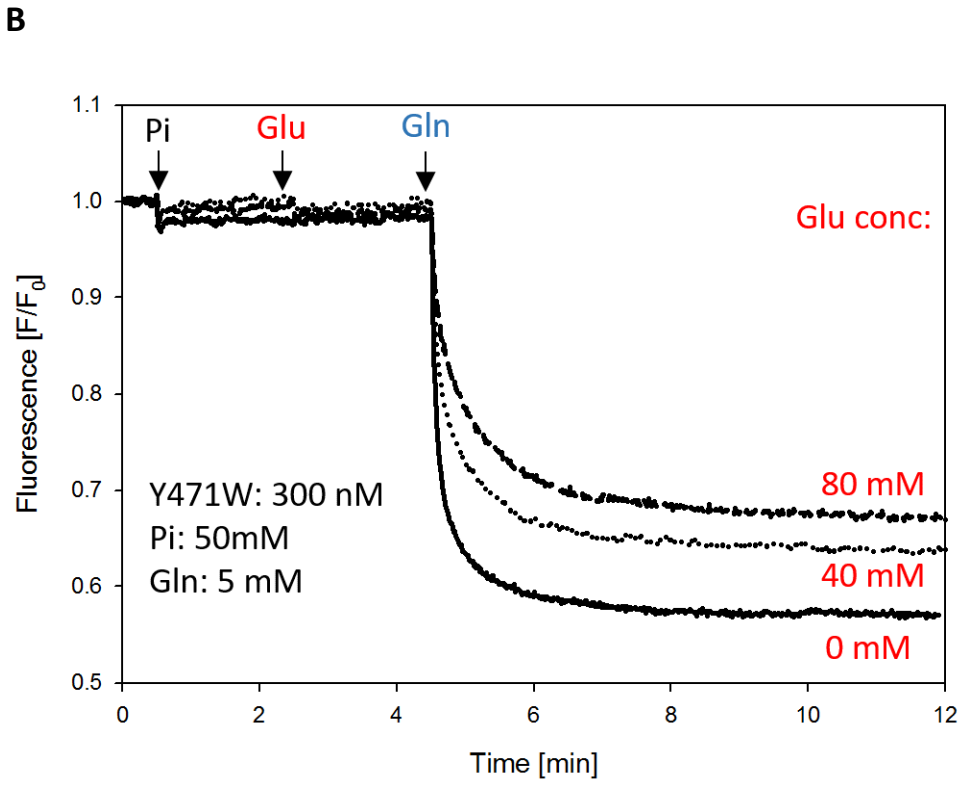
B
Pi
Glu
Gln
Glu conc:
80 mM
40 mM
0 mM
Y471W: 300 nM
Pi: 50mM
Gln: 5 mM
Fluorescence [F/F0]
Time [min]
1.1
1.0
0.9
0.8
0.7
0.6
0.5
0
2
4
6
8
10
12

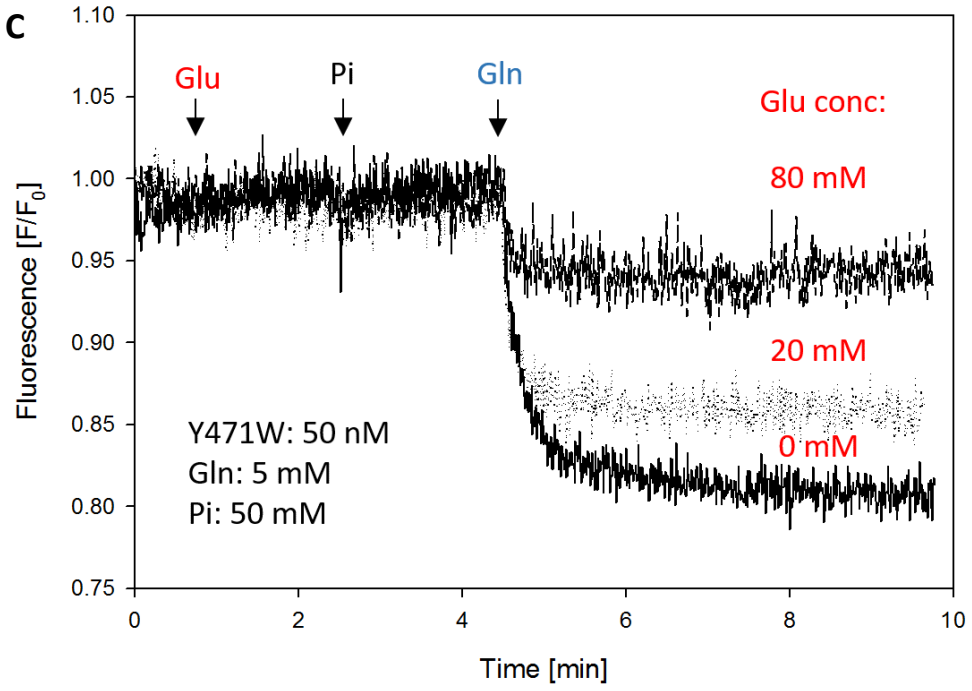
C
Glu
Pi
Gln
Glu conc:
80 mM
20 mM
0 mM
Y471W: 50 nM
Gln: 5 mM
Pi: 50 mM
Fluorescence [F/F0]
Time [min]
1.10
1.05
1.00
0.95
0.90
0.85
0.80
0.75
0
2
4
6
8
10

We began our studies of inhibitor effects on GAC(Y471W) tryptophan fluorescence with the allosteric inhibitor, CB-839, an analog of BPTES. CB-839 binds at the interface where two GAC dimers come together to form a tetramer and has been well-studied in *vivo*, currently undergoing clinical trials for treatment of triple negative breast cancer (5, 21). To test the effect of CB-839, in the real time fluorescence assay for glutamine binding, at 30 sec, we added CB-839 to 200 nM GAC(Y471W) and followed with the addition of 20 mM glutamine. Unlike anion activators (i.e., phosphate, sulfate), which do not have any effect on the GAC(Y471W) fluorescence signal by themselves, the addition of CB-839 resulted in a relatively small quench in tryptophan fluorescence (**Fig3.7 A**). Both the initial quench due to CB-839 and the subsequent quench due to glutamine addition were dependent on CB-839 concentration (**Fig.3.7 B**) and inversely correlated well with each other (**Fig.3.7 C**). The apparent IC_{50} of CB-839 was about 100 nM, agreeing well with previous direct binding assays and measurements using the glutaminase inhibition assay (22). The results shown in **Fig. 3.7** suggest that CB-839 functions by antagonizing the ability of GAC to bind glutamine and by this means inhibits its activity.

Taken together, these data suggest that CB-839 attenuates GAC activity by inhibiting substrate binding. However, the physical details remain unclear as the crystallographic data reveals that the distance between the CB-839 binding site (i.e., the activation loop) and the active site is about 12 Å, indicating an absence of a direct interaction between residues at each locus. Furthermore, on the opposite side of the

active site's water channel, there is a lid structure identified in Chapter II that allows easy access of glutamine. This makes it difficult to envision that a constraining conformational change at the activation loop following CB-839 binding would provide a direct block of glutamine binding as has been proposed (15). However, as discussed in Chapter II, there is good evidence for communication between the two sites via a peptide linkage, suggesting that a conformational change at the activation loop likely results in conformational changes in the glutamine binding pocket that in turn regulate glutamine binding affinity and, by this manner, give rise to the observed effects on glutaminase activity.

Figure 3.7 Allosteric inhibitor CB-839 reduces GAC activity by inhibiting substrate binding to the enzyme. A, Changes in GAC Y471W tryptophan fluorescence provide an assay to observe the influence of BPTES like molecules on glutamine binding. **B,** Addition of increasing concentrations of CB-839 reduces the degree of quenching induced by the addition of 20 mM glutamine. The concentration of GAC(Y471W) was 200 nM for all traces. **C,** The decrease of a glutamine induced quench is inversely correlated with the increase of the CB-839 dependent fluorescence quench.

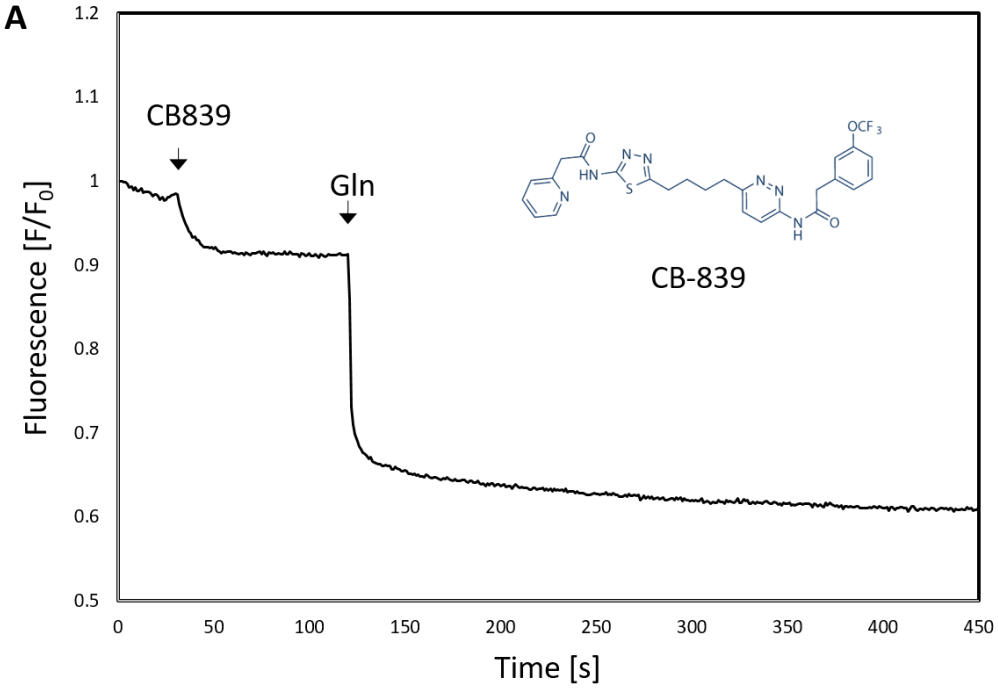
A
CB839
Gln
CB-839
Fluorescence [F/F0]
Time [s]
1.2
1.1
1
0.9
0.8
0.7
0.6
0.5
0
50
100
150
200
250
300
350
400
450

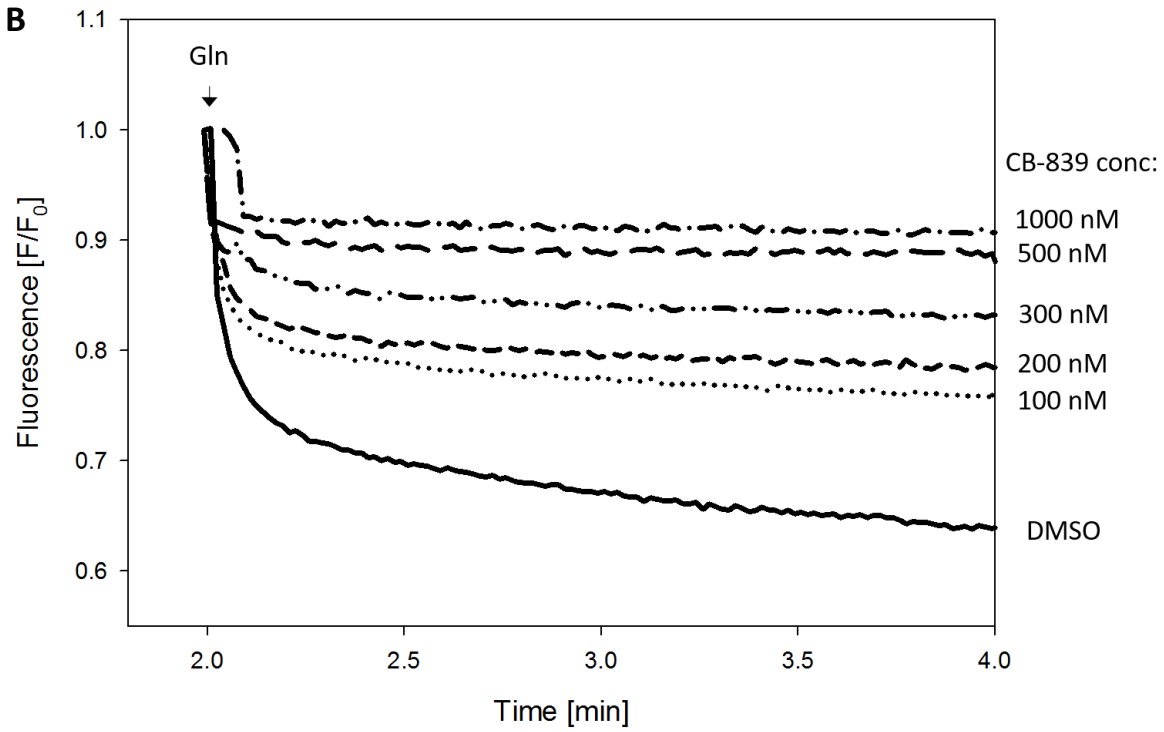
B
Gln
CB-839 conc:
1000 nM
500 nM
300 nM
200 nM
100 nM
DMSO
Fluorescence [F/F0]
Time [min]
1.1
1.0
0.9
0.8
0.7
0.6
2.0
2.5
3.0
3.5
4.0

C

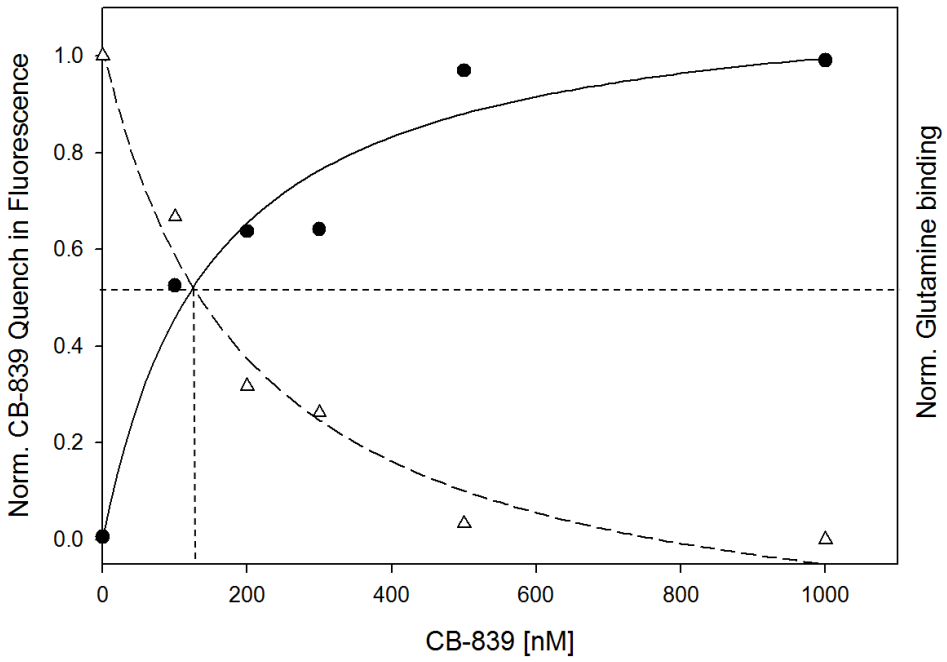
Norm. CB-839 Quench in Fluorescence
Norm. Glutamine binding
CB-839 [nM]
0.0
0.2
0.4
0.6
0.8
1.0
0
200
400
600
800
1000

DISCUSSION

Previous studies of tryptophan fluorescence as a readout of GAC conformational dynamics in the activation loop have provided a useful tool to monitor the binding of allosteric inhibitors (BPTES like molecules) and activators (phosphate) that interact proximal to the activation loop (19). Available structural data indicate that the distance between the activation loop and active site is approximately 12 Å, raising the question as to the mechanism by how activators and inhibitors near the activation loop communicate with the active site. Besides serving as a readout for inhibitor and activator binding at the activation loop, GAC(F327W) also distinguishes the binding of substrate (glutamine) and product (glutamate) by displaying a greater fluorescence increase with the former. This observation suggests that there is intramolecular communication between the activation loop and the active site. The implication is that glutamine binding at the active site affects the conformation of the activation loop and alters the microenvironment of F327W, which was reflected on the quenching of the fluorescence signal.

The observation that the GAC(F327W) tryptophan fluorescence signal selectively responds to glutamine binding led us to ask whether a tryptophan positioned in the GAC active site could serve as a sensor to detect changes between substrate (glutamine) and product (glutamate) binding as well. An analysis of the available structural data suggested that Y471 was an attractive candidate since the side chain –OH group of tyrosine formed a hydrogen bond with the amide group of the

bound glutamine side chain, which is oxidized to a carboxyl group in glutamate. As we have shown in this chapter, the GAC(Y471W) mutant exhibited a significant amount of fluorescence quenching (about 50%) with the addition of 20 mM glutamine, while there is less than 5% of quenching when 20 mM glutamate was added to the same concentration of GAC(Y471W). The observed difference in fluorescence quenching between substrate and product is mostly likely due to the charge difference between the amide group of glutamine and the carboxyl group of glutamate when they interact with the indole moiety of tryptophan 471. Tryptophan does not have the –OH group present in its sidechain needed to form the hydrogen bond with the substrate and position the H_2O molecule needed for the hydrolysis reaction. As a consequence, Y471W is able to bind glutamine but cannot carry out the catalytic deamination of glutamine. The loss of catalytic activity is illustrated by the results from the real time assay of Y471W when compared with wild-type GAC, where Y471W did not show any catalytic activity even with the addition of 50 mM phosphate (**Fig.3.4 A**). The GAC(Y471W) loss of activity was, in fact, advantageous, as it allowed us to uncouple substrate binding from hydrolysis, and made it possible to monitor directly substrate binding.

Having a tool in hand to monitor substrate binding, we proceeded to investigate whether different allosteric inhibitors and activators affect GAC activity by influencing glutamine binding. For the activator phosphate, the titration of GAC with glutamine in the presence of phosphate exhibited a significantly higher affinity of

glutamine for GAC(Y471W) than in the absence of phosphate (3.8 mM, 20 mM respectively). This result further supports a model where the conformational change that is induced by the addition of phosphate, indicated by the fluorescence changes in GAC(F327W) (**Fig.3.5 B**), altered the GAC-substrate binding interaction. Due to the lack of available phosphate bound GAC structures, the conformational change caused by phosphate binding remains speculative. However, based on earlier observations of phosphate driven oligomerization of GAC (23), phosphate binding has the duel effect of activating the enzyme and stabilizing its tetrameric form. Both tryptophan fluorescence and isothermal calorimetry demonstrate that the wild type GAC, but not the constitutively dimeric form of GAC(D391K), has the ability to bind glutamine. Therefore, the observed phosphate dependent enhancement of glutamine binding is likely a reflection of the shift from dimer to tetramer upon the addition of phosphate. Under the conditions of the fluorescence assay, the concentration of GAC was typically 50 nM and therefore a mixture of dimer and tetramer. Addition of phosphate increases the amount of tetramer and shifts the size distribution of the GAC population towards the higher affinity, active enzyme complex. This result provides evidence to explain how inorganic phosphate activates GAC by promoting high affinity substrate binding. As noted above, since the distance between the activation loop (the likely binding site for inorganic phosphate) and the substrate binding cleft is ~12 Å, it is likely that there is communication between the activation loop and the phosphate binding site via a peptide linker that acts as a conduit of communication between the two sites. It will

be of interest to see if the linker mutation described in Chapter II (GAC(G320A)) would uncouple phosphate binding from high affinity glutamine binding.

For the BPTES like inhibitors, GAC(Y471W) tryptophan fluorescence responded to the addition of the drug itself in a dose dependent quench, which at saturation is approximately 20% of the total fluorescence signal. This result is consistent with the observation made in Chapter II that, the conformational change of the activation loop can affect the active site and therefore would be predicted to influence the microenvironment of tryptophan 471. As shown in **Fig.3.6 B**, when the concentration of the inhibitor CB-839 is increased, the tryptophan fluorescence change induced by the same amount of glutamine (20 mM) was significantly decreased. Overall, these results suggest that the activation loop, which is locked into an inactive conformation by CB-839 binding, prevents glutamine from binding to the active site and in this way inhibits GAC activity.

In conclusion, the results presented here show that Y471W provides a tool for directly monitoring substrate binding to GAC. Our results reveal that the activation loop serves as a switch that regulates substrate affinity. Activators such as inorganic phosphate position the switch to enhance glutamine binding while inhibitors such as BPTES and CB-839 constrain the switch and block glutamine binding. In summary, we propose a model whereby the regulation of GAC activity entails a two-way communication between the activation loop and active site substrate binding cleft that

reciprocally sense each site's conformational changes, with the ultimate outcome of dictating glutamine affinity, which in turn, determines GAC glutaminase activity.

References

1. Wang, J., Erickson, J. W., Fuji, R., Ramachandran, S., Gao, P., Dinavahi, R., Wilson, K. F., Ambrosio, A. L. B., Dias, S. M. G., Chi, V., and Cerione, R. A. (2011) Targeting mitochondrial glutaminase activity inhibits oncogenic transformation. **18**, 207–219

2. Erickson, J. W., and Cerione, R. a (2010) Glutaminase: a hot spot for regulation of cancer cell metabolism? *Oncotarget*. **1**, 734–740

3. Levine, A. J., and Puzio-Kuter, A. M. (2010) The Control of the Metabolic Switch in Cancers by Oncogenes and Tumor Suppressor Genes. *Science (80-.).* **330**, 1340–1344

4. Robinson, M. M., McBryant, S. J., Tsukamoto, T., Rojas, C., Ferraris, D. V, Hamilton, S. K., Hansen, J. C., and Curthoys, N. P. (2007) Novel mechanism of inhibition of rat kidney-type glutaminase by bis-2-(5-phenylacetamido-1,2,4-thiadiazol-2-yl)ethyl sulfide (BPTES). *Biochem. J.* **406**, 407–14

5. Gross, M. I., Demo, S. D., Dennison, J. B., Chen, L., Chernov-Rogan, T., Goyal, B., Janes, J. R., Laidig, G. J., Lewis, E. R., Li, J., MacKinnon, A. L., Parlati, F., Rodriguez, M. L. M., Shwonek, P. J., Sjogren, E. B., Stanton, T. F., Wang, T., Yang, J., Zhao, F., and Bennett, M. K. (2014) Antitumor Activity of the Glutaminase Inhibitor CB-839 in Triple-Negative Breast Cancer. *Mol. Cancer Ther.* **13**, 890–901

6. Ahmadian, M. R., Wittinghofer, A., and Herrmann, C. (2002) Fluorescence methods in the study of small GTP-binding proteins. *GTPase Protoc.* **189**, 45–63

7. Antonny, B., Chardin, P., Roux, M., and Chabre, M. (1991) GTP Hydrolysis Mechanisms in ras p21 and in the ras-GAP Complex Studied by Fluorescence Measurements on Tryptophan Mutants. *Biochemistry*. **30**, 8287–8295

8. Annis, D. S., Mosher, D. F., and Roberts, D. D. (2009) Using tryptophan fluorescence to measure the stability of membrane proteins folded in liposomes. **27**, 339–351

9. Ghisaidoobe, A., and Chung, S. (2014) Intrinsic Tryptophan Fluorescence in the Detection and Analysis of Proteins: A Focus on Förster Resonance Energy

Transfer Techniques. *Int. J. Mol. Sci.* **15**, 22518–22538

10. Lee, F. S., Auld, D. S., and Vallee, B. L. (1989) Tryptophan Fluorescence as a Probe of Placental Ribonuclease Inhibitor Binding to Angiogenin. *Biochemistry*. **28**, 219–224

11. Faurobert, E., Otto-bruc, A., and Chardin, P. (1993) Tryptophan W207 in transducin Tac is the fluorescence sensor of the G protein activation switch and is involved in the effector binding. **12**, 4191–4198

12. Swain, S. D., Helgerson, S. L., Davis, A. R., Nelson, L. K., and Quinn, M. T. (1997) Analysis of Activation-induced Conformational Changes in p47 phox Using Tryptophan Fluorescence Spectroscopy *. *J. Biol. Chem.* **272**, 29502–29510

13. Lee, J., Pilch, P. F., Shoelson, S. E., and Scarlata, S. F. (1997) Conformational changes of the insulin receptor upon insulin binding and activation as monitored by fluorescence spectroscopy. *Biochemistry*. **36**, 2701–8

14. Stalnecker, C. A., Erickson, J. W., and Cerione, R. A. (2017) Conformational changes in the activation loop of mitochondrial glutaminase C: A direct fluorescence readout that distinguishes the binding of allosteric inhibitors from activators. *J. Biol. Chem.* **292**, 6095–6107

15. Cassago, A., Ferreira, A. P. S., Ferreira, I. M., Fornezari, C., Gomes, E. R. M., Greene, K. S., Pereira, H. M., Garratt, R. C., Dias, S. M. G., and Ambrosio, A. L. B. (2012) Mitochondrial localization and structure-based phosphate activation mechanism of Glutaminase C with implications for cancer metabolism. *Proc. Natl. Acad. Sci.* **109**, 1092–1097

16. Thangavelu, K., Pan, C. Q., Karlberg, T., Balaji, G., Uttamchandani, M., Suresh, V., Schuler, H., Low, B. C., and Sivaraman, J. (2012) Structural basis for the allosteric inhibitory mechanism of human kidney-type glutaminase (KGA) and its regulation by Raf-Mek-Erk signaling in cancer cell metabolism. *Proc. Natl. Acad. Sci.* **109**, 7705–7710

17. Delabarre, B., Gross, S., Fang, C., Gao, Y., Jha, A., Jiang, F., Song J., J., Wei, W., and Hurov, J. B. (2011) Full-length human glutaminase in complex with an allosteric inhibitor. *Biochemistry*. **50**, 10764–10770

18. Thangavelu, K., Chong, Q. Y., Low, B. C., and Sivaraman, J. (2014) Structural basis for the active site inhibition mechanism of human kidney-type glutaminase (KGA). *Sci. Rep.* **4**, 3827

19. Stalnecker, C. A., Ulrich, S. M., Li, Y., Ramachandran, S., McBrayer, M. K., DeBerardinis, R. J., Cerione, R. A., and Erickson, J. W. (2015) Mechanism by which a recently discovered allosteric inhibitor blocks glutamine metabolism in transformed cells. *Proc. Natl. Acad. Sci.* **112**, 394–399

20. Manuscript, A. (2015) Glutaminase regulation in cancer cells: a druggable chain of events. **19**, 450–457

21. Xiang, Y., Stine, Z. E., Xia, J., Lu, Y., O'Connor, R. S., Altman, B. J., Hsieh, A. L., Gouw, A. M., Thomas, A. G., Gao, P., Sun, L., Song, L., Yan, B., Slusher, B. S., Zhuo, J., Ooi, L. L., Lee, C. G. L., Mancuso, A., McCallion, A. S., Le, A., Milone, M. C., Rayport, S., Felsher, D. W., and Dang, C. V. (2015) Targeted inhibition of tumor-specific glutaminase diminishes cell-autonomous tumorigenesis. *J. Clin. Invest.* **125**, 2293–2306

22. Stalnecker, C. A. (2016) *TARGETING ALTERED CANCER CELL METABOLISM: MITOCHONDRIAL GLUTAMINASE REGULATION AND INHIBITION BY SMALL MOLECULES*. Ph.D. thesis

23. Ferreira, A. P. S., Cassago, A., De Almeida Gon??alves, K., Dias, M. M., Adamoski, D., Ascen????o, C. F. R., Honorato, R. V., De Oliveira, J. F., Ferreira, I. M., Fornezari, C., Bettini, J., Oliveira, P. S. L., Leme, A. F. P., Portugal, R. V., Ambrosio, A. L. B., and Dias, S. M. G. (2013) Active glutaminase C self-assembles into a supratetrameric oligomer that can be disrupted by an allosteric inhibitor. *J. Biol. Chem.* **288**, 28009–28020

CHAPTER IV

SUMMARY AND PERSPECTIVE

The mitochondrial glutaminase (GLS) enzymes are responsible for catalyzing the first critical step in glutamine metabolism, specifically, the deamination of glutamine to form glutamate and ammonia (1). Since cancer cells often turn to glutamine as an alternative to glucose for a metabolic fuel, it is not surprising that many cancer cells exhibit a high level of GLS expression. This overexpression is particularly the case for the GLS splice variant GAC, which we and others have shown to be the predominant isozyme in transformed cells (2, 3). While there may be small molecule activators of GAC yet to be identified or, alternatively, post-translational modifications of GAC that regulate its enzymatic activity, the data regarding the observed activity of GAC can be attributed to its overexpression, which by mass action, shifts GAC from an inactive dimer to active tetramers and higher oligomers. How this quaternary reorganization of inactive GAC monomers and dimers results in active tetramers is the central question addressed in this thesis. This work was undertaken with the premise that a detailed understanding of the activation mechanism of GAC would lead to insights pertaining to the development of better small molecule inhibitors that ultimately would lead to improved chemotherapeutic strategies.

Previous studies of GAC activation had suggested that the tetrameric state of the enzyme is critical for activation (4). In fact, GAC was observed to undergo even higher order oligomerization when it is activated by the addition of multivalent inorganic anions (5). Whether or not these higher order oligomers are physiologically

relevant, they underscore the tendency of GAC to self-assemble after adopting an active conformation. In order to better understand the mechanism of GAC activation, we sought to reduce the complexity of the active enzyme unit and deconstruct the mechanistic details of GAC in isolation.

We therefore set out to learn more about the minimal GAC unit that is capable of full activity. A close examination of the existing X-ray crystal structures of wild type GAC suggested that the allosteric inhibitor, BPTES, by stabilizing the tetrameric helical interface of GAC, might inhibit the enzyme activation by inducing conformational changes within what we refer to as the "activation loop". In Chapter II I demonstrated that by introducing the single charge reversal mutation at the helical interface of the GAC tetramer (i. e., GAC(D391K)), I can construct an inactive constitutively dimeric form of the enzyme. Upon solving the crystal structure of GAC(D391K) (**Fig.2.2 A**), a comparison of the purely dimeric form of glutaminase with existing GLS structures in the Protein Data Bank revealed a key feature shared by GAC(D391K) and those structures with GAC bound to the allosteric inhibitor BPTES: both had resolved, stationary activation loops. In contrast, wild-type GAC structures harbored flexible, unresolved conformations in this loop region. This suggested that the flexibility of the activation loop could be critical for enzyme activation and provided the rational for the alanine scanning of the activation loop (**Fig.2.3 A&B**). Examination of glutaminase activity for each of the loop mutants revealed that among the seven residues on the activation loop (residue 321-327), lysine 325 is critical for phosphate stimulated

activation as well as the formation of higher order oligomers induced by phosphate binding. Indeed, absent phosphate addition, recombinant GAC(K325A) exhibited the same *in vitro* level of activity as phosphate stimulated wild type GAC. In cell transfection experiments with ectopically expressed, V5-tagged GAC, both GAC(K325A) and GAC(K325A/D391K) mutants formed supramolecular polymers in the cytosol of transfected cells (**Fig.2.4 C&D**) although only recombinant GAC(K325A) did so *in vitro* as assayed by MALS. By taking advantage of an earlier study, where substitution of lysine 316 at the interface of GAC monomers prevented the formation of the super oligomers (6), I introduced the same mutation into the GAC(K325A/D391K) background and obtained a constitutively active GAC in the dimeric state. The triple mutant, GAC(K316Q/K325A/D391K) restored the normal mitochondrial localization of GAC while retaining greatly elevated, phosphate independent activity (**Fig.2.5 B&C**). This demonstrated that the minimal unit of glutaminase activity can be a dimeric form of the enzyme and thus allowed us to study the activation of the enzyme uncoupled from the need to form higher order oligomers. Having the properly localized, constitutively active form of the enzyme, I set out to test whether its expression in cells provided any growth advantage. I concluded that, by itself, high glutaminase activity does not result in a proliferative phenotype but rather, facilitates higher growth rates in transformed cells by augmenting nutrient flux to the rapidly dividing cells.

Another structural element critical to activation of GAC that we have identified was the conserved tyrosine-isoleucine-proline (YIP; **Fig. 2.5 A**) motif that forms a

“lid“ over the substrate-binding pocket upon the binding of substrate (**Fig. 2.5 B, C**). Substituting the highly conserved tyrosine to a phenylalanine resulted in an increase of the basal activity of wild-type GAC(Y254F) (**Fig.2.5 E**). The elevated basal activity of the GAC(Y254F) mutant appears to be a result of rapid substrate/product exchange (i.e., due to the opening of the lid and resulting increased access to the GAC active site), as suggested by the initial velocity analysis where the V_{max} of GAC(Y254F) was fivefold higher than wild-type GAC without a significant change in K_m (**Fig.2.5F**).

Previous studies in our laboratory using a tryptophan fluorescence readout of GAC at the activation loop (i. e., the GAC(F327W) mutant) have provided a useful tool for monitoring the binding of allosteric inhibitors (BPTES-like molecules) and activators (phosphate) that bind in close proximity to the activation loop (7). Because the distance between the activation loop and the active site is ~12 Å, the communication between activators and inhibitors at the activation loop and the active site became the next focus of my thesis research. Besides serving as a good real-time readout for inhibitor and activator binding at the activation loop, GAC(F327W) was also observed to have the ability to selectively respond to the binding of substrate (glutamine) but not product (glutamate). This strongly argues that there is linkage between the activation loop at the helical dimer-dimer interface and the glutamine binding active site. The reciprocal behavior of these two sites and the manner in which they regulate substrate affinity and thereby GAC activity is a central finding of this thesis work that is further explored in Chapter 3.

The ability of GAC(F327W) tryptophan fluorescence to selectively respond to glutamine binding suggested that a direct readout of substrate in the active site might also serve as a fluorescence readout to distinguish between substrate (glutamine) and product (glutamate) binding. A close examination of the contacts that GAC makes with substrate and product in the active site reveals how the active site cleft discriminates between glutamine and glutamate. I therefore focused on tyrosine 471 in the catalytic site of GAC as the crystal structures showed the Y471 side chain –OH group forms a hydrogen bond with the amide group of the glutamine, which is a carboxyl group in glutamate. Indeed, the Y471W mutant showed a significant amount of fluorescence quenching with the addition of glutamine, while the same concentration of glutamate showed little effect (**Fig.3.3 B&C**). This could be due to the charge difference between the amide group of glutamine and the carboxyl group of glutamate affecting their interaction with the indole sidechain of tryptophan 471. Because tryptophan does not have an –OH group on its sidechain to form a hydrogen bond with the substrate or position a water molecule for the hydrolysis reaction, Y471W is able to bind glutamine but is catalytically inactive. The usefulness of this real-time assay for glutamine binding becomes obvious as it allowed direct monitoring of only the binding event, distinct from catalysis (**Fig.3.4 C**). In this way, the inactivity of the Y471W mutant allowed us to separate substrate binding from subsequent events, and made it possible to monitor the substrate binding process in isolation. The apparent affinity of glutamine for the GAC(Y471W) mutant was determined to have a K_d of approximately 2.5 mM, in good agreement with the K_m measured with the wild-type GAC in activity assays. This

provides some confidence that the glutamine binding cleft conformation is relatively close to that of the active enzyme and thus can serve as a reliable readout for active site communication with the activation loop.

Having established the tryptophan substitution as a monitor for substrate binding to GAC(Y471W), I investigated how different types of allosteric inhibitors and activators affect glutamine binding. For the frequently studied activator phosphate, the fluorescent signal for glutamine binding displayed faster kinetics and a greater degree of quenching when 50 mM phosphate was added prior to the addition of glutamine. This result suggested that the conformational change induced by the binding of phosphate near the activation loop resulted in an increase in the substrate binding affinity for the enzyme. In the absence of a phosphate bound GAC structure, the conformational change caused by phosphate binding and the loop positioning in the active structure are clearly aims of future studies of GAC. Based on an earlier study of phosphate driven self-assembly of GAC (6), phosphate not only can activate the enzyme but also can stabilize tetramers and higher order oligomers. In addition, tryptophan fluorescence results comparing wild-type GAC and the dimeric form of GAC (D391K mutant) showed that only the tetrameric form of GAC has the ability to bind glutamine while the dimeric form of GAC does not bind phosphate or glutamine (**Fig.3.5 C**). Therefore, a plausible explanation for the phosphate binding enhancement of glutamine binding is that, at the concentration of the fluorescent assay (50 nM), GAC is a mixture of dimer and tetramer, but at this low concentration, most of the

population is in the dimeric form. The addition of phosphate then shifts the population of the enzyme toward the active tetramer, which has a higher affinity for glutamine (**Fig.3.5**). This result provides direct evidence as to how inorganic phosphate activates GAC: *by enhancing substrate binding*. Future work will be aimed toward a deeper understanding of the mechanism of communication between these two sites on GAC using the spectroscopic readouts developed here.

For the BPTES-like inhibitors, GAC(Y471W) tryptophan fluorescence was quenched in a dose dependent manner by up to 20% of the total signal upon addition of the drug (**Fig.3.6 A**). This result is consistent with the conclusion stated in Chapter II that the conformational change within the activation loop can affect the active site (in this case the micro-environment of tryptophan 471). As the concentration of the inhibitor (CB-839) was increased, the tryptophan fluorescence signal for the same amount of glutamine addition (20 mM) decreased from 50% to 0%. Moreover, the decrease of glutamine-induced quenching is inversely correlated with the increase of drug binding-induced quenching, meaning that the decreased glutamine binding (indicated by the quench of the tryptophan fluorescence signal) was caused by the binding of the inhibitor, CB-839 (**Fig.3.6 B&C**). Based on previous studies, BPTES analogs stabilize the activation loop in an inactive conformation. The results from the CB-839 + glutamine tryptophan fluorescence experiments add support to the idea that the inactive conformation of the activation loop, constrained by bound CB-839, can prevent glutamine from binding to the active site.

In summary, this thesis has explored the molecular details of the mechanism of tetramer and phosphate driven activation of GAC. The identification of a minimal enzymatic dimeric unit capable of full activity demonstrates that the formation of higher order oligomers is not an absolute pre-requisite for full enzyme activation. The results described in this thesis also highlight the importance of the communication between the activation loop and active site for enzyme catalysis and in particular, substrate binding. Finally, a method to monitor substrate binding independently from catalysis was developed, which allows us to observe the impact of binding allosteric activators and inhibitors on the activation of GAC in real time.

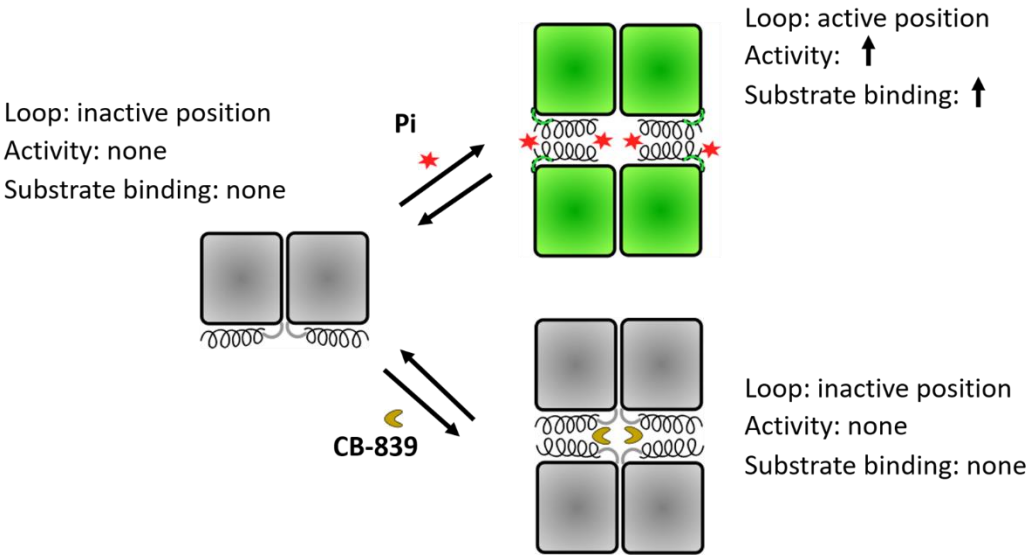

Inorganic phosphate enhances GAC tetramer formation and increases glutamine affinity. This higher substrate affinity results in the higher observed GAC activity.

FUTURE DIRECTIONS

The studies presented here suggest new and different areas worthy of further investigation. One aspect discussed in Chapter 2 concerns the dimeric mutant GAC(D391K), which provides a minimal unit to study the activation and inhibition of the enzyme without dealing with the complication presented by the formation of higher order oligomers. These findings also raise some possibilities regarding how specific types of posttranslational modifications within GAC might trigger enzyme activation. Such changes might include the modification of lysine residues through the addition of acetyl and succinyl moieties (8,9). Additionally, the mechanism of the "activation loop" directed activation of GAC provides some critical insights that will guide efforts to develop new small molecule inhibitors targeting GAC in glutamine addicted cancer cell lines. Future studies regarding this possibility might help us to understand how such modifications of GAC sustain a high level of enzyme activity without aggregating in cells.

Another aspect of these studies that might be expanded upon would be the further development of the utility of the tryptophan mutant GAC(Y471W), described in Chapter III. Since Y471W provides a very sensitive reporter to read out substrate binding independently from enzymatic activity, this mutant might be used in high throughput drug screens to identify inhibitors of GAC and how they influence glutamine binding. Also, the results from Y471W suggests the importance of the communication between the activation loop and the active site. Further studies,

including the point mutation of G320P, which, as we showed in Chapter II, uncouples the activation loop from the GAC active site by disrupting the peptide linkage between the two, could be incorporated in the GAC(Y471W) background in order to gain more information regarding the activation loop directed enzyme activation and the sequence specific requirements of this intramolecular communication. Lastly, since Y471 is a highly conserved residue among different types of GLS [liver-type (GLS2) and kidney-type (GLS)], the readout provided by its tryptophan substitution may well be useful for comparing the ability of substrate binding between different GLS isoforms and in what way these are affected by the addition of allosteric activators/inhibitors. In this regard, these read outs may ultimately serve to be very useful in future drug development efforts, as they are amenable to high throughput screening protocols that will allow for the identification of isoform specific small molecule inhibitors of GLS and GLS2.

References

1. Kovacevic, Z., and McGivan, J. D. (1983) Mitochondrial metabolism of glutamine and glutamate and its physiological significance. *Physiol. Rev.* **63**, 547–605

2. Lukey, M. J., Greene, K. S., Erickson, J. W., Wilson, K. F., and Cerione, R. A. (2016) The oncogenic transcription factor c-Jun regulates glutaminase expression and sensitizes cells to glutaminase-targeted therapy. *Nat. Commun.* **7**, 11321

3. Xiang, Y., Stine, Z. E., Xia, J., Lu, Y., O'Connor, R. S., Altman, B. J., Hsieh, A. L., Gouw, A. M., Thomas, A. G., Gao, P., Sun, L., Song, L., Yan, B., Slusher, B. S., Zhuo, J., Ooi, L. L., Lee, C. G. L., Mancuso, A., McCallion, A. S., Le, A., Milone, M. C., Rayport, S., Felsher, D. W., and Dang, C. V. (2015) Targeted inhibition of tumor-specific glutaminase diminishes cell-autonomous tumorigenesis. *J. Clin. Invest.* **125**, 2293–2306

4. Cassago, A., Ferreira, A. P. S., Ferreira, I. M., Fornezari, C., Gomes, E. R. M., Greene, K. S., Pereira, H. M., Garratt, R. C., Dias, S. M. G., and Ambrosio, A. L. B. (2012) Mitochondrial localization and structure-based phosphate activation mechanism of Glutaminase C with implications for cancer metabolism. *Proc. Natl. Acad. Sci.* **109**, 1092–1097

5. Suzuki, S., Tanaka, T., Poyurovsky, M. V., Nagano, H., Mayama, T., Ohkubo, S., Lokshin, M., Hosokawa, H., Nakayama, T., Suzuki, Y., Sugano, S., Sato, E., Nagao, T., Yokote, K., Tatsuno, I., and Prives, C. (2010) Phosphate-activated glutaminase (GLS2), a p53-inducible regulator of glutamine metabolism and reactive oxygen species. *Proc. Natl. Acad. Sci.* **107**, 7461–7466

6. Ferreira, A. P. S., Cassago, A., De Almeida Gonalves, K., Dias, M. M., Adamoski, D., Asceno, C. F. R., Honorato, R. V., De Oliveira, J. F., Ferreira, I. M., Fornezari,

C., Bettini, J., Oliveira, P. S. L., Leme, A. F. P., Portugal, R. V., Ambrosio, A. L. B., and Dias, S. M. G. (2013) Active glutaminase C self-assembles into a supratetrameric oligomer that can be disrupted by an allosteric inhibitor. *J. Biol. Chem.* **288**, 28009–28020

7. Stalnecker, C. A., Erickson, J. W., and Cerione, R. A. (2017) Conformational changes in the activation loop of mitochondrial glutaminase C: A direct fluorescence readout that distinguishes the binding of allosteric inhibitors from activators. *J. Biol. Chem.* **292**, 6095–6107

8. Xiong, Y., and Guan, K.-L. (2012) Mechanistic insights into the regulation of metabolic enzymes by acetylation. *J. Cell Biol.* **198**, 155–164

9. Hirschey, M. D., and Zhao, Y. (2015) Metabolic Regulation by Lysine Malonylation, Succinylation, and Glutarylation. *Mol. Cell. Proteomics*. **14**, 2308–2315